

**“Evaluation of the *Pseudomonas aeruginosa* Quorum Sensing
proteins PqsD, PqsBC and MvfR as novel anti-virulence
targets”**

Dissertation

zur Erlangung des Grades

des Doktors der Naturwissenschaften

der Naturwissenschaftlich-Technischen Fakultät

der Universität des Saarlandes

von

M. Sc. Giuseppe Allegretta

Saarbrücken

2017

Tag des Kolloquiums: 8th Februar 2017

Dekan: Prof. Dr. Guido Kickelbick

Vorsitz: Prof. Dr. C.-M. Lehr

Berichterstatter: Prof. Dr. R. W. Hartmann
Dr. A. Titz

Akad. Mitarbeiter: Dr. S. Böttcher

Die vorliegende Arbeit wurde von Januar 2013 bis Dezember 2016 unter Anleitung von Herrn Univ.-Prof. Dr. Rolf W. Hartmann in der Fachrichtung Pharmazie der Naturwissenschaftlich-Technischen Fakultät der Universität des Saarlandes sowie am Helmholtz-Institut für Pharmazeutische Forschung Saarland (HIPS) in der betailung Drug design and Optimizationn (DDOP), angefertigt.

*Dedicated to my wife
and my family.*

*“È sapiente solo chi sa di non sapere”
“The only true wisdom is in knowing you know nothing”
– Socrates –*

Table of contents

1	ZUSAMMENFASSUNG	vi
2	ABSTRACT	vii
3	PAPERS INCLUDED IN THE THESIS	viii
4	CONTRIBUTION REPORTS	ix
5	FURTHER PUBLICATION OF THE AUTHOR	x
6	ABBREVIATIONS	xi
7	INTRODUCTION	1
7.1	Brief history of antibiotic research	1
7.2	<i>Pseudomonas aeruginosa</i>	2
7.2.1	Clinical importance	2
7.2.2	Virulence factors production during infection	3
7.2.3	Quorum Sensing	4
7.2.4	Proof of Concept: Quorum Sensing inhibition as anti-virulence strategy	5
7.3	The <i>pqs</i> system	5
7.3.1	The <i>pqs</i> -related small molecules and their biosynthesis	6
7.3.2	Targeting the biosynthetic pathway	7
7.3.3	The transcriptional regulator MvfR	9
7.3.4	Targeting the transcriptional regulator	9
8	AIM OF THE THESIS	11
9	RESULTS	12
9.1	From <i>in vitro</i> to <i>in cellulo</i> : structure-activity relationship of (2-nitrophenyl)methanol derivatives as inhibitors of PqsD in <i>Pseudomonas aeruginosa</i>	12
9.2	Catechol-based substrates of chalcone synthase as a scaffold for novel inhibitors of PqsD.	24
9.3	Elucidation of the profile of MvfR-regulated small molecules in <i>Pseudomonas aeruginosa</i> after Quorum Sensing Inhibitors treatment	34
10	DISCUSSION	55
10.1	Development of PqsD inhibitors	55
10.1.1	Ligand-based approach	55
10.1.2	Similarity-guided approach	58
10.1.3	Common characteristics of the two classes	60
10.2	Evaluation of PqsBC inhibitors and MvfR antagonists	61
10.2.1	Effects of MvfR antagonists on <i>pqs</i> -small molecules	62
10.2.2	Effects of PqsBC inhibitors on <i>pqs</i> -small molecules	63
10.2.3	Effects of MvfR antagonists and PqsBC inhibitors on antibiotic tolerance	63
10.2.4	Comparison between PqsBC inhibitors and MvfR antagonists	63
11	CONCLUSIONS AND OULOOKS	65
12	REFERENCES	67
13	ANKNOWLEDGEMENTS	74

1 ZUSAMMENFASSUNG

Pseudomonas aeruginosa ist ein Gram-negatives Pathogen, das bei Patienten mit defekten Abwehrbarrieren schwere Infektionen verursacht. Wegen der Entwicklung von Stämmen, die gegen mehrere Antibiotika resistent sind, ist eine neue antiinfektive Strategie dringend nötig. Das Target die intrabakterielle Kommunikation, genannt Quorum Sensing (QS), scheint der ideale Ansatz. Dieses System koordiniert die *Pseudomonas*-Virulenz und seine Blockade unterdrückt effizient die bakterielle Pathogenität, ohne das Wachstum zu beeinflussen. Unter den verschiedenen QS Systemen wurde das *pqs* System aufgrund seiner einzigartigen Präsenz in *P. aeruginosa* als Ziel ausgewählt.

Die zwei biosynthetischen Proteine PqsD und PqsBC, die für die Signalmolekülproduktion notwendig sind, und der Transkriptionsregulator MvfR (PqsR) wurden als potentielle Target für die Blockierung dieses Systems ausgewählt. Zwei verschiedene Strategien wurden verwendet, um neue PqsD-Inhibitoren zu entwerfen und zu synthetisieren, die sowohl in zellfreien als auch ganzen Zelltests aktiv waren. Weiterhin wurden alle bei der Signalmoleküle-Biosynthese produzierten Substanzen nach der Inkubation mit PqsBC-Inhibitoren oder MvfR-Antagonisten untersucht. Interessanterweise wurde ein einzigartiges Profil für jede Klasse von QS-Inhibitoren beobachtet. Am Ende half diese Studie beim Verstehen, dass MvfR das beste Target ist, um das *pqs*-System zu blockieren und ein effizienteste Ergebnis zu erzielen.

2 ABSTRACT

Pseudomonas aeruginosa is a Gram-negative pathogen which causes severe infections in patients with compromised defense barriers. Because of the development of more and more resistant strains to multiple antibiotics, a new strategy for treating these bacterial infections is highly required. Targeting a type of cell-to-cell communication, called Quorum Sensing (QS), seems to be the ideal approach. This system is needed for coordinating *Pseudomonas* virulence and its blockage efficiently suppresses the bacterial pathogenicity without affecting growth. Among the different cell-to-cell communication systems, the *pqs* system was chosen as target because of its unique presence in *P. aeruginosa*.

Three proteins were selected as potential targets for blocking this system, such as the two biosynthetic proteins PqsD and PqsBC, necessary for signal molecule production, and the transcriptional regulator MvfR (PqsR). Two different strategies were employed for designing and synthesizing novel PqsD inhibitors which revealed to be active both in cell-free and whole cell assays. Furthermore, the production of all main compounds produced during signal molecule biosynthesis after incubation with PqsBC inhibitors or MvfR antagonists was investigated. Interestingly, a unique profile for each class of QS inhibitor was observed. In the end, this study helps in understanding that MvfR would be the best target to inhibit for blocking the *pqs* system and having the most efficient result.

3 PAPERS INCLUDED IN THE THESIS

The present thesis is divided into two publications and one manuscript to be submitted which are referred to in the text by their letter:

A. From *in vitro* to *in cellulo*: structure-activity relationship of (2 nitrophenyl)methanol derivatives as inhibitors of PqsD in *Pseudomonas aeruginosa*

Michael P. Storz, Giuseppe Allegretta, Benjamin Kirsch, Martin Empting, Rolf W. Hartmann

Org. Biomol. Chem. (2014). 12 (32), 6094 – 6104.

B. Catechol-based substrates of Chalcone Synthase as a scaffold for novel inhibitors of PqsD

Giuseppe Allegretta, Elisabeth Weidel, Martin Empting, Rolf W. Hartmann

Eur. J. Med. Chem. (2015). 90, 351 – 359.

C. Elucidation of the profile of MvfR-regulated small molecules in *Pseudomonas aeruginosa* after Quorum Sensing Inhibitors treatment

To be submitted.

4 CONTRIBUTION REPORTS

The author would like to clarify his contribution to **A – C** which compose his PhD thesis.

- A.** The author synthesized and characterized the compounds **71 – 76** included in the paper, while the rest of tested molecules were synthesized and characterized by Dr. Michael P. Storz. The author contributed in reviewing the manuscript of the publication.

- B.** The author designed, synthesized and characterized all the published compounds. In addition, he contributed in interpreting the Structure-Activity Relationship and the SPR results. The author significantly contributed in writing the manuscript.

- C.** The PhD student synthesized and characterized the **XVI**. He developed, optimized and validated the HPLC-MS/MS method for the quantification of 2'-aminoacetophenone, dihydroxyquinoline, 4-hydroxy-2-heptylquinoline, 4-hydroxy-2-heptylquinoline-N-oxide and *Pseudomonas* Quinolone Signal in *Pseudomonas aeruginosa* cultures. In addition, the author performed all the whole-cell assays. He significantly contributed in writing the manuscript.

5 FURTHER PUBLICATION OF THE AUTHOR

D. Mild and catalyst-free microwave-assisted synthesis of 4,6-disubstituted 2-methylthiopyrimidines – exploiting tetrazole as an efficient leaving group

Andreas Thomann, Jens Eberhard, Giuseppe Allegretta, Martin Empting, Rolf W. Hartmann
Synlett. (2015). 26 (18), 2606 – 2610

6 ABBREVIATIONS

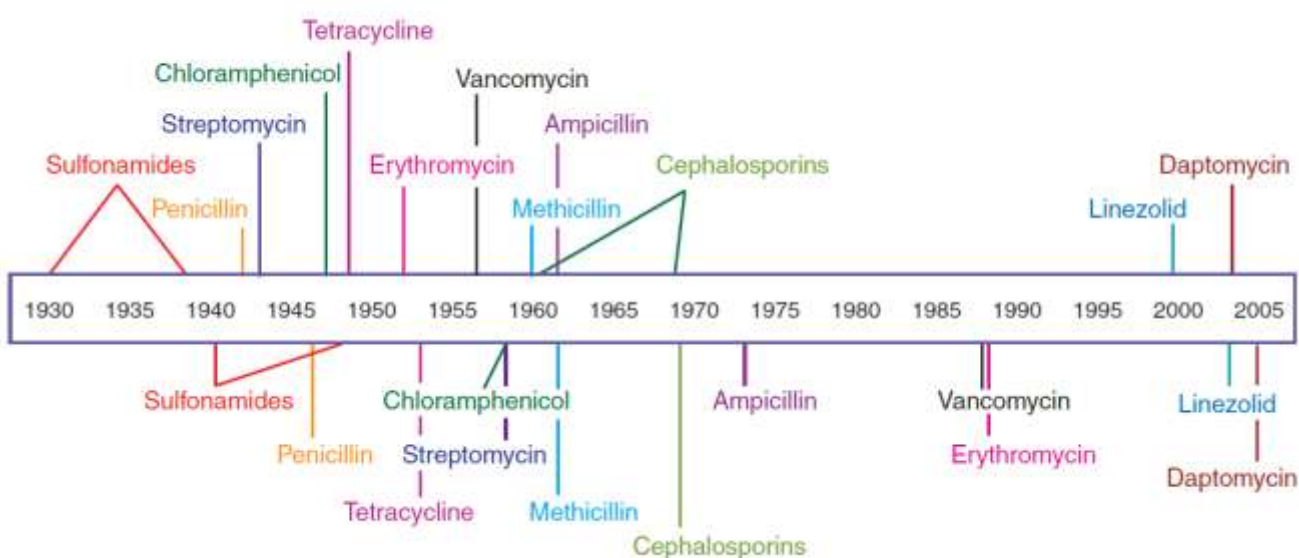
MDR	: Multidrug Resistant
<i>P. a.</i>	: <i>Pseudomonas aeruginosa</i>
QS	: Quorum Sensing
AI	: Auto-inducer
C ₄ -HSL	: <i>N</i> -butanoyl-L-homoserinelactone
3-oxo-C ₁₂ -HSL	: <i>N</i> -(3-oxododecanoyl)-L-homoserinelactone
IQS	: 2-(2-hydroxyphenyl)-thiazole-4-carbaldehyde
PQS	: <i>Pseudomonas</i> Quinolone Signal
QSI	: Quorum Sensing Inhibitor
HSL	: Homoserinelactone
MvfR	: Multiple virulence factor Regulator
AA	: Anthranilic acid
CoA	: Coenzyme A
A-CoA	: Anthraniloyl-Coenzyme A
2-ABA-CoA	: 2'-aminobenzoylacetate-Coenzyme A
M-CoA	: Malonyl-Coenzyme A
2-ABA	: 2'-aminobenzoylacetate
HHQ	: 4-hydroxy-2-heptylquinoline
DHQ	: Dihydroxyquinoline
2-AA	: 2'-aminoacetophenone
2-HABA	: 2'-hydroxylaminobenzoylacetate
HQNO	: 4-hydroxy-2-heptylquinoline- <i>N</i> -oxide
AQ	: Alkyl-quinoline
LTTR	: Lys-type transcriptional regulator
FabH	: β -ketoacyl-ACP synthase III
SAR	: Structure-Activity Relationship
SPR	: Surface Plasmon Resonance
IC ₅₀	: Concentration of inhibitor necessary for blocking the 50% of conversion
EWG	: Electron withdrawing group
EDG	: Electron donating group
CHS2	: Chalcone Synthase
PKS	: Polyketide Synthase

7 INTRODUCTION

7.1 Brief history of antibiotic research

The discovery of penicillin, the first antibacterial agent against *Staphylococcus* and *Streptococcus*, by Fleming in 1928 (Fleming, 1929) was a milestone in the history of medicine. From that year, the "Golden Age" of antibiotic research started and, until the late 1960s, the scientific community identified new classes of antibiotics with different spectra width capable to block all the main targets of bacterial metabolism. However, the misuse of these precious tools during the XX century in clinics and agriculture induced a natural selection in the bacterial community of resistant strains towards these drugs (Fig. 1) (Brown, Wright, 2016).

Antibiotic deployment



Antibiotic resistance observed

Fig. 1 Timeline of the first employment of the antibacterial agents (above the timeline) and the first assessment of resistance towards the drug (below the timeline) (Clatworthy *et al.*, 2007).

Actually, the number of new clinical isolates with acquired antibiotic resistance increased years after years (Schäberle, Hack, 2014). Because of their spread in clinics and environment, and the difficulties in developing new antibacterial drugs in last three decades, the treatment of infections caused by bacteria resistant towards more than three antibiotics, named multidrug resistant (MDR) (Obritsch *et al.*, 2004), has become increasingly complicated. Among the prokaryotes, the ESKAPE pathogens (*Enterococcus faecium*, *Staphylococcus aureus*, *Klebsiella pneumoniae*, *Acinetobacter baumannii*, *Pseudomonas aeruginosa*, and *Enterobacter* species) (Pendleton *et al.*, 2013) are the most dangerous ones because of their capability to become MDR. Actually, around 26000 patients die each year only in EU from MDR bacterial infections and the estimated costs for treating patients affected by these superbugs are at least 1.5 billion € per year (ECDC/EMA Joint Working Group, 2009). Consequently, an urgent need of new anti-infectives is

present for avoiding a threatening scenario in which mankind will not have any shield as protection against MDR bacteria.

7.2 *Pseudomonas aeruginosa*

7.2.1 *Clinical importance*

Pseudomonas aeruginosa (*P. a.*) is a facultative anaerobe Gram-negative bacterium (Pendleton *et al.*, 2013) belonging to the family of the *Pseudomonaceae*. It is an opportunistic pathogen which is the cause of severe hospital-acquired infections (Lister *et al.*, 2009). It affects mainly patients with compromised immune system, for example people with burned wounds (Tredget *et al.*, 2004), suffering from cystic fibrosis (Gómez, Prince, 2007) or infected by HIV (Busi Rizzi *et al.*, 2006). The eradication of *P. a.* is becoming more and more difficult because of the wide occurrence of MDR strains. For example, in the period 1993 – 2002 an increase from 4 % to 14 % (Obritsch *et al.*, 2004) causing a mortality of 39 % among the infected patients from 1998 to 2001 (Kang *et al.*, 2003). This pathogen showed to be less sensitive to ciprofloxacin, imipenem, tobramycin and aztreonam (Obritsch *et al.*, 2004) which are the first-line antipseudomonal antibiotics (Hill *et al.*, 2005). The resistance towards these drugs was acquired over time by this bacterium through two main mechanisms, such as imported or chromosomally encoded (Lister *et al.*, 2009). The first type is based on plasmid transfer among bacteria carrying genes for expressing β -lactamases (Livermore, Woodford, 2006) or aminoglycosides modifying enzymes (Hancock, 1998). The second mechanism occurs by mutation in the bacterial genome causing a target mutation, as in the gyrase gene transferring quinolone resistance, or a different expression of transport proteins in the bacterial membranes, for example upregulation of efflux pumps and downregulation of porines (Lister *et al.*, 2009; Hancock, 1998).

In both cases, the resistance was acquired by the pathogen because the antibiotic affected bacterial growth and, for survival, the bacterial community developed the tools for reducing the compounds' activity. Consequently, a different approach should be considered for blocking *P. a.* infections without interfering with the life cycle of the pathogen.

Recently, a potential efficient strategy has been identified through the blockage of the production and/or the expression of virulence factors necessary for acute and/or chronic infection without killing the pathogen, the so-called “Anti-virulence strategy” (Maura *et al.*, 2016; Wagner *et al.*, 2016; Clatworthy *et al.*, 2007). One important advantage of this approach would be the potentially low rate of resistance because the survival of the bacterium will not be affected by the active agent itself. Consequently, the bacterial community would not have the pressure to develop tools for inactivating the target compounds (Allen *et al.*, 2014; Rasko, Sperandio, 2010).

7.2.2 Virulence factors production during infection

Acute *P. a.* infections follow three main steps, adhesion, invasion and systemic dissemination, in which the pathogen attacks the host using several cell-associated and extracellular virulence factors (Todar, 2009).

After damage of the host natural barriers, as the skin, or reduced efficiency of the immune system, as in patients affected by AIDS, the bacterium has the possibility to adhere on the epithelial cells using sugar binding proteins as fimbriae (known also as polar type IV pili) (Persat *et al.*, 2015), flagella (Feldman *et al.*, 1998) and LecA and LecB lectins (Stateva, Mitov, 2011). Then, the pathogen starts producing the elastases LasA and LasB which hydrolyse elastine, an essential protein of the connective tissue (Galloway, 1991), and surfactant peptides, important tools of the lung innate immunity (Mariencheck *et al.*, 2002). In addition, it expresses alkaline protease necessary for the degradation of complement components and inflammatory cytokines (Laarman *et al.*, 2012). Furthermore, *P. a.* enhances the production of rhamnolipids and hemolytic phospholipase C which are responsible of the dissolution and hydrolyzation of phospholipids, especially phosphatidylcholine, present in the eukaryotic membranes and lung surfactants (Stateva, Mitov, 2011). Moreover, the bacterium synthesizes the redox toxin pyocyanin which interferes with multiple mammalian cell functions (Stateva, Mitov, 2011) as the cell respiration, and several siderophores, for example pyochelin and pyoverdine, important for iron-uptake and, consequently, bacterial growth (Hoergy *et al.*, 2014). After colonizing and growing in the infection site, *P. a.* can disseminate in the whole body through the blood stream using the same virulence factors employed in the adhesion and invasion steps (Stateva, Mitov, 2011). In addition, the exposition of lipid A, the lipophilic moiety of the lipopolysaccharides present in the outer membrane, to the blood is the main cause of the Gram-negative septicemia (Stateva, Mitov, 2011).

Moreover, the pathogen can start building biofilms in the colonized sites, which are composed of a complex mixture of exopolysaccharides, rhamnolipids, extracellular DNA and proteins (Flemming, Wingender, 2010), causing the establishment of a chronic infection (Wagner *et al.*, 2016). This heterogeneous structure is formed around the cells for improved adhesion and stabilization on host tissues, and for creating a physical barrier to several biocides, as reactive chemicals (bleach or superoxides), the immune system, UV light and antimicrobial agents (Hall-Stoodley *et al.*, 2004). Furthermore, the bacterial community is not homogeneous in the biofilm. Actually, the cells present in the middle of this heterogeneous matrix are less metabolically active compared to the ones located on the surface because of a lower access to oxygen. So, these bacteria become dormant. Taking into consideration that the antibiotics block metabolic pathways, these drugs can kill only pathogens with an active metabolism, such as the cells on the surface, and not the one inside the biofilm which are, then, called "persisters" (Walter III *et al.*, 2003). When the concentration of the antibiotic reaches sub-inhibitory levels, the persister cells can switch their metabolic pathways on and repopulate the tissue. Consequently, the presence of dormant cells leads to recalcitrant infections very difficult to eradicate (Lewis, 2010).

7.2.3 Quorum Sensing

The behavior of *P. a.* in acute and chronic infections is controlled by a complex regulatory system called Quorum Sensing (QS) (Wagner *et al.*, 2016).

The QS is a cell-to-cell communication system used by both Gram-positive and Gram-negative in which the bacteria synthesize and release small molecules, so called auto-inducers (AIs), depending on bacterial cell density and nutrient concentrations, for examples phosphate or iron. These molecular signals diffuse in the community and interact with their respective regulators for coordinating the expression of specific genes. Among these are the ones necessary for virulence factors and biofilm production, and for the synthesis of the signal molecules (Lee, Zhang, 2014).

P. a. employs at least four different QS networks interconnected to each other, such as the *las*, *rhl*, *iqs* and *pqs* (Fig. 2). These systems employ transcriptional regulators, respectively LasR, RhIR, IqsR and PqsR (also called Multiple virulence factor Regulator, MvfR), which, after binding their specific AIs, activate the expression of selected genes connected to virulence (Lee, Zhang, 2014).

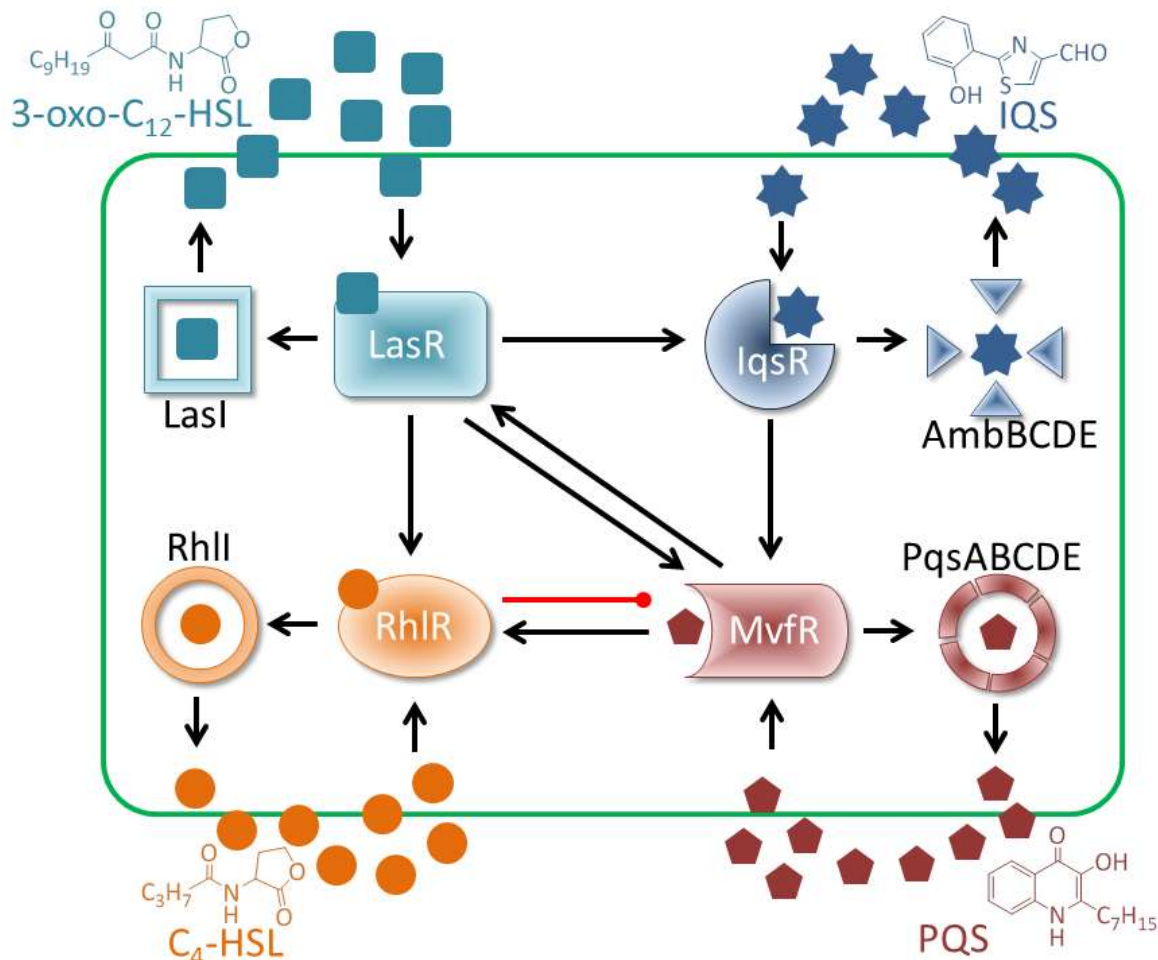


Fig. 2 Quorum Sensing networks in *Pseudomonas aeruginosa*. Black line-arrows: activation. Red line-dots: inhibition. (Edited picture from Lee, Zhang, 2014; Maura *et al.*, 2016).

The *las* system makes use *N*-butanoyl-L-homoserinelactone (C₄-HSL) as signal molecule and it induces the expression of LasA and LasB elastases, alkaline protease, MvfR, RhlR, IqsR and the cognate synthetase LasI. The *rhl* system employs a molecule of *N*-(3-oxododecanoyl)-L-homoserinelactone (3-oxo-C₁₂-HSL) as AI and it favors the production of rhamnolipids, LasB elastase, pyocyanin, hydrogen cyanide, the related signal molecule biosynthetic protein RhlI and the downregulation of *mvfR* (Lee, Zhang, 2014). The most recent discovered *iqs* employs 2-(2-hydroxyphenyl)-thiazole-4-carbaldehyde (IQS) and it positively regulates the *pqs* system, but further investigations are necessary for better understanding of its role in *P. a.* infections (Lee *et al.*, 2013). The *pqs* system utilizes *Pseudomonas* Quinolone Signal (PQS) as QS molecule and it activates the synthesis of pyocyanin, hydrogen cyanide, LecA lectin, the enzymes needed for PQS biosynthesis, the expression of RhlR (Lee, Zhang, 2014) and LasR (Maura *et al.*, 2016). In addition, the *las*, *rhl* and *pqs* systems coordinate biofilm formation (Christensen *et al.*, 2007; Hurley *et al.*, 2012; Smith, Iglewski, 2003).

7.2.4 Proof of Concept: Quorum Sensing inhibition as anti-virulence strategy

Based on the importance of QS in regulating virulence factors and biofilm formation, the scientific community considered these cell-to-cell communication systems as potential drug targets. Actually, *in vivo* studies demonstrated that strains lacking in the expression of the transcriptional regulators and/or of the AI biosynthetic pathways provoked a lower mortality of mice compared to the animals treated with the wild-type *P. a.*. So, these findings were the proof that the QS is a valuable target for the anti-virulence strategy (Christensen *et al.*, 2007; Rumbaugh *et al.*, 1999; Xiao *et al.*, 2006a). Consequently, three possible approaches could be considered for the development of Quorum Sensing Inhibitors (QSIs), such as inhibition of the AI syntheses, inactivation of the signal molecules and interference with the transcriptional regulators (Wagner *et al.*, 2016).

7.3 The *pqs* system

Several Gram-negative bacteria, for example *Vibrio fischeri* and *Pantoea sterwatii*, make use of signal molecules belonging to the class of homoserinelactones (HSL) for their QS systems as *P. a.* (Fugua *et al.*, 2001; Miller, Bassler, 2001). On the contrary, quinolone-like quorum sensors are employed only by *P. a.* (Pesci *et al.*, 1999) and some species of *Burkholderia* (Vial *et al.*, 2008; Diggle *et al.*, 2006). Taking into consideration that *P. a.* causes severe infections in patients with compromised barriers and immune system, a selective anti-*Pseudomonas* therapy would be preferable. Consequently, the ideal cell-to-cell communication system to be targeted would be the *pqs* as it would be possible to develop selective inhibitors without having side effects on other bacteria, as the Gram-negative *Escherichia coli* which lives in symbiosis with us in our gut (Zhang *et al.*, 2015).

7.3.1 The *pqs*-related small molecules and their biosynthesis

As previously mentioned, the *pqs* system employs as signal molecules the quinolone PQS (Pesci *et al.*, 1999) and its precursor HHQ (Xiao *et al.*, 2006a). Their biosynthesis require several enzymes which are expressed by the polycistronic operon *pqsABCDE* (Gallagher *et al.*, 2002; Déziel *et al.*, 2004; McGrath *et al.*, 2004), and *pqsH* (Gallagher *et al.*, 2002) (Fig. 3).

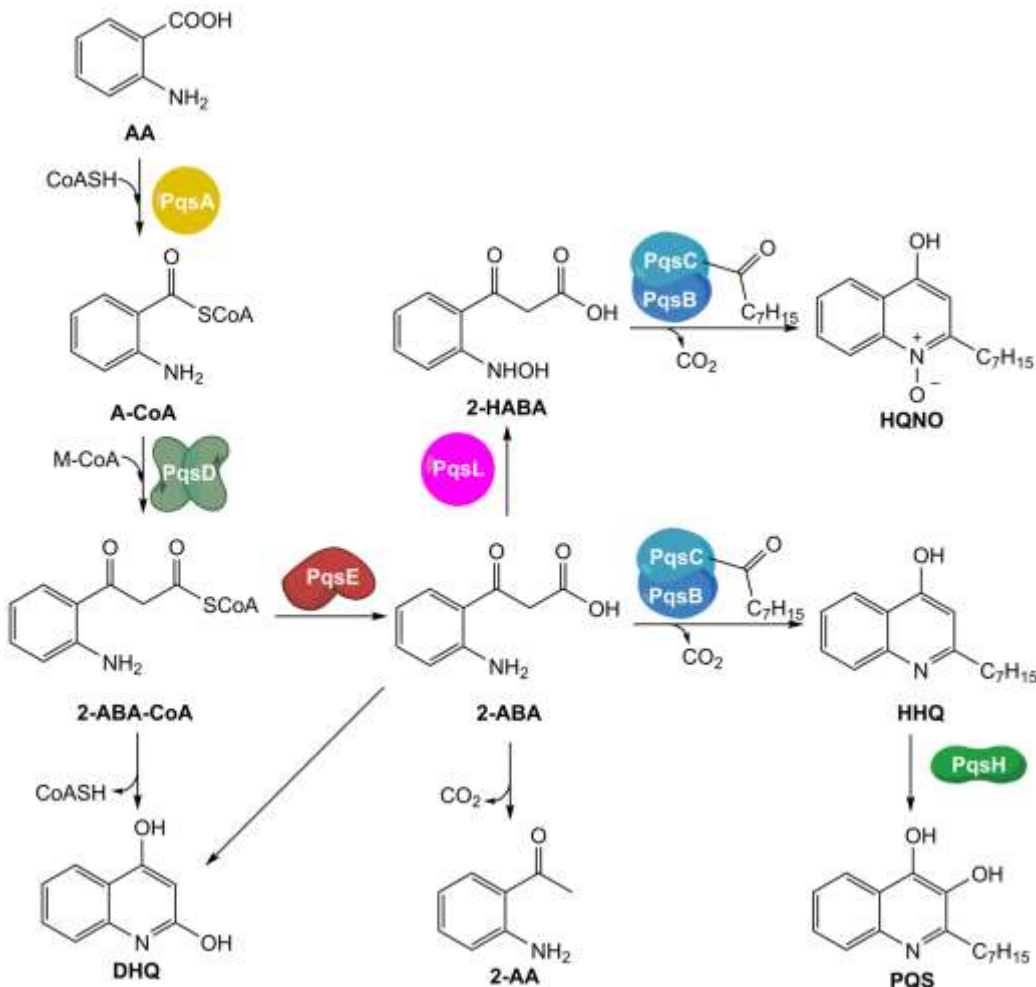


Fig. 3 Current model of the biosynthetic pathway of MvfR-related small molecules. AA: anthranilic acid. CoASH: Coenzyme A. A-CoA: anthraniloyl-CoA. M-CoA: malonyl-CoA. 2-ABA-CoA: 2'-aminobenzoylacetate-CoA. 2-ABA: 2'-aminobenzoylacetate. DHQ: dihydroxyquinoline. 2-AA: 2'-aminoacetophenone. 2-HABA: 2'-hydroxylaminobenzoylacetate. HHQ: 4-hydroxy-2-heptylquinoline. HQNO: 4-hydroxy-2-heptylquinoline-*N*-oxide. PQS: *Pseudomonas* Quinolone Signal.

The production of the signal molecule starts from a molecule of anthranilic acid (AA) which is transformed into anthraniloyl-CoA (A-CoA) by the Coenzyme A (CoA) ligase PqsA (Coleman *et al.*, 2008). Then, the thioester A-CoA is converted by PqsD into 2'-aminobenzoylacetate-CoA (2-ABA-CoA) after reacting with a molecule of malonyl-CoA (M-CoA) (Dulcey *et al.*, 2013). So, the thioesterase PqsE cleaves the thioester bond of 2-ABA-CoA for getting the reactive intermediate 2'-aminobenzoylacetate (2-ABA) (Drees, Fetzner, 2015) which is transformed into 4-hydroxy-2-heptylquinoline (HHQ) after condensation with a molecule of octanoyl-CoA by the hetero-dimer PqsBC (Dulcey *et al.*, 2013). Finally, HHQ is oxidized by the flavin monooxygenase PqsH into PQS

(Schertzer *et al.*, 2010). Moreover, 2-ABA-CoA and 2-ABA are important intermediates for the biosynthesis of other compounds important for *P. a.* infection. Actually, both molecules can undergo to an intramolecular cyclization resulting in the formation of dihydroxyquinoline (DHQ). In addition, 2-ABA can be decarboxylated and transformed into the volatile molecule 2'-aminoacetophenone (2-AA). Finally, 2-ABA could be oxidized by PqsL into the hydroxylamine analogue which would be converted into 4-hydroxy-2-heptyl-quinoline-*N*-oxide (HQNO) by PqsBC (Dulcey *et al.*, 2013; Déziel *et al.*, 2004).

Even if a deep analysis of the biosynthetic products of the *pqs* system revealed that *P. a.* produces more than 50 *pqs*-related small molecules (Lépine *et al.*, 2004), the bacterium synthesizes mainly PQS, HHQ, HQNO, DHQ and 2-AA and their role in *Pseudomonas* infections was elucidated. PQS and HHQ behave as signal molecules of the *pqs* system binding the transcriptional regulator MvfR, but with different potency. Actually, the dihydroxyl-quinoline is 100 times more potent than the monohydroxyl-analogue (Xiao *et al.*, 2006a; Diggle *et al.*, 2007). Nonetheless, the analysis of these alkyl-quinolines (AQs) in *in vivo* studies, such as clinical cases and animal experiments, revealed that the amount of HHQ is higher than PQS in the infection sites (Que *et al.*, 2011; Xiao *et al.*, 2006a). It is plausible to assume that the pathogen produces HHQ and exports it in the extracellular space by the efflux pump MexEF-OprN (Lamarche, Déziel, 2011). Consequently, the molecule permeates in the bacteria, is oxidized by PqsH into PQS and finally transported outside the cells through membrane vesicles traffic (Mashburn, Whiteley, 2005; Déziel *et al.*, 2004). Moreover, because of the presence of the 3,4-dihydroxyl moiety, PQS is important in iron homeostasis based on its capability to chelate ferric ions and favoring its transport into the cell (Diggle *et al.*, 2007). Furthermore, PQS, but not HHQ, is essential for full production of the redox-toxin pyocyanin (Xiao *et al.*, 2006a). HQNO is necessary for coordinating the autolysis of the prokaryotic cells for the consequent release of DNA in the extracellular space, a fundamental component of the bacterial biofilm (Hazan *et al.*, 2016). Furthermore, the *N*-oxide quinoline inhibits the proliferation of Gram-positive bacteria, as *Staphylococcus aureus*, and, consequently, it helps *P. a.* to colonize the environmental niche of infection (Déziel *et al.*, 2004; Machan *et al.*, 1992). DHQ is used by the pathogen as toxin against epithelial cells for inhibiting their cellular growth (Zhang *et al.*, 2008) and is necessary for *Pseudomonas* pathogenicity, as pyocyanin production (Gruber *et al.*, 2016). The small volatile molecule 2-AA is fundamental for the transition from acute to chronic infection favoring the formation of persister cells within the bacterial community (Kesarwani *et al.*, 2011; Que *et al.*, 2013).

7.3.2 Targeting the biosynthetic pathway

Blocking the biosynthesis of the signal molecules has been shown to be an efficient strategy for reducing PQS and HHQ production in *P. a.* cultures and, consequently, reduce its virulence (Wagner *et al.*, 2016). Among the enzymes necessary for the synthesis of the *pqs*-related small molecules, the two oxidases PqsH and PqsL have not been considered attractive targets as the

respective *P. a.* mutants would be still capable to synthesize the QS signal molecules (Lépine *et al.*, 2004; Déziel *et al.*, 2004; Gallagher *et al.*, 2002). Furthermore, even if PqsE is important for the cleavage of the thioester bond of 2-ABA-CoA for releasing 2-ABA, its function in the biosynthetic pathway can be taken over by the non-specific thioesterase TesB as *P. a. pqsE* mutant still produce HHQ and PQS (Drees, Fetzner, 2015). So, the enzymes to target for blocking the Aqs production would be PqsA, PqsD and the dimer PqsBC as their *P. a.* mutants were not able to generate any signal molecules (Zhang *et al.*, 2008). As the crystal structure of PqsA has not been elucidated until now, the most attractive proteins for designing QSIs would be PqsD and PqsBC based on the important information obtained from the X-ray data (Bera *et al.*, 2009; Drees *et al.*, 2016).

Both PqsD and PqsBC belong to the β -ketoacyl-ACP synthase III (FabH) family, a class of condensing enzymes which employ substrates conjugated to CoA by thioester bonds (Bera *et al.*, 2009). Another characteristic of FabH-like proteins is the presence of the catalytic triad Cys-His-Asp which is fully present in PqsD, while partially in PqsC as Cys-His diad and completely absent in PqsB (Bera *et al.*, 2009; Drees *et al.*, 2016).

PqsD is constituted by 337 aminoacids and it exists as a homo-dimer in the bacterial cytosol (Bera *et al.*, 2009). This protein catalyzes the conversion of A-CoA into 2-ABA-CoA through two steps: 1) the anthranilate is transferred onto Cys₁₁₂ through trans-thioesterification releasing one CoA molecule; 2) the complex anthranilate-PqsD reacts with M-CoA through a nucleophilic substitution leading to the loss of a CO₂ molecule and release of 2-ABA-CoA (Bera *et al.*, 2009; Dulcey *et al.*, 2013). Furthermore, through a similar mechanism, PqsD can catalyze *in vitro* the conversion of A-CoA into HHQ using a molecule of β -ketodecanoic acid (Pistorius *et al.*, 2011).

Several strategies were used for designing PqsD inhibitors, such as ligand-based and similarity-guided approaches (Wagner *et al.*, 2016). The first method was based on the transition state of the first enzymatic step in which there is the formation a tetrahedral intermediate. Starting from substrate analogues followed by structure simplification, the PqsD inhibitor **I** was obtained highly active in reducing HHQ production both *in vitro* and *in cellulo* assays (Fig. 4) (Storz *et al.*, 2012).

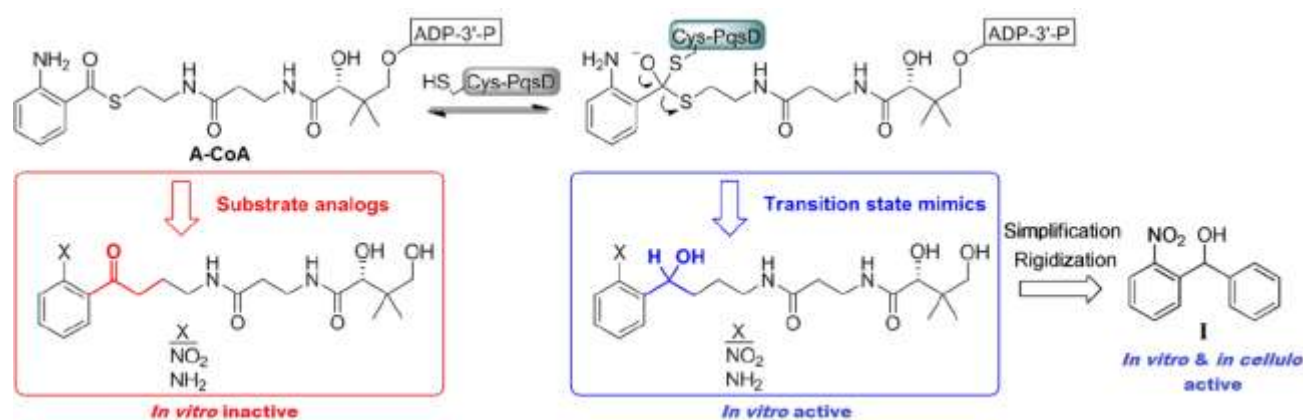


Fig. 4 Ligand-based design concept based on the transition state of the first PqsD enzymatic reaction. (Edited figure from Storz *et al.*, 2012).

The second approach started considering the similarities between the PqsD and FabH families and from known inhibitors of the latter class of proteins novel inhibitors of the bacterial enzyme were designed capable to reduce efficiently HHQ and PQS production *in vitro* (Hinsberger *et al.*, 2014; Weidel *et al.*, 2013). These results demonstrated that the inhibition of PqsD is a valuable tool for reducing QS molecules production and, consequently, further investigations were required for optimizing the lead QSI and for identifying novel inhibitors.

PqsBC is a hetero-dimer formed by the subunit B and C consisting of 283 and 350 aminoacids, respectively. While the role of PqsB is still unclear, PqsC is necessary for the condensation of 2-ABA with an octanoyl chain through a three steps-reaction: 1) the octanoyl-CoA is transferred onto Cys₁₂₉ of the catalytic pocket through a trans-thioesterification reaction; 2) 2-ABA loses a CO₂ molecule forming a reactive enolate; 3) the carbanion attacks the electrophilic thioester for getting an intermediate which spontaneously cyclizes into HHQ (Drees *et al.*, 2016).

Considering that the enzymatic mechanism was only recently elucidated, only few compounds could be developed against this target until today (Starkey *et al.*, 2014). So, more efforts should be put in studying the effects of PqsBC inhibitors on the *pqs* system. Based on the findings obtained, the scientific community would have additional information for understanding the impact of these QSIs on the *pqs* biosynthetic machinery and, consequently, further elucidating its functionality.

7.3.3 *The transcriptional regulator MvfR*

As previously described, the *pqs* system makes use of the transcriptional regulator MvfR which belongs to the family of LysR-type transcriptional regulators (LTTR) (Xiao *et al.*, 2006a). This protein is constituted by 332 aminoacids and it has a DNA-binding domain at the *N*-terminus used for binding the promotor of the genes to be expressed, and a ligand-binding domain at the *C*-terminus in which the signal molecule interacts with the regulator (Schell, 1993). MvfR is a membrane-associated protein that is mainly expressed in the late exponential phase of bacterial growth (Cao *et al.*, 2001). After binding the signal molecule, the protein forms a dimer or a tetramer and, then, strongly binds the promoter regions of the genes under its regulation activating their transcription (Cao *et al.*, 2001; Xiao *et al.*, 2006b; Kirsch *et al.*, unpublished data). Subsequently, when the bacterial culture enters in stationary phase, the MvfR is translocated in the extracellular space and cleaved by a protease which causes the inactivation of the transcriptional regulator (Cao *et al.*, 2001).

7.3.4 *Targeting the transcriptional regulator*

The transcriptional functionality of MvfR can be positively or negatively modulated based on the interactions established by small molecules in the ligand-binding pocket of the protein. For decreasing the *P. a.* pathogenicity the ideal approach is reducing the protein activity through the administration of antagonists (Wagner *et al.*, 2016). The scientific community developed several

classes of MvfR antagonists applying different strategies, such as those based on the scaffold of the natural ligands (Lu *et al.*, 2014; Ilangonav *et al.*, 2013), or guided by the analysis of small fragments binding to the protein (Klein *et al.*, 2012; Zender *et al.*, unpublished data), or highthroughput screening (Starkey *et al.*, 2014). The results obtained have in common that the compounds were capable to reduce *pqs* transcription, signal molecule biosynthesis, virulence factors production, like pyocyanin and rhamnolipids, and biofilm formation (Lu *et al.*, 2014; Ilangonav *et al.*, 2013; Klein *et al.*, 2012; Zender *et al.*, unpublished data; Starkey *et al.*, 2014). These findings highlighted the efficiency of this approach in inhibiting the *pqs* system and, consequently, *P. a.* pathogenicity. However, a complete analysis of the *mvfR*-related small molecules biosynthesis after the treatment of the bacteria with MvfR antagonists was not performed. Actually, a deeper evaluation of their effects on 2-AA, DHQ, HQNO, HHQ and PQS production would help in better understanding the biosynthetic machinery and, in addition, indicating the optimal dosage of QSI to administer for treating *P. a.* infections.

8 AIM OF THE THESIS

Among the human pathogens, the opportunistic bacterium *P. a.* has been considered to be a serious health problem because of the difficulties in eradicating this prokaryote through antibiotic therapies due to its resistance mechanisms. Actually, after circa a century of antibacterial drugs usage, the natural selection let the bacteria become less sensitive towards these compounds which consequently have lost their therapeutic efficiency. Among the novel strategies proposed for treating *P. a.* infections, blocking the *pqs* cell-to-cell communication system was proven to successfully reduce the bacterial virulence blocking both the key enzymes of the signal molecule biosynthesis PqsD and PqsBC, and the transcriptional regulator MvfR.

The first goal of the thesis was to optimize the activity of the PqsD inhibitor **I** discovered by Storz and coworkers in the cell-free assay and studying the Structure-Activity Relationship (SAR) of this class of QSIs. Furthermore, the effect of the substituents on the time-dependent onset of inhibition was investigated *in vitro*. In addition, the efficacy of the developed QSIs in reducing signal molecule production was assessed in the whole-cell assay and a correlation of the results between *in vitro* and *in cellulo* settings was attempted.

Based on the promising results got from the application of the similarity-guided approach, the second aim of the thesis was to examine enzymes having common features and similar function with PqsD in nature. Subsequently, the substrates of this protein were evaluated in the cell-free assay and, through chemical modifications of the scaffold, an SAR was evaluated. Furthermore, the binding mode of this class of PqsD inhibitors was analyzed using Surface Plasmon Resonance (SPR). Then, the activity of these QSIs was examined in *P. a.* cultures.

The third aim of the thesis was to investigate the effects of PqsBC inhibitors and MvfR antagonists on *pqs*-related small molecules production after incubation with *P. a.* strains for understanding more deeply the signal molecules biosynthetic machinery. Moreover, the influence of these QSIs on the persistence phenotype was evaluated.

9 RESULTS

9.1 From *in vitro* to *in cellulo*: structure-activity relationship of (2-nitrophenyl)methanol derivatives as inhibitors of PqsD in *Pseudomonas aeruginosa*.

Publication A

Authors: Michael P. Storz, Giuseppe Allegretta, Benjamin Kirsch, Martin Empting, Rolf W. Hartmann

Journal: Org. Biomol. Chem. (2014). 12 (32), 6094 – 6104.



Cite this: *Org. Biomol. Chem.*, 2014, **12**, 6094

From *in vitro* to *in cellulo*: structure–activity relationship of (2-nitrophenyl)methanol derivatives as inhibitors of PqsD in *Pseudomonas aeruginosa*†

Michael P. Storz,^a Giuseppe Allegretta,^a Benjamin Kirsch,^a Martin Empting^{a,*} and Rolf W. Hartmann^{a,b}

Recent studies have shown that compounds based on a (2-nitrophenyl)methanol scaffold are promising inhibitors of PqsD, a key enzyme of signal molecule biosynthesis in the cell-to-cell communication of *Pseudomonas aeruginosa*. The most promising molecule displayed anti-biofilm activity and a tight-binding mode of action. Herein, we report on the convenient synthesis and biochemical evaluation of a comprehensive series of (2-nitrophenyl)methanol derivatives. The *in vitro* potency of these inhibitors against recombinant PqsD as well as the effect of selected compounds on the production of the signal molecules HHQ and PQS in *P. aeruginosa* were examined. The gathered data allowed the establishment of a structure–activity relationship, which was used to design fluorescent inhibitors, and finally, led to the discovery of (2-nitrophenyl)methanol derivatives with improved *in cellulo* efficacy providing new perspectives towards the application of PqsD inhibitors as anti-infectives.

Received 3rd April 2014,
Accepted 29th May 2014
DOI: 10.1039/c4ob00707g
www.rsc.org/obc

Introduction

Until recently, bacterial communities were seen as nothing more than an accumulation of autonomous single-celled organisms. But today, we are aware that bacteria use cell-to-cell communication systems like *quorum sensing* (QS) to behave collectively rather than as individuals.¹ Small diffusible molecules are produced by single bacterial cells that can be released into the environment and detected by surrounding bacteria. Upon proliferation, the extracellular signal molecule concentrations increase along with cell density. Once a certain threshold is reached, receptors are activated by these autoinducers resulting in population-wide changes in gene expression. This concerted switch from low- to high-cell-density mode allows single bacterial cells to limit their group-beneficial efforts to those cell densities which guarantee an effective group outcome. Even if QS may not be directly essential for the survival of a singular bacterial cell, it is very important for bacteria–host interactions and pathogenesis upon bacterial infections in

general. In this regard, QS regulates a variety of virulence factors, which contribute to breaking the first line defences and damaging surrounding tissues leading to dissemination, systemic inflammatory-response syndrome, multiple organ failure, and, finally, death of the host.² Furthermore, QS contributes to the collective coordination of biofilm formation, a key reason for bacterial resistance against conventional antibiotics in clinical use.³ Thus, the importance of these regulatory systems could be exploited for the design of novel anti-infectives.

Several groups have successfully targeted QS, which is discussed as an alternative to the traditional treatment using bactericidal or bacteriostatic agents (for reviews see ref. 4 and 5). Novel anti-virulence compounds ideally decrease pathogenicity without affecting bacterial survival or growth, whereas it is believed that no or less selection pressure is posed on the bacteria. Hence, a reduced rate of newly occurring resistances, which gradually render existing antibiotics ineffective, is expected.⁶

Among bacteria, very different communication systems based on distinct autoinducers are utilized. Gram-positive bacteria primarily use modified oligopeptides, whereas *N*-acyl homoserine lactones are a major class of signal molecules in Gram-negative bacteria.¹ The opportunistic pathogen *P. aeruginosa* additionally utilizes a characteristic *pqs* system, which is based on the quinolone PQS (*Pseudomonas* Quinolone Signal) and its biosynthetic precursor HHQ (2-heptyl-4-quinolone) (Fig. 1).⁷

^aHelmholtz-Institute for Pharmaceutical Research Saarland (HIPS), Campus C23, 66123 Saarbrücken, Germany. E-mail: rolf.hartmann@helmholtz-hz1.de; Fax: +49 681 302 70308; Tel: +49 681 302 70300

^bPharmaceutical and Medicinal Chemistry, Saarland University, Campus C23, 66123 Saarbrücken, Germany

† Electronic supplementary information (ESI) available: Synthesis and analytics of all synthetic intermediates and all substrates used in the enzyme inhibition assay as well as procedure of the mutagenicity test; HHQ and PQS inhibition in the PA14 wild-type strain. See DOI: 10.1039/c4ob00707g



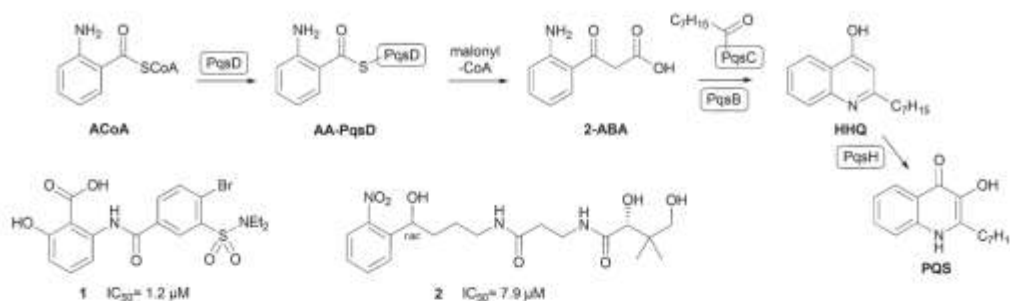


Fig. 1 Role of PqsD in HHQ and PQS biosynthesis (top). Structures of previously reported PqsD inhibitors 1 and 2.

Both are able to activate the transcriptional regulator PqsR leading to the production of various virulence factors like pyocyanin and hydrogen cyanide (HCN).⁵ We have shown, that PqsR antagonists efficiently decrease pyocyanin production and pathogenicity of *P. aeruginosa* PA14.^{5,10} Furthermore, HHQ and PQS contribute to the formation of biofilms.³

Biosynthesis of HHQ and PQS is accomplished by proteins encoded by the *pqsABCD* operon. Thereby, experiments using transposon knockout mutants identified PqsD as key enzyme in the cellular signal molecule production route.^{11,12} Recently, Dulcey *et al.* reported that cytoplasmic PqsD catalyses the condensation of anthraniloyl-CoA (ACoA) and malonyl-CoA to 2-aminobenzoylacetate (2-ABA, Fig. 1).¹³ The resulting reactive intermediate is then processed to HHQ by PqsC using octanoic acid as substrate. This second reaction step is supported by PqsB by an unknown mechanism. Interestingly, PqsD alone is also capable of generating HHQ *in vitro* directly from ACoA using β -ketodecanoic acid as secondary substrate.¹⁴ This enzymatic reaction has been routinely exploited by us to evaluate PqsD inhibitors.^{14–18} Inhibition of PqsD is an attractive strategy to interfere with QS-controlled infection mechanisms, since it is essential for cellular HHQ/PQS formation. A *pqsD* transposon mutant strain of *P. aeruginosa* PAO1, which is deficient in PQS formation, shows decreased levels of pyocyanin and HCN as well as reduced lethality in nematodes.¹¹ Furthermore, putative inhibitors of PqsA, an enzyme involved in earlier stages of HHQ biosynthesis, block the cellular production of the corresponding signal molecules, prevent systemic dissemination, and attenuate mortality in infected mice.¹⁹

Derived from compounds active against FabH, a structurally and functionally related enzyme, we have identified and optimized the first PqsD inhibitors demonstrating IC_{50} values in the single-digit micromolar range (Fig. 1, 1).^{14,15} Unfortunately, these compounds had no pronounced effect on the extracellular signal molecule levels in cell-based assays using *P. aeruginosa* PA14 (unpublished data). Recently, in a ligand-based approach we have identified compound 2 as a novel inhibitor of PqsD (Fig. 1).¹⁶ Ligand efficiency-guided optimisation led to compound 3 (Fig. 2), which was used for an initial examination of the effects on PA14 cells mediated by

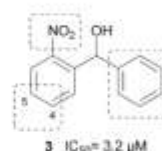


Fig. 2 Systematically varied structural features of inhibitor 3.

PqsD inhibition.¹⁶ Indeed, this compound was capable of reducing the HHQ and PQS levels. Furthermore, biofilm formation was significantly inhibited and no antibiotic effects were observed.

Binding studies of 3 revealed apparent irreversibility and that binding occurs near the active site residues.¹⁷ Both enantiomers showed similar affinity but contrary thermodynamic profiles. Based on site-directed mutagenesis, isothermal titration calorimetry (ITC) analysis, and molecular docking, explicit binding modes were proposed. In these predicted enzyme-inhibitor complexes both enantiomers reside in nearly identical positions with the main difference being the orientation of the hydroxyl group at the stereogenic center.¹⁷

Herein, we present a target-oriented (*in vitro*) structure-activity relationship and optimization of this compound class based on the (2-nitrophenyl)methanol scaffold by systematic structure variation (Fig. 2) investigating also the time-dependent onset of inhibition. Previously, we reported, that a tetrahedral geometry including an acceptor function is favoured for the linker between both phenyl rings.¹⁶ However, the intrinsic nitrophenyl moiety bears an increased risk of toxic, mutagenic and carcinogenic side effects.²⁰ Thus, we evaluated the mutagenicity in Ames *Salmonella* assays and investigated suitable chemical replacements. Additionally, the influences of substituents with opposed electronic and hydrophilic properties in 4- and 5-position of the nitrophenyl moiety were studied. Furthermore, a variety of aliphatic and aromatic residues instead of the second phenyl ring were examined.

The gathered information enabled us to design fluorescent inhibitors, which may be useful tools to investigate enzyme inhibitor interactions and to visualize the target in cells.^{21,22}



Finally, selected compounds were examined regarding their potency to inhibit signal molecule production in *P. aeruginosa* PA14 cells. Thereby, we additionally applied a novel strategy to reduce costs and time by the usage of a *pqsH*-deficient mutant which has been selected from a transposon mutant library.²³ This procedure allows to evaluate the potency of a compound solely by quantification of HHQ instead of two signal molecules. In this way we identified compounds with increased *in cellulo* activity while a low molecular weight is retained (<250 Da). These optimized fragment-like molecules provide the potential for further improvements by a fragment growing approach. Additionally, an attempt to correlate *in vitro* data with the effects observed in the cellular assays is made.

Results and discussion

Chemistry

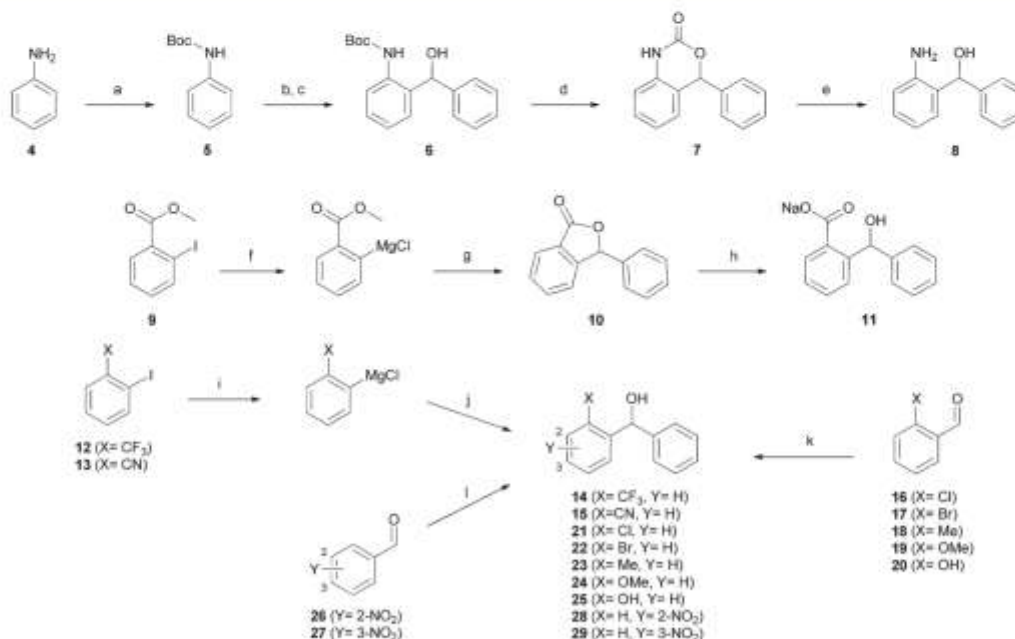
In order to find alternatives to the nitro group, a variety of molecules with different chemical functionalities were synthesized (Scheme 1). Assembly of (2-aminophenyl)(phenyl)methanol **8** started with the formation of Boc-protected aniline **5**. Ortho-lithiation by *tert*-butyllithium and subsequent reaction with benzaldehyde yielded the alcohol **6**. The desired product **8** was obtained by a two-step deprotection using

trifluoroacetic acid and basic hydrolysis. This route also provided access to the cyclic carbamate **7**.

The carboxylate **11** was prepared by iso-propylmagnesium chloride-mediated iodine-magnesium exchange on methyl 2-iodobenzoate **9** and subsequent addition to benzaldehyde. This reaction is followed by spontaneous cyclisation yielding lactone **10**, which was hydrolyzed under basic conditions to yield the desired carboxylate. An analogous method employing iodine-magnesium exchange was used for synthesis of the trifluoromethyl and nitril derivatives **14** and **15**. In the case of compounds **21–25** and **28–29**, corresponding aldehyde precursors were commercially available. Hence, the desired products were prepared by direct addition of phenylmagnesium chloride.

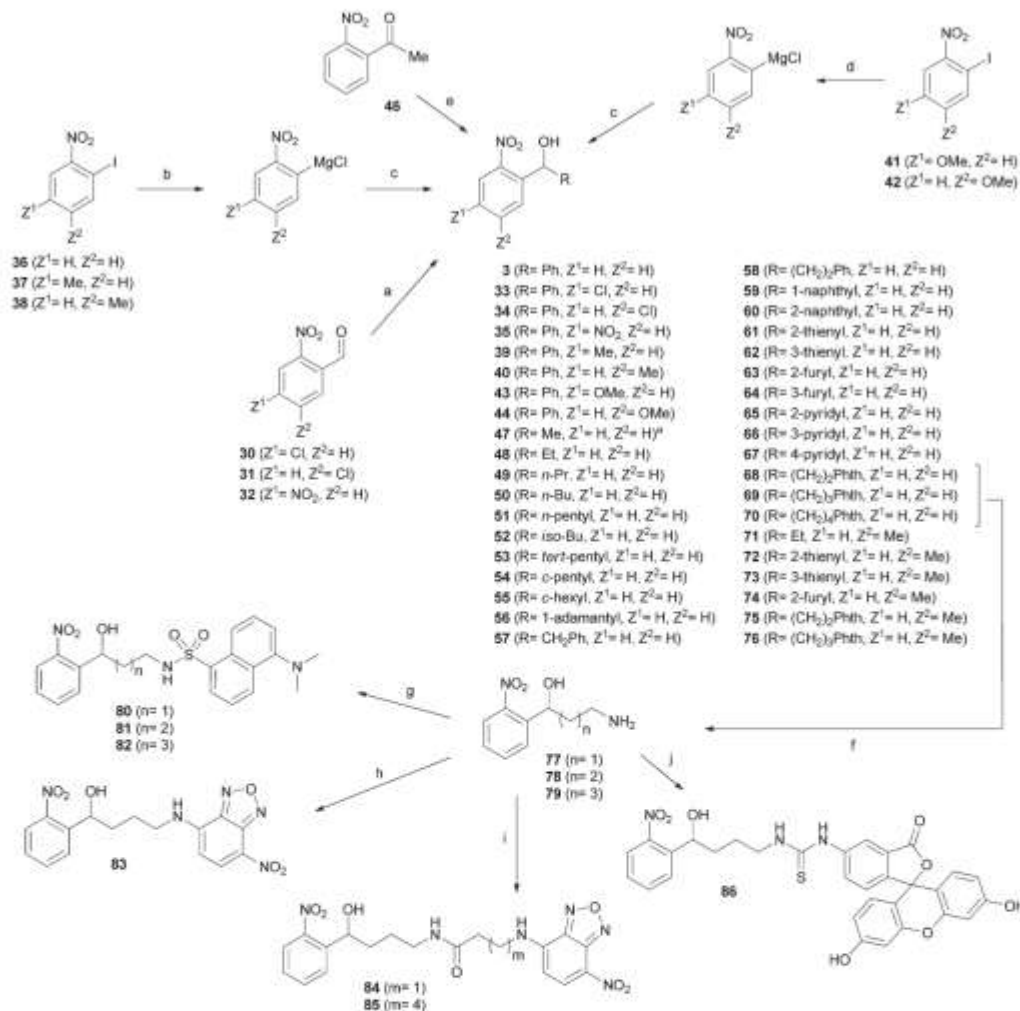
The synthesis of (2-nitrophenyl)methanol derivatives **3**, **33–35**, **39**, **40**, **43–44**, and **47–86** followed the general pathways outlined in Scheme 2. For all compounds, in which Z¹ or Z² were exclusively substituted by hydrogen or methyl, phenylmagnesium chloride was added to **36–38** to accomplish iodine-magnesium exchange in *ortho* position to NO₂ as described by Knochel and coworkers.²⁴ The generated Grignard reagents were reacted with the appropriate aldehydes to form the desired products.

For synthesis of the methoxy derivatives **43** (Z¹ = OMe) and **44** (Z² = OMe) from **41** and **42** we utilized 4-methoxyphenylmagnesium bromide as novel reagent to accomplish



Scheme 1 Synthesis of compounds **8**, **11**, **14–15**, **21–25**, and **28–29**. Reagents and conditions: (a) Boc₂O, THF, reflux, 38%; (b) *t*BuLi, THF, –60 °C; (c) benzaldehyde, THF, –20 °C, 35% (2 steps); (d) TFA, DCM, 0 °C–room temp, 78%; (e) KOH, MeOH–H₂O, reflux, 17%; (f) *i*PrMgCl, THF, –40 °C; (g) benzaldehyde, THF, –40 °C, 63% (2 steps); (h) NaOH, MeOH–H₂O, 50 °C, 39%; (i) *i*PrMgCl, THF, –40 °C; (j) benzaldehyde, THF, –40 °C, 47–71% (2 steps); (k) PhMgCl, THF, 0–50 °C, 36–92%; (l) PhMgCl, THF, –40 °C, 7–12%.





Scheme 2 Synthesis of compounds 3, 33–35, 39–40 and 43–44 and 47–86. Reagents and conditions: (a) PhMgCl, THF, $-40\text{ }^\circ\text{C}$; 20–58%; (b) PhMgCl, THF, $-40\text{ }^\circ\text{C}$; (c) aldehyde, THF, $-40\text{ }^\circ\text{C}$, 11–86% (2 steps); (d) 4-methoxyphenylmagnesium bromide, THF, $-40\text{ }^\circ\text{C}$; (e) NaBH₄, MeOH, $0\text{ }^\circ\text{C}$ –room temp, 62%; (f) hydrazine hydrate, EtOH, reflux, 62–89%; (g) NBD chloride, NaHCO₃, MeOH, room temp – $50\text{ }^\circ\text{C}$, 40%; (h) HOOC-(CH₂)_n-NBD (84), 85(i), EDC·HCl, HOBT·H₂O, NMM, acetonitrile, room temp, 32–46%; (i) dansyl chloride, TEA, DCM, room temp, 29–45%; (j) fluorescein iso-thiocyanate, DIEA, DMF, room temp, 36%.

iodine-magnesium exchange in *ortho*-iodo-nitrobenzenes. Application of this method to a broader range of substrates will be discussed elsewhere.

Fluorescent derivatives were prepared by cleavage of the phthalimide moiety of 68–70 *via* the Ing-Manske procedure. The released amines 77–79 served as a starting point for the introduction of fluorophores. Coupling these amines with dansyl chloride yielded derivatives 80–82. Direct attachment of NBD to the amine 78 using NBD-chloride afforded 83, whereas 84 and 85 were synthesized by coupling with the NBD contain-

ing carboxylic acids. The fluorescein derivative 86 was formed upon reaction with fluorescein iso-thiocyanate.

Essentiality of the nitro-group and Ames test

After synthesis, compounds were evaluated regarding their inhibitory activity against heterologously expressed and purified PqsD using ACoA and β -ketodecanoic acid as substrates.¹⁴ Until recently, β -ketodecanoic acid instead of malonyl-CoA has been considered as the second substrate in HHQ synthesis, since it has been shown, that addition of β -ketodecanoic acid

to the anthraniloyl-PqsD complex leads to HHQ formation *in vitro*.¹⁴ We have clearly shown that (2-nitrophenyl)methanol derivatives interfere with the formation of the anthraniloyl-PqsD complex itself, which allows further usage of β -ketodecanoic acid independently of its function in the bacterial cells.¹⁷

First, a variety of substituents replacing the nitro group in *ortho* position were tested. An amino group (**8**) in analogy to ACoA, which served as template for the inhibitor design,¹⁰ led to an inactive compound. This was also true for substituents with electron-withdrawing properties similar to the nitro group, as trifluoromethyl (**14**), nitril (**15**) and halogens (**21**, **22**). Furthermore, no activity was observed for molecules bearing potential hydrogen bond acceptors like **7**, **10**, the carboxylate **11**, **24** and **25**. Since the nitro group seems to be essential for activity, we shifted the position in *meta* or *para* position (**28**, **29**), but inhibitory potency was again completely abolished. An initial toxicity study provided promising results, since no toxic effect against human THP-1 macrophages was observed at 250 μ M of compound **3**.¹⁰ To assess the mutagenic risk of the compound class, Ames *Salmonella* assays were performed. Compound **3** was tested on *Salmonella typhimurium* derived strains TA100, TA1535 and TA102 with and without metabolic activation by liver homogenate (S9 mix). No biologically relevant increase in the number of revertant colonies was observed at dose levels up to 5000 μ g per plate. Thus, the nitro group was retained and we focused our efforts on the improvement of inhibitory activity by introduction of additional substituents into the nitrophenyl moiety.

In vitro SAR

Recently, we have reported extensive studies on the mode of action of the (2-nitrophenyl)methanol scaffold.¹⁷ In this regard, we demonstrated a time-dependent onset of inhibition based on a slow non-covalent (reversible) interaction. As we have observed that inhibition onset levels out after 20 min of preincubation for compound **3**,¹⁷ we consider a period of 30 min appropriate for the rapid evaluation of the set of novel compounds ($n \sim 50$) described herein. Additionally, we measured the inhibitory activity using only 10 min of preincubation to gain qualitative insight into the effect of inhibitor modifications on binding behaviour.

This examination is relevant, as it has been reported that time-dependency of enzyme-inhibitor interactions can have significant impact in the efficacy of compounds in the cellular system.²⁵

First, we re-evaluated our starting compound **3** applying an optimized protocol for the prolonged pre-treatment period of enzyme with inhibitor (Table 1). As described earlier,¹⁷ an improvement of potency was observed rendering this compound now a sub-micromolar PqsD inhibitor.

In a subsequent step, we investigated the effect of different substituents within the nitrophenyl moiety. Compounds bearing electron-withdrawing substituents (EWG) as chlorine (**33**, **34**) or nitro (**35**) showed diminished inhibitory activity (Table 1). However, concerning target affinity (IC_{50} at 30 min of preincubation) the *para* substitution pattern (Z^2 in Table 1)

seems to be more favourable. In contrast, introduction of the electron-donating (EDG) methyl (**39**, **40**) or methoxy (**43**, **44**) groups led to potent compounds with IC_{50} values in the range of the unsubstituted **3**. Again, a preference for the introduction of substituents at Z^2 was observed (**40**, **44**). These observations are in accordance with our proposed binding mode reported earlier,¹⁷ as the *para* position to the nitro group provides more space to accommodate additional substituents. An explanation for the general detrimental effect of EWGs on affinity could be that the nitro group functions as hydrogen bond acceptor (as in our proposed binding model). This ability might possibly be diminished by electron-withdrawing substituents. Unfortunately, none of the modifications installed in this part of the scaffold led to an improvement of inhibitor potency. However, comparing the determined IC_{50} for 10 min and 30 min, it seems that the Z^2 position provides the opportunity to modulate the binding behaviour. Through the choice of either methyl (EDG) or chloro (EWG) substituents, the onset (see IC_{50} at 10 min) can be either slightly accelerated (**3** vs. **40**) or slowed down (**3** vs. **34**).

In light of the results gathered so far, we kept the unsubstituted nitrophenyl moiety constant and turned our attention to the second residue R of the methanol moiety. Hydrogen or linear alkyl chains of different length were introduced (**45**, **47–51**). Thereby, shorter residues up to ethyl (**45**, **47**, and **48**) were favoured over longer variants (**49–51**). A plausible explanation is the increasing entropic penalty caused by the limitation of rotational freedom upon formation of the inhibitor-enzyme complex.

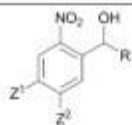
Except iso-butyl-bearing compound **52**, branched and cyclic isomers **53–56** generally inhibited PqsD less efficiently than their linear congeners. This might be due to the narrow entrance channel, which hampers the binding of the bulky residues.

Short alkyl linkers were inserted between the tetrahedral carbon and the phenyl group, but neither compound **57** nor **58** showed improved IC_{50} values compared to **3**. Thus, we concluded that direct attachment to the methanol moiety brings the aromatic residue in an optimal position and fused a second benzene ring. But the resulting 1-naphthyl and 2-naphthyl isomers **59** and **60** were less potent PqsD inhibitors.

Hence, monocyclic heteroaromatic residues were introduced. For all the thiophene and pyridine derivatives **61**, **62**, and **65–67** moderate activity without further improvement was observed. The furane derivatives showed conspicuous behaviour, since the differences in activity between the oxygen in 2- or 3-position were tremendous. While the 3-furyl derivative **64** was almost inactive, the 2-furyl isomer **63** shows improved PqsD inhibition. The synthetic route towards fluorescent (2-nitrophenyl)methanol derivatives provided additional inhibitors of PqsD with non-fluorescent residues R as intermediates. The amines **77–79** may be considered as direct derivatives of the alkyl compounds **49–51**, whereas the terminal methyl was substituted by an amino group, which is expected to be protonated under assay conditions. In contrast



Table 1 PqsD inhibition by (2-nitrophenyl)methanol derivatives



Compounds	Z ¹	Z ²	R	IC ₅₀ [μM] (10 min) ^{a,b}	IC ₅₀ [μM] (30 min) ^{c,d}
3	H	H	Ph	3.2 ± 0.1	0.5 ± 0.1
33	Cl	H	Ph	11.4 ± 1.4	11.2 ± 0.9
34	H	Cl	Ph	15.0 ± 0.6	1.6 ± 0.1
35	NO ₂	H	Ph	15.4 ± 2.0	5.8 ± 1.0
39	Me	H	Ph	3.7 ± 0.5	1.6 ± 0.1
40	H	Me	Ph	1.9 ± 0.4	0.6 ± 0.1
43	OMe	H	Ph	2.2 ± 0.5	1.6 ± 0.3
44	H	OMe	Ph	3.0 ± 0.4	0.5 ± 0.1
45	H	H	H	1.6 ± 0.5	0.7 ± 0.2
47	H	H	Me	1.3 ± 0.3	0.8 ± 0.1
48	H	H	Et	1.1 ± 0.2	0.8 ± 0.1
49	H	H	<i>n</i> -Pr	2.8 ± 0.4	1.0 ± 0.4
50	H	H	<i>n</i> -Bu	5.2 ± 0.8	2.9 ± 0.1
51	H	H	<i>n</i> -Pentyl	4.9 ± 0.9	1.0 ± 0.4
52	H	H	<i>iso</i> -Bu	7.9 ± 1.0	1.2 ± 0.3
53	H	H	<i>tert</i> -Pentyl	15.9 ± 1.1	6.7 ± 0.1
54	H	H	<i>c</i> -Pentyl	4.9 ± 1.0	1.4 ± 0.2
55	H	H	<i>c</i> -Hexyl	10.1 ± 1.4	4.5 ± 0.2
56	H	H	1-Adamantyl	11.6 ± 2.2	2.7 ± 0.1
57	H	H	CH ₃ Ph	5.4 ± 0.6	0.8 ± 0.1
58	H	H	CH ₂ CH ₂ Ph	4.6 ± 1.0	0.9 ± 0.1
59	H	H	1-Naphthyl	10.8 ± 2.5	5.8 ± 0.2
60	H	H	2-Naphthyl	13.1 ± 1.9	2.4 ± 0.5
61	H	H	2-Thienyl	14.3 ± 1.9	1.5 ± 0.2
62	H	H	3-Thienyl	5.9 ± 0.9	6.4 ± 1.9
63	H	H	2-Furyl	1.8 ± 0.4	0.9 ± 0.1
64	H	H	3-Furyl	28% @ 50 μM	13.1 ± 2.8
65	H	H	2-Pyridyl	6.7 ± 1.2	1.2 ± 0.1
66	H	H	3-Pyridyl	11.7 ± 2.1	1.7 ± 0.1
67	H	H	4-Pyridyl	6.8 ± 1.4	2.2 ± 0.1
68	H	H	(CH ₂) ₂ Phth	1.2 ± 0.1	0.3 ± 0.1
69	H	H	(CH ₂) ₃ Phth	1.9 ± 0.3	0.7 ± 0.2
70	H	H	(CH ₂) ₄ Phth	1.7 ± 0.5	1.6 ± 0.4
71	H	Me	Et	0.7 ± 0.3	0.6 ± 0.1
72	H	Me	2-Thienyl	6.2 ± 1.8	2.7 ± 0.5
73	H	Me	3-Thienyl	3.3 ± 0.5	1.6 ± 0.3
74	H	Me	2-Furyl	0.9 ± 0.1	1.1 ± 0.1
75	H	Me	(CH ₂) ₃ Phth	0.9 ± 0.1	0.7 ± 0.1
76	H	Me	(CH ₂) ₄ Phth	0.7 ± 0.1	0.7 ± 0.2
77	H	H	(CH ₂) ₂ NH ₂	34.7 ± 4.6	40.0 ± 3.7
78	H	H	(CH ₂) ₃ NH ₂	44% @ 50 μM	27.8 ± 1.7
79	H	H	(CH ₂) ₄ NH ₂	8.2 ± 2.1	22.4 ± 4.3
80 ^e				3.5 ± 0.1	5.8 ± 0.2
81 ^e				3.0 ± 1.3	4.0 ± 0.7
82 ^e				3.2 ± 0.4	1.4 ± 0.3
83 ^e				4.3 ± 0.5	3.4 ± 0.2
84 ^e				46.5 ± 2.1	12.5 ± 4.2
85 ^e				13.1 ± 1.5	10.0 ± 0.7
86 ^e				1.3 ± 0.7	1.5 ± 0.3

^a *P. aeruginosa* PqsD (recombinantly expressed in *Escherichia coli*), anthraniloyl-CoA (5 μM), and β-ketodecanoic acid (70 μM). ^b IC₅₀ values were determined using a 10 min preincubation period of inhibitor and enzyme followed by a 40 min reaction time. ^c IC₅₀ values were determined using a 30 min preincubation period of inhibitor and enzyme followed by a 40 min reaction time. ^d For the structure of the fluorescent derivatives 80–86 see Scheme 2.

to the alkyl compounds, the amines 77–79 showed low activity. This result was expected, as the entrance of the substrate tunnel is decorated with arginine side chains providing a repulsive positive surface polarization.

The phthalimides 68–70, on the other hand, also differing in the length of the alkyl linker, showed potent PqsD inhibition. Compound 68 even demonstrated the lowest IC₅₀ value within the investigated set of compounds of around 300 nM.

So far, novel interesting derivatives with retained potency and reduced molecular weight (45, 47, 48, and 63) or even improved target affinity (68) have been identified. Moreover, some compounds showed a pronounced difference between the IC_{50} values measured *via* the 10 min and 30 min protocol (34, 52, 61, and 66) indicating a slow onset of inhibition. As described above, introduction of a methyl group in *para* position to the nitro group resulted in a reduction of time-dependency while retaining activity for compound 40. These results encouraged us to synthesize additional selected derivatives possessing this methyl group (71, 72). Indeed, all of these methyl-containing compounds showed a fast onset of inhibition (Table 1) while being potent inhibitors of PqsD in the single-digit micromolar to submicromolar range. However, no further improvement in target affinity has been gained compared to the most potent compound 68. Nevertheless, together with the unmethylated congeners (48, 61–63, 68, and 69) interesting pairs of PqsD inhibitors for further evaluation *in cellulo* have been yielded.

Apparently, various substituents of R are tolerated by PqsD, which encouraged us to introduce fluorescent groups in this position. Since promising inhibitory activity was observed for compound 2, we substituted the pantothenate moiety by dansyl (5-(dimethylamino)-naphthalene-1-sulfonyl), NBD (7-nitrobenz-2-oxa-1,3-diazol-4-yl) and fluorescein fluorophores. The flexible linker of 2 was conserved to provide sufficient degrees of conformational freedom to adopt to the sterical requirements of the substrate tunnel. In the case of the dansyl derivatives 80–82, the chain length of the alkyl linker was only slightly varied with the intention to position the hydrophobic fluorophore within the channel. For the more hydrophilic NBD derivatives 83–85 additional acyl linkers were introduced as well, thereby shifting the fluorophore towards the protein surface. Fortunately, an acceptable *in vitro* activity was observed for the dansyl derivatives 80–82, and compounds with NBD (83) or fluorescein (86) directly attached to the amine 78. However, the NBD fluorophores 84 and 85 containing an additional acyl-linker were less potent. Unfavourable interactions and/or entropic penalties might be possible reasons.

Inhibition of signal molecule production in a *P. aeruginosa* *pqsH* mutant

In an attempt to elucidate the physicochemical and/or functional requirements for high *in cellulo* efficacy, we tested selected compounds regarding their ability to reduce the signal molecule levels in *P. aeruginosa* PA14 (Table 2).

In the wild-type strain, HHQ is converted into PQS by PqsH and the expression of *pqsH* depends on the growth period.²⁶ Thus, we quantified HHQ in a *pqsH* mutant, which is not able to perform this oxidation, to increase simplicity and reproducibility of this cell-based assay. To ensure the validity of this novel methodology, we compared the results gathered using the *pqsH* mutant with additionally determined PA14 wild-type data for three selected compounds and observed a good correlation between both data sets (see ESI†).

Table 2 Comparison of inhibitory potency regarding HHQ production in a *P. aeruginosa* *pqsH* mutant with physicochemical properties

Cmpd	MW ^a	Log <i>P</i> ^{b,d}	LE ^{c,e}	IC ₅₀ (10 min)/IC ₅₀ (30 min) ^f	% HHQ inhibition ^g
3	229.23	2.47	0.52	6.4	43 ± 6
33	263.68	3.16	0.39	1.2	n.i.
34	263.68	3.12	0.45	9.4	n.i.
35	274.23	2.14	0.37	2.7	10 ± 4
39	243.26	2.93	0.45	2.3	20 ± 3
40	243.26	2.93	0.48	3.2	19 ± 7
43	259.26	2.69	0.43	1.4	n.i.
44	259.26	2.55	0.46	6.0	n.i.
45	153.14	0.76	0.78	2.3	13 ± 1
47	167.16	1.11	0.71	1.6	26 ± 6
48	181.19	1.64	0.66	1.4	61 ± 2
49	195.22	2.17	0.60	2.8	22 ± 7
50	209.24	2.71	0.52	1.7	n.i.
51	223.27	3.24	0.53	4.9	n.i.
61	235.26	2.15	0.51	8.7	64 ± 6
62	235.26	2.15	0.45	0.8	74 ± 6
63	219.19	1.63	0.53	2.0	51 ± 15
64	219.19	1.63	0.43	n.d. ^h	73 ± 2
68	326.30	2.61	0.38	4.0	n.i. @ 125 μM
69	340.33	2.84	0.34	2.7	n.i. @ 125 μM
70	354.36	2.98	0.31	1.1	n.i. @ 125 μM
71	195.22	2.10	0.62	1.2	n.i.
72	249.24	2.61	0.46	2.3	24 ± 0.2
73	249.24	2.61	0.48	2.1	23 ± 7
74	233.22	2.09	0.49	0.8	20 ± 2
75	340.33	3.07	0.34	1.3	n.i. @ 125 μM
76	354.36	3.30	0.33	1.0	n.i. @ 100 μM
80	429.49	3.71	0.24	0.6	n.i. @ 75 μM
81	443.52	3.94	0.24	0.8	n.i. @ 75 μM
82	457.54	4.08	0.26	2.3	n.i. @ 25 μM
83	373.32	1.10	0.28	1.3	n.i. @ 150 μM
84	444.40	2.15	0.21	3.7	17 ± 3
85	486.48	2.65	0.20	1.3	27 ± 1
86	599.61	2.94	0.19	0.9	n.i.

^a Molecular weight (MW), calculated partition coefficient (log *P*), ligand efficiency index (LE), and the ratio of IC_{50} values measured using different preincubation periods. ^b Calculated by ACD/Labs 2012 using the ACD/Log *P* Classic algorithm. ^c Values calculated as $LE = 1.4 (-\log IC_{50})/N$ using the IC_{50} value for the prolonged incubation time (30 min) and *N* meaning number of non-hydrogen atoms. ^d Planctonic *P. aeruginosa* PA14 *pqsH* mutant, Inhibitor concentration 250 μM as not indicated otherwise. Percentage of inhibition was normalized regarding OD600. n.i. no significant inhibition (<10%). ^e n.d. means "not determined".

If soluble, all compounds were tested at 250 μM. The *in cellulo* results are summarized in Table 2 together with relevant parameters like molecular weight (MW), calculated partition coefficient (log *P*), ligand efficiency index (LE), and the ratio of IC_{50} values measured using different preincubation periods.

Inhibitor 3, which served as a starting point, decreased HHQ production by 43%. Introduction of methyl groups into the nitro-phenyl moiety (39 and 40) reduced inhibitory potency, whereas methoxy substituents (43 and 44) led to inactivity. These results are disappointing, since two of the compounds showed submicromolar *in vitro* activity. A similar result was obtained for molecules bearing a substituent in the nitrophenyl moiety: the chloro compounds 33 and 34 as well as the dinitrophenyl-derivative 35 showed no or only low



activity in the cells. Furthermore, no effects on HHQ production despite of most promising IC_{50} values were observed for the phthalimides 68–70, 75, and 76, which were tested at 100–125 μ M due to limited solubility.

All congeners of the homologous series 45–51 containing unbranched alkyl residues showed good activity in the enzymatic assay, whereas the *in vitro* activity slightly decreased for the larger alkanes. In the cellular test system, the largest residues (50 and 51) led to inactivity, while a maximum HHQ inhibition was observed for ethyl (48). This compound showed an improved cellular activity compared to the starting point 3. Interestingly, the variant with methyl in *para* position to the nitro group (71) was inactive, although it possesses a slightly improved IC_{50} value.

Surprisingly, all four compounds containing hetero-aromatic pentacycles 61–64 potently reduced the HHQ formation. These compounds were not among the most potent PqsD inhibitors *in vitro*. Moreover, 64 showed only a moderate activity in the double-digit micromolar range against recombinant PqsD. We can only speculate whether additional alternative cellular targets are involved or whether the furanyl residue is converted into a more active compound inside the cell. Multiple examples for the instability of furan are reported in the literature. However, the thiophene 62 is the most potent inhibitor of cellular HHQ formation reported so far. Again, the methyl modification in Z^2 of the nitrophenyl moiety resulting in compounds 72–74 was detrimental to *in cellulo* efficacy.

Finally, we examined the effect of fluorophore-labelled derivatives 80–86 on *P. aeruginosa* to evaluate their potential for applications in cellular systems. Unfortunately, neither the dansyl- nor fluorescein-labelled inhibitors (80–82 and 86) were able to reduce HHQ formation at 250 μ M. Consequently, their application is restricted to studies using lysed cells or isolated biomolecules. The best results were obtained for NBD derivatives 84 and 85, which showed at least slight inhibition. This opens up avenues towards intracellular labelling experiments, which might be conducted in the future.

Interpretation of *in vitro* and *in cellulo* data

A first conclusion which can be drawn from the detailed experimental data reported herein is that in the case of (2-nitrophenyl)methanol derivatives *in vitro* potency expressed either as IC_{50} or ligand efficiency (LE, Table 2) does not directly translate into *in cellulo* activity. However, this observation is not utterly surprising as Gram-negative bacteria, in general, and *P. aeruginosa*, in particular, are known to provide challenging barriers for the effective inhibition of intracellular targets.^{27–29} The orthogonal sieving ability of the two bacterial cell membranes blocking larger hydrophobic compounds (outer membrane) as well as smaller hydrophilic entities (inner membrane) from entering the cytoplasm is only one obstacle which an anti-infective agent has to overcome.^{37,38} Additionally, an arsenal of efflux pumps and degrading/metabolizing enzymes may hinder a drug from reaching its target.²⁹ Hence, the physicochemical, structural, and functional

features of compounds displaying intracellular activity are all the more worthwhile to investigate.

In this context, time-dependent inhibition was one characteristic of the presented compound class that has first drawn our attention. Reversible target interaction (inhibition) is characterized by inhibitor binding (k_{on} , “on-rate”) and dissociation (k_{off} , “off-rate”). Thus, a slow binding behaviour in combination with promising (nanomolar) IC_{50} values would imply long drug-residence times as the “off-rate” should also be attenuated along with the inhibition onset (“on-rate”). Such an effective (long-lasting) enzyme blockade can be considered a favourable scenario in order to shut down cellular signal molecule synthesis. However, we were not able to establish a correlation between this phenomenon and improved HHQ reduction. Some compounds with either high or low ratios of IC_{50} values measured using 10 min or 30 min of preincubation were effective inhibitors of signal molecule production (compare for example 3 and 61 with 62 and 70). Indeed, we showed that the methyl modification at the nitrophenyl core results in compounds with only low time-dependent onset of inhibition along with a decreased or even abolished *in cellulo* efficacy (48 vs. 71 and 61 vs. 72). Nevertheless, the most potent inhibitor in our cell assays was 62 showing almost no time-dependency of PqsD inhibition.

A parameter which seems to have direct influence on intracellular activity, though, was molecular weight. Most compounds with MW > 300 Da were inactive inside the cells. The only exceptions within the set of tested compounds were NBD-tagged fluorophores 84 and 85 showing only a moderate reduction of HHQ production. This observed mass cut-off is much lower than the general value of 600 Da reported for Gram-negative bacteria and should not be considered a strict criteria due exceptions mentioned above.³⁰ This finding might be explained by the described low permeability of outer membrane of *P. aeruginosa* compared to other Gram-negative bacteria.³¹

Another important physicochemical parameter for cellular availability is hydrophobicity usually expressed as the octanol-water partition coefficient $\log P$. None of the fragment-like compounds reported herein can be considered as strongly lipophilic as none of them exceeds $\log P \approx 4$ while the majority possesses a value below 3. However, it has been proposed by others that even lower $\log P$ values are beneficial or actually a prerequisite for activity against Gram-negative bacteria.³⁰ Indeed, our most active compound *in cellulo* possess a $\log P$ below 2.5.

Noteworthy, we have identified compounds within the set of tested (2-nitrophenyl)methanol derivatives that are interesting exceptions to the described MW/ $\log P$ criteria. Compound 71, for example, has low molecular weight (195.22 Da) and $\log P$ (0.62) combined with a substantial *in vitro* activity ($IC_{50} = 0.6$) but no relevant *in cellulo* activity. We account this finding to the general detrimental effect of the methyl group in *para* position to the nitro group which we have also found for the other compounds bearing this substitution pattern. On the other hand, developed NDB-tagged inhibitors possess



increased molecular weight and hydrophobicity, yet show moderate activity on signal molecule production. Hence, further optimization of our fragment-like molecules towards drug-like compounds *via* fragment growing approaches may be a rewarding endeavour.

Conclusions

More than fifty derivatives of (2-nitrophenyl)methanol **3** have been synthesized and tested for *in vitro* activity. In this regard, we demonstrated that 4-methoxyphenylmagnesium bromide is a suitable reagent to accomplish efficient I-Mg exchange for compound **42**. Whereas the nitro group in *ortho* position turned out to be essential for *in vitro* PqsD inhibition, no mutagenicity was observed for compound **3** in an Ames test. Improved potency was achieved by the replacement of the eastern phenyl residue. This position turned out to be very tolerant for various moieties, which allowed the design of fluorescence-labelled inhibitors.

For a straightforward evaluation of PqsD inhibitors in the cellular context, signal molecule production was investigated using a *pqsH*-deficient *P. aeruginosa* PA14 strain. Some of our compounds showed significantly improved inhibition of signal molecule production. An attempt to correlate *in vitro* data with *in cellulo* results has been made identifying low molecular weight and hydrophobicity as important, but not stringent, criteria for intracellular activity. Nevertheless, the presented work emphasizes the notion that optimization of intracellular activity is a challenging multi-parameter problem which requires further intense research.

Finally, novel PqsD inhibitors presented in this work possess a fragment-like size and improved efficiency *in cellulo*. Together with the structural insight provided by our studies regarding the mode of action, we have delivered the basis for a fragment-growing optimization process towards PqsD-targeting anti-infectives.

Experimental section

General

(2-Nitrophenyl)methanol **45** was purchased from Sigma-Aldrich and used for biological assays without further purification. Starting materials were purchased from ABCR, Acros, Sigma-Aldrich and Fluka and were used without further purification. All reactions were conducted under a nitrogen atmosphere. During workup drying was achieved by anhydrous sodium sulfate. Flash chromatography was performed using silica gel 60 (40–63 μm) and the reaction progress was determined by TLC analysis on ALUGRAM SIL G/UV254 (Macherey-Nagel). Visualization was accomplished through excitation using UV light. Purification by semi-preparative HPLC was carried out on an Agilent 1200 series HPLC system from Agilent Technologies, using an Agilent Prep-C18 column (30 \times 100 mm/10 μm) as stationary phase with acetonitrile–water as

eluent. The purity of compounds used in the biological assays was $\geq 95\%$ as measured by LC/MS, monitored at 254 nm. The methods for LC/MS analysis and a table with analytical data (including melting points) for all tested compounds are provided in the purity section of the ESI† All chiral alcohols were isolated as racemates. ^1H and ^{13}C NMR spectra were recorded on a Bruker DRX-500 instrument at 300 K. Chemical shifts are reported in δ values (ppm) and the hydrogenated residues of deuterated solvents were used as internal standard (acetone- d_6 : 2.05, 29.84. CDCl_3 : δ = 7.26, 77.16. $\text{MeOH}-d_4$: δ = 3.31, 49.00. $\text{DMSO}-d_6$: δ = 2.50, 39.52). Splitting patterns describe apparent multiplicities and are designated as s (singlet), d (doublet), dd (doublet of doublet), t (triplet), td (triplet of doublet), q (quartet), m (multiplet). All coupling constants (J) are given in hertz (Hz). Mass spectra (ESI) were measured on a Thermo Scientific Orbitrap. Mass spectra (EI) were measured on a DSQII instrument (ThermoFisher). Melting points of samples were determined in open capillaries using a SMP3 Melting Point Apparatus from Bibby Sterilin and are uncorrected. Infrared spectra were measured on a PerkinElmer Spectrum 100 FT-IR spectrometer.

General method A for synthesis of **3**, **39**, **40**, **48–76**

A solution of 2-iodo-nitrobenzene **36** or a close derivative (1.0 eq.) in THF (10 ml g^{-1} reagent) was cooled to $-40\text{ }^\circ\text{C}$ and a solution of phenylmagnesium chloride (2 M in THF, 1.1 eq.) was added dropwise. After stirring for 30 min at $-40\text{ }^\circ\text{C}$, the aldehyde (1.0 eq.) was added. Then, the reaction mixture was continuously stirred at $-40\text{ }^\circ\text{C}$ until complete conversion (checked by TLC). The reaction was quenched with a saturated solution of NH_4Cl (5 ml) and diluted with water (5 ml). The aqueous phase was extracted with ethyl acetate (three times) and the combined organic layers were washed with brine, dried, and concentrated under reduced pressure. The residue was purified by column chromatography over silica gel to give the desired product.

General method B for synthesis of **10**, **14**, and **15**

A solution of the iodobenzene **9**, **12** or **13** (1.00 g, 1.0 eq.) in 30 ml THF was cooled to $-40\text{ }^\circ\text{C}$ and a solution of iso-propylmagnesium chloride (2 M in THF, 1.1 eq.) was added dropwise. The solution was stirred for 60 min at $-40\text{ }^\circ\text{C}$, benzaldehyde (1.0 eq.) was added and the reaction was completed at $-40\text{ }^\circ\text{C}$ (checked by TLC). The workup was carried out as described in method A.

General method C for synthesis of **21–25**

To a solution of phenylmagnesium chloride (2 M in THF, 1.5 eq.) in 8 ml THF at $0\text{ }^\circ\text{C}$ aldehydes **16–20** (1 eq.) were slowly added and the solution was stirred at $50\text{ }^\circ\text{C}$ for 30 min. The mixture was cooled to $0\text{ }^\circ\text{C}$, quenched with a saturated solution of NH_4Cl (5 ml), and diluted with water (5 ml). The aqueous phase was extracted with diethyl ether (three times) and the combined organic layers were dried and concentrated under reduced pressure. The residue was purified by column chromatography over silica gel to give the desired product.



General method D for synthesis of 28 and 29

To a solution of phenylmagnesium chloride (3.31 ml, 2 M in THF, 6.62 mmol) in 20 ml THF at $-40\text{ }^{\circ}\text{C}$ nitrobenzaldehyde 26 or 27 (1.00 g, 6.62 mmol) was added slowly. The reaction mixture was stirred continuously at $-40\text{ }^{\circ}\text{C}$ until complete conversion (checked by TLC). The mixture was quenched with a saturated solution of NH_4Cl (5 ml) and diluted with water (5 ml). The workup was carried out as described in method A, followed by purification of the crude product by flash chromatography (petroleum ether–ethyl acetate 6 : 1).

General method E for synthesis of 77–79

To a solution of the phthalimides 68–70 (1.53 mmol, 1 eq.) in ethanol (40 ml) hydrazine hydrate (9.18 mmol, 6 eq.) was added and the mixture was refluxed for 3 h. Ethanol was removed *in vacuo* and ethyl acetate was added. The solution was washed with water and extracted twice with EtOAc. The organic phase was dried and the solvent was evaporated to yield the desired product in sufficient purity.

Expression and purification of recombinant PqsD

Expression and purification of recombinant PqsD was conducted as previously described.¹⁶ Briefly, BL21 (λ DE3) *E. coli* transformed with expression vector pT28b(+)/pqsD were induced with IPTG overnight. After harvesting and lysis through sonication, recombinant PqsD possessing a His₆-tag was isolated *via* immobilized metal ion affinity chromatography (IMAC) followed by gel filtration. The affinity tag was removed by thrombin cleavage and a second IMAC step.

Enzyme inhibition assay using recombinant PqsD

The standard assay for determination of IC_{50} values was performed monitoring the enzyme activity by measuring the HHQ concentration as described recently.¹⁴ PqsD was preincubated with inhibitor for 10 min or 30 min prior to addition of the substrates ACoA and β -ketodecanoic acid. Quantification of HHQ was performed analogously, but with some modifications: The flow rate was set to $750\ \mu\text{l}\ \text{min}^{-1}$ and an Accucore RP-MS column, $150 \times 2.1\ \text{mm}$, $2.6\ \mu\text{m}$, (Thermo Scientific) was used. All test compound reactions were performed in sextuplicate. Synthesis of ACoA and β -ketodecanoic acid was performed as described in the ESL†

Cultivation of *P. aeruginosa* PA14 pqsH mutant

For determination of extracellular HHQ levels, cultivation was performed in the following way: cultures of *P. aeruginosa* PA14 pqsH transposon mutant²³ (initial $\text{OD}_{600} = 0.02$) were incubated with or without inhibitor (final DMSO concentration 1%, v/v) at $37\text{ }^{\circ}\text{C}$, 200 rpm and a humidity of 75% for 16 h in 24-well Greiner Bio-One Cellstar plates (Frickenhäuser, Germany) containing 1.5 ml medium per well. Cultures were generally grown in PPGAS medium (20 mM NH_4Cl , 20 mM KCl, 120 mM Tris-HCl, 1.6 mM MgSO_4 , 0.5% (w/v) glucose, 1% (w/v) Bacto™ Tryptone). For each sample, cultivation and sample work-up were performed in triplicates.

Determination of extracellular HHQ levels

Extracellular levels of HHQ were determined according to the method of Lépine *et al.* with the following modifications.^{32,33} An aliquot of 500 μl of bacterial cultures were supplemented with 50 μl of a 10 μM methanolic solution of the internal standard (IS) 5,6,7,8-tetradeutero-2-heptyl-4(1H)-quinolone (HHQ-*d*₄) and extracted with 1 ml of ethyl acetate by vigorous shaking. After centrifugation, 400 μl of the organic phase were evaporated to dryness in LC glass vials. The residue was re-dissolved in methanol. UHPLC-MS/MS analysis was performed as described in detail recently.¹⁶ The following ions were monitored (mother ion [*m/z*], product ion [*m/z*], scan time [s], scan width [*m/z*], collision energy [V], tube lens offset [V]): HHQ: 244, 159, 0.5, 0.01, 30, 106; HHQ-*d*₄ (IS): 248, 163, 0.1, 0.01, 32, 113. Xcalibur software was used for data acquisition and quantification with the use of a calibration curve relative to the area of the IS.

Calculation of log *P* values

Experimental values of 67 and 79 were determined by Sirius T3 titrator from Sirius Analytical. Comparison with values calculated by ACD/Labs 2012 (Build 1996, 31. May 2012) revealed, that ACD/Log *P* Classic is the most appropriate algorithm. Consequently, the latter was used for the values given in Table 2.

Abbreviations

2-ABA	2-Aminobenzoylacetate
ACoA	Anthraniloyl-CoA
dansyl	5-(Dimethylamino)-naphthalene-1-sulfonyl
EDG/EWG	Electron-donating/withdrawing group
HHQ	2-Heptyl-4-quinolone
LE	Ligand efficiency
log <i>P</i>	Octanol–water partition coefficient
MW	Molecular weight
NBD	7-Nitrobenz-2-oxa-1,3-diazol-4-yl
PQS	2-Heptyl-3-hydroxy-4-quinolone
QS	Quorum sensing

Acknowledgements

We thank Carina Scheid, Simone Amann, and Christine Maurer for performing the PqsD and cellular assays. Furthermore, we thank Prof. Dr Susanne Häufler for kindly supplying the *P. aeruginosa* PA14 wild-type strain and PA14 pqsH mutant and Michael Hoffmann for performing HRMS measurements.

Notes and references

- 1 S. Swift, J. A. Downie, N. A. Whitehead, A. M. Barnard, G. P. Salmund and P. Williams, *Adv. Microb. Physiol.*, 2001, **45**, 199.

- 2 For a review see: L. C. M. Antunes, R. B. R. Ferreira, M. M. C. Buckner and B. B. Finlay, *Microbiology*, 2010, **156**, 2271.
- 3 L. Yang, M. Nilsson, M. Gjermansen, M. Givskov and T. Tolker-Nielsen, *Mol. Microbiol.*, 2009, **74**, 1380.
- 4 T. B. Rasmussen and M. Givskov, *Microbiology*, 2006, **152**, 895.
- 5 J. C. A. Janssens, S. C. J. De Keersmaecker, D. E. De Vos and J. Vanderleyden, *Curr. Med. Chem.*, 2008, **15**, 2144.
- 6 For a critical discussion see: T. Defoirdt, N. Boon and P. Bossier, *PLoS Pathog.*, 2010, **6**, e1000989.
- 7 E. C. Pesci, J. B. Milbank, J. P. Pearson, S. L. McKnight, A. Kende, E. P. Greenberg and B. Iglewski, *Proc. Natl. Acad. Sci. U. S. A.*, 1999, **96**, 11229.
- 8 J.-F. Dubern and S. P. Diggle, *Mol. BioSyst.*, 2008, **4**, 882.
- 9 C. Lu, B. Kirsch, C. Zimmer, J. C. de Jong, C. Henn, C. K. Maurer, M. Müsken, S. Häussler, A. Steinbach and R. W. Hartmann, *Chem. Biol.*, 2011, **19**, 381.
- 10 C. Lu, C. K. Maurer, B. Kirsch, A. Steinbach and R. W. Hartmann, *Angew. Chem., Int. Ed.*, 2014, **53**, 1109.
- 11 L. A. Gallagher, S. L. McKnight, M. S. Kuznetsowa, E. C. Pesci and C. Manoil, *J. Bacteriol.*, 2002, **184**, 6472.
- 12 Y.-M. Zhang, M. W. Frank, K. Zhu, A. Mayasundari and C. O. Rock, *J. Biol. Chem.*, 2008, **283**, 28788.
- 13 C. E. Dulcey, V. Dekimpe, D.-A. Fauvelle, S. Milot, M.-C. Groleau, N. Doucet, L. G. Rahme, F. Lépine and E. Déziel, *Chem. Biol.*, 2013, **20**, 1481.
- 14 D. Pistorius, A. Ullrich, S. Lucas, R. W. Hartmann, U. Kazmaier and R. Müller, *ChemBioChem*, 2011, **12**, 850.
- 15 E. Weidel, J. C. de Jong, C. Brengel, M. P. Storz, A. Braunschhausen, M. Negri, A. Plaza, A. Steinbach, R. Müller and R. W. Hartmann, *J. Med. Chem.*, 2013, **56**, 6146.
- 16 M. P. Storz, C. K. Maurer, C. Zimmer, N. Wagner, C. Brengel, J. C. de Jong, S. Lucas, M. Müsken, S. Häussler, A. Steinbach and R. W. Hartmann, *J. Am. Chem. Soc.*, 2012, **134**, 16143.
- 17 M. P. Storz, C. Brengel, E. Weidel, M. Hoffmann, K. Hollemeyer, A. Steinbach, R. Müller, M. Empting and R. W. Hartmann, *ACS Chem. Biol.*, 2013, **8**, 2794.
- 18 J. H. Sahnner, C. Brengel, M. P. Storz, M. Groh, A. Plaza, R. Müller and R. W. Hartmann, *J. Med. Chem.*, 2013, **56**, 8656.
- 19 B. Lesic, F. Lépine, E. Déziel, J. Zhang, Q. Zhang, K. Padfield, M.-H. Castonguay, S. Milot, S. Stachel, A. A. Tzika, R. G. Tompkins and L. G. Rahme, *PLoS Pathog.*, 2007, **3**, e126.
- 20 R. Padda, C. Wang, J. Hughes, R. Kutty and G. Bennett, *Environ. Toxicol. Chem.*, 2003, **22**, 2293.
- 21 S. Xu, A. N. Butkevich, R. Yamada, Y. Zhou, B. Debnath, R. Duncan, E. Zandi, N. A. Petasis and N. Neamati, *Proc. Natl. Acad. Sci. U. S. A.*, 2012, **109**, 16348.
- 22 K. A. Kozlowski, F. H. Wezeman and R. M. Schultz, *Proc. Natl. Acad. Sci. U. S. A.*, 1984, **81**, 1135.
- 23 N. T. Liberati, J. M. Urbach, S. Miyata, D. G. Lee, E. Drenkard, G. Wu, J. Villanueva, T. Wei and F. M. Ausubel, *Proc. Natl. Acad. Sci. U. S. A.*, 2006, **103**, 2833.
- 24 I. Sapountzis and P. Knochel, *Angew. Chem., Int. Ed.*, 2002, **41**, 1610.
- 25 R. A. Copeland, D. L. Pompliano and T. D. Meek, *Nat. Rev. Drug Discovery*, 2006, **5**, 730.
- 26 E. Déziel, F. Lépine, S. Milot, J. He, M. N. Mindrinos, R. Tompkins and L. G. Rahme, *Proc. Natl. Acad. Sci. U. S. A.*, 2004, **101**, 1345.
- 27 L. L. Silver, *Clin. Microbiol. Rev.*, 2011, **24**, 71.
- 28 H. Nikaido, *Antimicrob. Agents Chemother.*, 1989, **33**, 1831.
- 29 K. Poole, *J. Mol. Microbiol. Biotechnol.*, 2001, **3**, 255.
- 30 R. O'Shea and H. E. Moser, *J. Med. Chem.*, 2008, **51**, 2871.
- 31 B. L. Angus, A. M. Carey, D. A. Caron, A. M. Kropinski and R. E. Hancock, *Antimicrob. Agents Chemother.*, 1982, **21**, 299.
- 32 C. K. Maurer, A. Steinbach and R. W. Hartmann, *J. Pharm. Biomed. Anal.*, 2013, **86**, 127.
- 33 F. Lépine, F. E. Déziel, S. Milot and L. G. Rahme, *Biochim. Biophys. Acta*, 2003, **1622**, 36.



9.2 Catechol-based substrates of chalcone synthase as a scaffold for novel inhibitors of PqsD.

Publication B

Authors: Giuseppe Allegretta, Elisabeth Weidel, Martin Empting, Rolf W. Hartmann

Journal: Eur. J. Med. Chem. (2015). 90, 351 – 359.



Short communication

Catechol-based substrates of chalcone synthase as a scaffold for novel inhibitors of PqsD

Giuseppe Allegretta^a, Elisabeth Weidel^a, Martin Empting^a, Rolf W. Hartmann^{a, b, *}^a Helmholtz-Institute for Pharmaceutical Research Saarland (HIPS), Campus C2, 66123 Saarbrücken, Germany^b Pharmaceutical and Medicinal Chemistry, Saarland University, Campus C2, 66123 Saarbrücken, Germany

ARTICLE INFO

Article history:

Received 2 September 2014

Received in revised form

24 November 2014

Accepted 26 November 2014

Available online 27 November 2014

Keywords:

Pseudomonas aeruginosa

PqsD

HHQ

SPR

Quorum sensing

ABSTRACT

A new strategy for treating *Pseudomonas aeruginosa* infections could be disrupting the *Pseudomonas* Quinolone Signal (PQS) quorum sensing (QS) system. The goal is to impair communication among the cells and, hence, reduce the expression of virulence factors and the formation of biofilms. PqsD is an essential enzyme for the synthesis of PQS and shares some features with chalcone synthase (CHS2), an enzyme expressed in *Medicago sativa*. Both proteins are quite similar concerning the size of the active site, the catalytic residues and the electrostatic surface potential at the entrance of the substrate tunnel. Hence, we evaluated selected substrates of the vegetable enzyme as potential inhibitors of the bacterial protein. This similarity-guided approach led to the identification of a new class of PqsD inhibitors having a catechol structure as an essential feature for activity, a saturated linker with two or more carbons and an ester moiety bearing bulky substituents. The developed compounds showed PqsD inhibition with IC₅₀ values in the single-digit micromolar range. The binding mode of these compounds was investigated by Surface Plasmon Resonance (SPR) experiments revealing that their interaction with the protein is not influenced by the presence of the anthranilic acid bound to active site cysteine. Importantly, some compounds reduced the signal molecule production *in cellulo*.

© 2014 Published by Elsevier Masson SAS.

1. Introduction

Pseudomonas aeruginosa is an opportunistic Gram-negative bacterium, which is the etiological agent of chronic infections in immunocompromised patients [1] and in people affected by cystic fibrosis (CF) [2]. The treatment of the infections caused by this pathogen is very difficult due to its high intrinsic tolerance towards common antibiotics and the development of new resistant strains [3]. Consequently, novel therapeutic options are urgently needed for *P. aeruginosa*-related diseases. A potential approach could be targeting the quorum sensing (QS) which is a cell-to-cell communication system important for the regulation and coordination of

the lifestyles of bacterial cells using diffusible small signal molecules [4].

P. aeruginosa employs three interconnected QS systems. The *las* and *rhl* systems use homoserine lactones as signal molecules (*N*-(3-oxo-dodecanoyl)-L-homoserine lactone and *N*-(butanoyl)-L-homoserine lactone, respectively) which are commonplace among Gram-negative bacteria [5]. The *pqs* system, on the other hand, is employed only by some *Pseudomonas* and *Burkholderia* species and operates via the autoinducers PQS (*Pseudomonas* Quinolone Signal; 2-heptyl-3-hydroxy-4(1*H*)-quinolone) and its precursor HHQ (2-heptyl-4(1*H*)-quinolone) [6]. PQS and HHQ interact with the transcriptional regulator PqsR (also called MvR) controlling the production of virulence factors, such as pyocyanin, elastase and hydrogen cyanide [7], as well as the formation of biofilms [8]. Finally, activation of this receptor promotes expression of the enzymes encoded by the *pqsABCDE* operon is important for the synthesis of the HAQs themselves [9].

PqsD is encoded by this operon and is a key enzyme in the synthesis of the quinolone-based signal molecules catalyzing the conversion of anthraniloyl-CoA (ACoA) into the reactive 2-aminobenzoyl acetate (2-ABA) [10]. Subsequently, this

Abbreviations: QS, quorum sensing; SPR, surface plasmon resonance; CF, cystic fibrosis; PQS, pseudomonas quinolone signal; HHQ, 2-heptyl-4(1*H*)-quinolone; ACoA, anthraniloyl coenzyme A; CoA, Coenzyme A; DMF, dimethylformamide; THE, tetrahydrofuran; BOP, (benzotriazol-1-yl)oxytris(dimethylamino)phosphonium hexafluorophosphate; TFA, trifluoroacetic acid; HRMS, high-resolution mass spectrum; IS, internal standard.

* Corresponding author. Helmholtz-Institute for Pharmaceutical Research Saarland (HIPS), Saarland University, Campus C2, 66123 Saarbrücken, Germany.

E-mail address: rolf.hartmann@helmholtz-hzi.de (R.W. Hartmann).

<http://dx.doi.org/10.1016/j.ejmech.2014.11.055>

0223-5234/© 2014 Published by Elsevier Masson SAS.

intermediate reacts with PqsC which bears an octanoic acid residue, and, with the support of PqsB, gives the quinolone HHQ [10]. PqsD belongs to the β -ketoacyl-ACP synthase III (FabH)-type condensing enzyme family and possesses some functional and mechanistic properties of the polyketide synthase (PKS) family [11]. Another enzyme that belongs to the PKS family is the chalcone synthase (CHS2) expressed in *Medicago sativa* (alfalfa) [12]. Physiologically, this vegetable protein transforms *p*-coumaroyl-CoA into the flavanone naringenin, the central intermediate for the biosynthesis of several classes of flavonoids [12,13]. However, CHS2 accepts other substrates *in vitro*, such as cinnamic acid [14], caffeic acid [14], ferulic acid [13].

Comparing PqsD with CHS2, some matches were found. In fact, both are condensing enzymes with a similar volume of the active sites, 923 Å³ for CHS2 and 890 Å³ for PqsD [11], and use the same catalytic residues, such as cysteine, histidine, and asparagine [11–13]. Moreover, both the proteins accept malonyl-CoA as secondary substrate and the deepness of the binding pockets is comparable, 16 Å for CHS2 [12] and 15 Å for PqsD [11]. Finally, the entrances of the active sites of both enzymes are decorated with basic amino acid side chains [11,12].

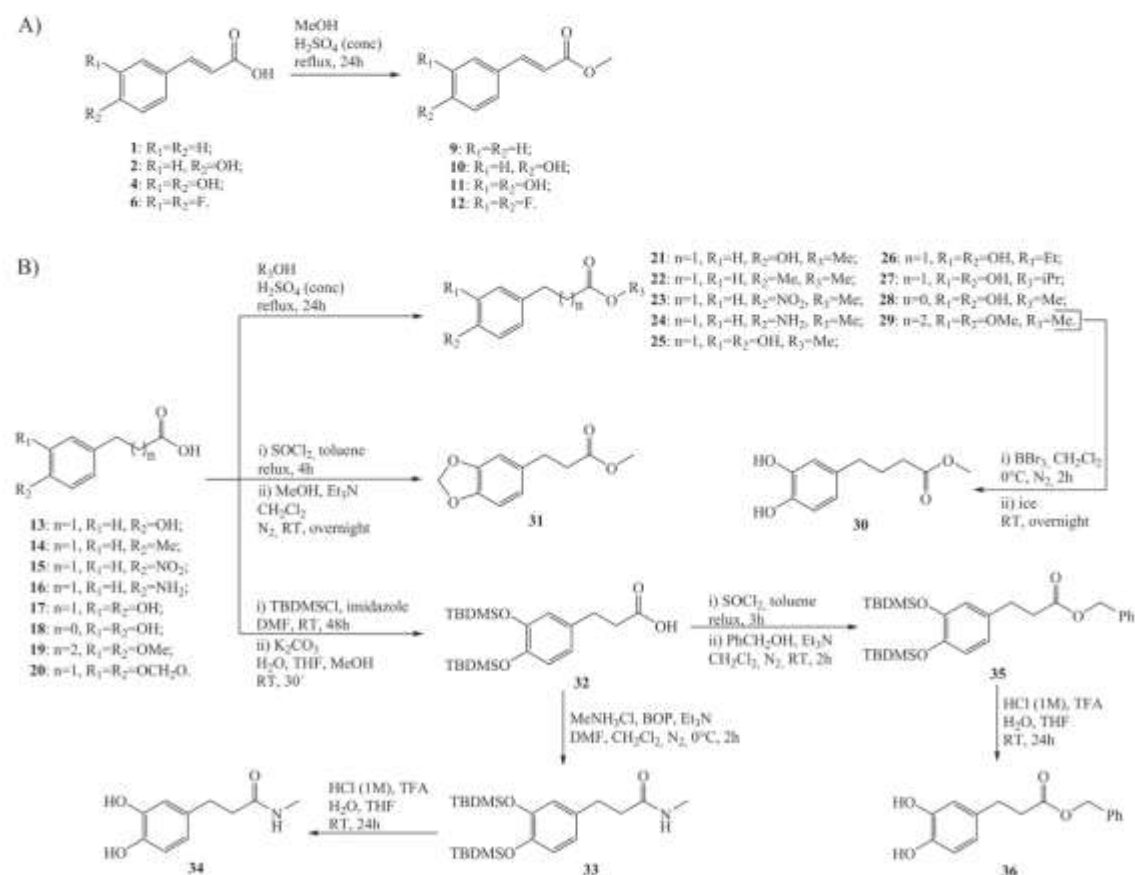
Guided by the results of our previous work showing that the inhibition of PqsD is a promising approach for reducing the

production of HHQ, PQS and biofilm [15], and the aim of this study was to identify and develop a new class of PqsD inhibitors using the molecular scaffold of described CHS2 substrates and understanding the binding mode of this series of compounds.

2. Results and discussion

2.1. Chemistry

The esters **9–12**, **21–29** of the respective carboxylic acids **1**, **2**, **4**, **6** and **13–19** were synthesized by a Fischer esterification with alcohol, as reactant and solvent, and drops of sulfuric acid 98% as catalyst (Scheme 1). **29** was demethylated by BBr₃ in dichloromethane obtaining **30**. **31** was synthesized by a two-step reaction starting with the conversion of **20** into the respective acyl chloride through thionyl chloride in toluene followed by subsequent methanolysis. The intermediate **32** was obtained by treating **17**, first, with *tert*-butyldimethylsilyl chloride (TBDMSCl) in DMF and, then, with potassium carbonate in THF/water/methanol for protecting the hydroxyl groups of the starting material. **32** was converted into the methyl amide **33** by BOP coupling and methylamine. Moreover, **32** was transformed into the benzyl ester **35** through acyl chloride intermediate formation and addition of benzyl alcohol.



Scheme 1. General synthesis of **9–12**, **21–29**, **30–31**, **34** and **36**.

Finally, the silyl ethers present in **33** and **35** were cleaved by acid hydrolysis with hydrochloric acid and TFA giving the respective final compounds **34** and **36**.

2.2. Biology

PqsD is not only able to catalyze the reaction between malonyl-CoA and ACoA producing 2-ABA, it is also capable to transform ACoA into HHQ *in vitro* using β -ketodecanoic acid [16]. The inhibitory activities of the test compounds were evaluated quantifying the amount of HHQ produced after incubation of the enzyme with the potential inhibitor as described in Experimental section.

The substrates of CHS2 and their analogues (compounds **1–5**, Fig. 1) were tested in our PqsD assay. Compounds **1**, **2**, **4** showed an inhibition over 20% at 50 μ M (see Table 1). Although activity was observed for **2** and **4**, compound **3** (the meta-isomer of **2**), however, was inactive. Consequently, the hydroxyl-group in *para* position is important for the activity while an OH in *meta* is tolerated by the enzyme. Exchange of the 3,4-dihydroxy (**4**) by the 3,4-difluoro substituents (**6**) results in a decrease of PqsD inhibition.

Compounds **7** and **8** have been reported as unnatural substrates of a homologue of CHS2 namely CHS expressed in *S. baicalensis* [17]. Evaluation in our PqsD assay revealed an inhibitory activity below 15% at 50 μ M. These results show that the phenyl ring is more favorable as a molecular core than thiophene and furane, at least within the set of tested compounds.

The methyl ester **10** showed a decreased inhibitory activity on PqsD compared to the carboxylic acid **2**. Interestingly, we observed a higher potency for the catechol-containing methyl ester **11** with an IC_{50} value of 51 μ M in comparison to the corresponding free acid **4** (26% of inhibition at 50 μ M). On the contrary, **9** and **12** did not inhibit the bacterial enzyme.

As the α,β -unsaturated system has often been found to be a toxicophor [18], we replaced the double bond of **11** by a saturated linker. The resulting compound **17** showed an IC_{50} value of 27 μ M (Scheme 1B) rendering the ethylene bridge a favorable modification of the general scaffold. Further attempts to improve activity included synthesis of derivatives with different substituents on the phenyl ring as well as the ester moiety (**21–27**, **31** and **36**). Compounds **21–24** were completely inactive at the test concentration of 50 μ M, while **31** inhibited PqsD by only 37%. Interestingly, inhibitors **25**, **26**, **27** and **36** showed promising activity in the cell-free assay with IC_{50} values of 23, 14, 8.6 and 5.9 μ M, respectively. These results highlight that the catechol is an essential structural feature for inhibitory activity while the potency increases with the size of the substituent on the ester moiety. The length of the alkylene linker was varied for investigating its influence on PqsD inhibition (**28** and **30**). The propylene bridge present in **30** was favorable for inhibitor potency compared to **25** and **28** with a shorter linker (Table 1). Methyl amide **34** was evaluated as an isostere of the

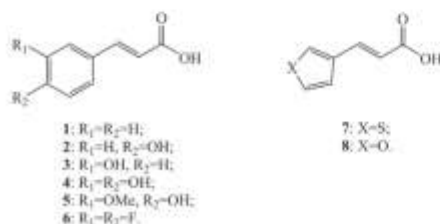


Fig. 1. Cinnamic acid analogs tested in PqsD assay. (1) Cinnamic acid; (2) p-coumaric acid; (3) m-coumaric acid; (4) caffeic acid; (5) ferulic acid; (6) 3,4-difluorocinnamic acid; (7) 3-(3-thienyl)acrylic acid; (8) 3-(3-furyl)acrylic acid.

Table 1
Biological activity of tested compounds.

Compound	R_1	R_2	n	Y	X	PqsD IC_{50} (μ M)	% HHQ inhibition in PA14 <i>pqsH</i> at 250 μ M	cLogP ^a
1	H	H	OH			33% @50 μ M	n.i.	2.13
2	H	OH	OH			30% @50 μ M	n.i.	1.63
3	OH	H	OH			n.i.	n.d.	1.63
4	OH	OH	OH			26% @50 μ M	10% @500 μ M	1.32
5	OMe	OH	OH			n.i.	n.d.	1.70
6	F	F	OH			18% @50 μ M	n.d.	2.25
7			OH			5 12% @50 μ M	n.i.	1.03
8			OH			0 12% @50 μ M	n.d.	1.33
9	H	H	OMe			n.i.	n.d.	2.49
10	H	OH	OMe			22% @50 μ M	n.i.	1.74
11	OH	OH	OMe			51 \pm 4	31 \pm 2	2.01
12	F	F	OMe			n.i.	n.i.	2.67
17	OH	OH	1 OH			27 \pm 2	n.i.	1.01
21	H	OH	1 OMe			n.i.	n.d.	1.89
22	H	Me	1 OMe			n.i.	n.d.	2.71
23	H	NO ₂	1 OMe			n.i.	n.d.	2.24
24	H	NH ₂	1 OMe			n.i.	n.d.	1.64
25	OH	OH	1 OMe			23 \pm 1	17 \pm 1	2.00
26	OH	OH	1 OEt			14 \pm 1	17 \pm 1	2.47
27	OH	OH	1 OIPr			8.6 \pm 0.6	16	2.77
28	OH	OH	0 OMe			23 \pm 1	24 \pm 3	1.31
30	OH	OH	2 OMe			7.9 \pm 0.2	18 \pm 2	2.47
31	O-CH ₂		1 OMe			37% @50 μ M	n.i.	2.33
34	OH	OH	1 NHMe			20 \pm 4	n.i.	0.76
36	OH	OH	1 OCH ₂ Ph			5.9 \pm 1.2	n.i.	3.13

n.d. = not determined.

n.i. = no significant inhibition (<10%).

^a Calculated by ACD/Labs 2012 using ACD/LogP GALAS algorithm.

corresponding ester **25**. Both compounds displayed comparable activity with IC_{50} s of 20 μ M and 23 μ M, respectively.

To date, we have identified two modes of action for reported PqsD inhibitors mainly differing in the binding site of a given compound [19–21]. The addressed inhibitors either interacted directly with the active site residues or blocked the entrance of the enzyme substrate channel. To shed light on the binding mode of the novel compound class described herein, two specifically designed SPR experiments were performed following a protocol described by Weidel E. et al. [20]. The first experiment deals with the analysis of binding between untreated PqsD and the compounds (Fig 2A, Case I). The second SPR run was performed for evaluating the interactions between the protein, preincubated with ACoA, and the inhibitors (Fig 2A, Case II). If the binding sites of the inhibitor and the anthraniloyl-PqsD adduct do not overlap similar association and dissociation curves should be observed for both SPR experiments (Fig 2B). The esters **9**, **10**, **11**, **27**, **30** and **36** were tested at 500 μ M and 250 μ M in both the assays. Considering the sensograms of the first experiment, all the α,β -unsaturated compounds **9**, **10** and **11** did not disassociate completely (Fig. 2C, Fig S1A). This may have two reasons: either these compounds possess a slow

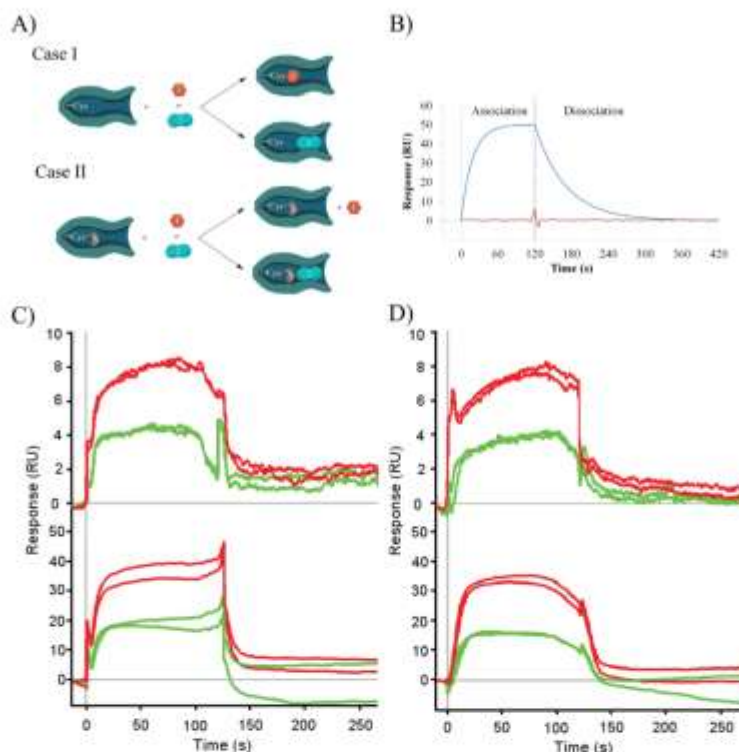


Fig. 2. Clarification of the binding mode by SPR. (A) Representative schemes of the two possible inhibition mechanisms of PqsD. 1 is a competitor of ACoA in the active site, 2 is an inhibitor that bind the channel before the active site. Case I: PqsD with the compounds. Case II: PqsD, preincubated with ACoA ("A"), with the inhibitors. (B) Theoretical SPR response curves of PqsD pretreated with ACoA drawn using the equations described by O'Shannessy et al. [22]. Blue curve: channel blocker inhibitor still binds PqsD after the treatment with ACoA. Red curve: ACoA competitor inhibitor doesn't bind at all the bacterial enzyme. Response curves of **11** and **36** at 250 μ M (green sensograms) and at 500 μ M (red sensograms) with PqsD without the treatment with ACoA (C) and after the preincubation with ACoA (D). (For interpretation of the references to colour in this figure legend, the reader is referred to the web version of this article.)

dissociation rate or they are covalent binders. On the contrary, **27**, **30** and **36** were completely released by the enzyme (Fig. 2D, Fig. S1B). The evaluation of the results of the second assay revealed that all substances except **9** were able to bind the anthraniloyl-PqsD complex and showed a binding behavior similar to the first experiment (Fig. 2, Fig. S1).

These data indicate that this compound class does not compete with ACoA upon binding to the enzyme. Thus, it is more likely that these novel PqsD inhibitors interact with the upper region of the substrate tunnel behaving like channel-blockers as also observed for previously reported compounds [20,21]. The determined response curves for compounds with the saturated linker were in accordance with the measured inhibitory potencies as **36** gave a higher response than **30** and **27**. Hence, the combination of the phenyl ring on the ester moiety with the ethylene linker fits better in the channel of PqsD increasing, consequently, the affinity of the ligand towards the bacterial protein.

Selected compounds were also tested in a cell-based assay using a PA14 *pqsH* mutant strain of *P. aeruginosa* at a final concentration of 250 μ M following a previously described protocol [15] (see Table 1). Among the tested compounds, the catechol derivatives possessing an ester moiety (**11**, **25**, **26**, **27**, **28** and **30**) were able to reduce the production of HHQ in the bacterial cultures without affecting cellular growth (Table 1). In contrast to the results of the

cell-free assay, the olefin **11** performed better than its saturated analogue **25**, while the methylene derivative **28** was slightly more potent than the longer linkers (**25** and **30**). The *in cellulo* activity is also influenced by the size of the ester moiety. While the methyl (**25**), ethyl (**26**) and isopropyl (**27**) variants showed the same reduction of signal molecule, the bulky benzyl derivative did not exhibit inhibition HHQ production. Finally, while in the PqsD assay the ester **25** and the amide **34** were equally potent, the latter compound was completely inactive in the cell-based assay. These observations together with our recently reported study regarding a different class of PqsD inhibitors [23] emphasize the challenging task to develop *in cellulo* active QSI following a target-based approach. Nevertheless, considering the intrinsic low permeability of the outer membrane of *P. aeruginosa* [24] and the high efficiency of the efflux pumps, for example the MexAB-OprM complex [25], the *in cellulo* activity of some compounds highlights that the scaffold has good properties for crossing the external barriers of Gram-negative bacteria. Further investigations are needed for increasing the *in vitro* and *in cellulo* potency.

3. Conclusions

Based on similarities between CHS2 and PqsD, the substrates of the former enzyme and their analogues were evaluated for their

activity on the bacterial signal molecule synthase. This led to the discovery of a novel class of inhibitors possessing a catechol moiety as an essential motif for activity, connected to an ester moiety through an alkylene linker with at least two carbons. A structure activity relationship was derived resulting in compounds **27**, **30** and **36** with promising inhibitory activities in the single-digit micromolar range. The binding mode of compounds possessing the saturated linker between the catechol and the ester moiety was investigated by SPR revealing that these inhibitors do not bind directly at the active site residues of PqsD, but more likely at the entrance of the substrate channel. In ongoing studies we are investigating a possible covalent mechanism of inhibition of this catechol-based class of compounds. Notably, several derivatives of this compound class were active *in cellulose* emphasizing favorable properties of the scaffold enabling the compounds to cross the Gram-negative outer membrane and to address cytoplasmic targets. Despite the inhibitory activity needs to be further optimized, the discovered scaffold has some potential for the development of novel anti-infectives for treating *P. aeruginosa* infections.

4. Experimental part

4.1. General

Starting materials were bought from Acros Organics, Sigma Aldrich and Alfa Aesar and were used without further purifications. Column chromatography was performed using silica gel 60 (63–200 μm) and the reactions were checked by TLC analysis using TLC Silica gel 60 F₂₅₄ (Merck) under UV light. Purification by semi-preparative HPLC was executed on an Agilent 1200 series HPLC system from Agilent Technologies using an Agilent C18 column (30 \times 100 mm/10 μm) as stationary phase and a gradient of water and acetonitrile as eluent. The purity of the compounds was checked by analytical HPLC using a SpectraSYSTEM (ThermoFisher) with a Macherey–Nagel C18 column (3 \times 125 mm/5 μm) installed. Mass spectra (ESI) were measured on a Finnigan Surveyor MSQ Plus (ThermoFisher). Mass spectra (EI) were measured on a DSQII instrument (ThermoFisher). All compounds were obtained with a purity $\geq 95\%$. ^1H and ^{13}C NMR spectra were recorded on a Bruker DRX-500 instrument at 300 K. Chemical shifts are reported in δ values (ppm) and the hydrogenated residues were used as internal standard (acetone- d_6 : $^1\text{H} = 2.05$, $^{13}\text{C} = 29.84$; CDCl_3 : $^1\text{H} = 7.26$, $^{13}\text{C} = 77.16$). Splitting patterns are designated as follows: s, singlet; d, doublet; dd, doublet of doublet; ddd, doublet of doublet of doublet; t, triplet; ddt, doublet of doublet of triplet; qua, quartet; qui, quintet; hep, heptet; ws, wide singlet; m, multiplet. The coupling constants (J) are given in hertz (Hz). The melting points of the compounds were determined by SMP3 Melting Point Apparatus from Bibby Sterling using capillaries with one end open. The cLogP were calculated using ACD/Percepta Platform (ACD/Percepta, 2203 – released 2012, Advanced Chemistry Development, Inc., Toronto, ON, Canada, www.acdlabs.com, 2014) via the GALAS algorithm. High-resolution mass spectra were recorded on a Dionex Ultimate 3000 RSLC system using a Waters BEH C18, 50 \times 2.1 mm, 1.7 μm dp column by injection of two μl methanolic sample. Separation was achieved by a linear gradient with (A) $\text{H}_2\text{O} + 0.1\%$ formic acid to (B) ACN + 0.1% formic acid at a flow rate of 600 $\mu\text{L}/\text{min}$ and 45 $^\circ\text{C}$. The gradient was initiated by a 0.33 min isocratic step at 5% B, followed by an increase to 95% B in 9 min to end up with a 1 min flush step at 95% B before reequilibration under the initial conditions. UV and MS detection were performed simultaneously. Coupling the HPLC to the MS was supported by an Advion Triversa Nanomate nano-ESI system attached to a Thermo Scientific Orbitrap. Mass spectra were acquired in centroid mode ranging from 100 to 1000 m/z or from 200 to 2000 m/z at a

resolution of $R = 30,000$. The theoretical exact masses refer to the protonated species.

4.2. Synthesis

4.2.1. General procedure for the synthesis of compounds **9–12** and **21–29**

After dissolving the carboxylic acid in the alcohol, three drops of H_2SO_4 95% were added to the solution and the mixture was refluxed for 24 h. The solvent was evaporated under reduced pressure and water was added to the crude mixture. The pH of the aqueous layer was adjusted to 7 adding drops of a saturated solution of NaHCO_3 and brine was added in the mixture. The aqueous layer was extracted three times with ethyl acetate; the organic layer was dried over Na_2SO_4 and the solvent was evaporated under reduced pressure yielding the final compound. Further purification step was made when it was necessary.

4.2.1.1. Methyl cinnamate (9). The carboxylic acid **1** (200 mg, 1.35 mmol) and MeOH (15 ml) were used. 155 mg (71%) of yellow crystalline solid were obtained. ^1H NMR (500 MHz, acetone- d_6): 3.75 (s, 3H), 6.55 (d, $J = 16.1$, 1H), 7.43–7.44 (m, 3H), 7.67–7.70 (m, 3H). ^{13}C NMR (125 MHz, acetone- d_6): 51.7, 118.8, 129.0, 129.8, 131.2, 135.4, 145.3, 167.5. MS (ESI) m/z : $[\text{M} + \text{MeCN} + \text{H}]^+ = 204.06$. Purity = 98.19%. Mp = 36–38 $^\circ\text{C}$. HRMS: calculated $m/z = 163.07536$, experimental $m/z = 163.07517$.

4.2.1.2. Methyl (E)-3-(4-hydroxyphenyl)acrylate (10). The carboxylic acid **2** (150 mg, 0.91 mmol) and MeOH (15 ml) were used. 162 mg (100%) of yellow crystalline solid were obtained. ^1H NMR (500 MHz, acetone- d_6): 3.72 (s, 3H), 6.34 (d, $J = 16.0$, 1H), 6.88–6.91 (m, 2H), 7.54–7.57 (m, 2H), 7.60 (d, $J = 15.6$, 1H), 8.86 (s, 1H). ^{13}C NMR (125 MHz, acetone- d_6): 51.5, 115.3, 116.7, 127.0, 130.9, 145.4, 160.6, 167.9. MS (ESI) m/z : $[\text{M} + \text{MeCN} + \text{H}]^+ = 220.02$. Purity = >99%. Mp = 129–132 $^\circ\text{C}$. HRMS: calculated $m/z = 179.07027$, experimental $m/z = 179.07029$.

4.2.1.3. Methyl (E)-3-(3,4-dihydroxyphenyl)acrylate (11). The carboxylic acid **4** (500 mg, 2.77 mmol) and MeOH (50 ml) were used. 543 mg (100%) of orange crystalline solid were obtained. ^1H NMR (500 MHz, acetone- d_6): 3.71 (s, 3H), 6.28 (d, $J = 15.8$, 1H), 6.87 (d, $J = 8.2$, 1H), 7.04 (dd, $J = 8.2$, $J = 2.5$, 1H), 7.15 (d, $J = 2.5$, 1H), 7.53 (d, $J = 15.6$, 1H), 8.17 (ws, 1H), 8.44 (ws, 1H). ^{13}C NMR (125 MHz, acetone- d_6): 51.5, 115.2, 115.4, 116.4, 122.5, 127.6, 145.7, 146.3, 148.8, 167.8. MS (ESI) m/z : $[\text{M} + \text{MeCN} + \text{H}]^+ = 235.93$. Purity = >99%. Mp = 160–162 $^\circ\text{C}$. HRMS: calculated $m/z = 195.06519$, experimental $m/z = 195.06533$.

4.2.1.4. Methyl (E)-3-(3,4-difluorophenyl)acrylate (12). The carboxylic acid **6** (250 mg, 1.36 mmol) and MeOH (25 ml) were used. 265 mg (100%) of white crystalline solid were obtained. ^1H NMR (500 MHz, acetone- d_6): 3.75 (s, 3H), 6.58 (d, $J = 15.7$, 1H), 7.37–7.43 (m, 1H), 7.54–7.57 (m, 1H), 7.64 (d, $J = 16.6$, 1H), 7.74 (ddd, $J = 11.7$, $J = 7.8$, $J = 2.2$, 1H). ^{13}C NMR (125 MHz, acetone- d_6): 51.9, 117.4 (d, $J = 18$, J_2), 118.7 (d, $J = 18$, J_2), 120.2 (d, $J = 3$, J_4), 126.5 (dd, $J = 7$, $J = 3$, J_3 , J_4), 133.2 (dd, $J = 7$, $J = 3$, J_3 , J_4), 143.0, 150.7 (dd, $J = 102$, $J = 15$, J_1 , J_2), 152.7 (dd, $J = 105$, $J = 15$, J_1 , J_2), 167.2. MS (EI) m/z : $[\text{M}]^+ = 197.9$. Purity = >99%. Mp = 78–80 $^\circ\text{C}$. HRMS: calculated $m/z = 199.05651$, experimental $m/z = 199.05641$.

4.2.1.5. Methyl 3-(4-hydroxyphenyl)propanoate (21). The carboxylic acid **13** (150 mg, 0.90 mmol) and MeOH (15 ml) were used. 100 mg (62%) of yellow crystalline solid were obtained. ^1H NMR (500 MHz, acetone- d_6): 2.55 (t, $J = 7.8$, 2H), 2.80 (t, $J = 7.8$, 2H), 3.60 (s, 3H), 6.73–6.76 (m, 2H), 7.03–7.07 (m, 2H), 8.08 (s, 1H). ^{13}C NMR

(125 MHz, acetone- d_6): 30.8, 36.6, 51.5, 116.0, 130.1, 132.4, 156.7, 173.5. MS (ESI) m/z : $[M + H_2O]^+$ = 198.02. Purity = 97.02%. Mp = 46–48 °C. HRMS: calculated m/z = 181.08592, experimental m/z = 181.08604.

4.2.1.6. Methyl 3-(*p*-tolyl)propanoate (22). The carboxylic acid **14** (100 mg, 0.61 mmol) and MeOH (10 ml) were used, 80 mg (73%) of yellow crystalline solid were obtained. 1H NMR (500 MHz, acetone- d_6): 2.27 (s, 3H), 2.58 (t, J = 8.0, 2H), 2.86 (t, J = 7.2, 2H), 3.60 (s, 3H), 7.07–7.12 (m, 4H). ^{13}C NMR (125 MHz, acetone- d_6): 21.1, 31.2, 36.3, 51.6, 129.1, 129.9, 136.3, 138.8, 173.5. MS (ESI) m/z : $[M + MeCN + H]^+$ = 220.02. Purity = 95.34%. Mp = 40–42 °C. HRMS: calculated m/z = 179.10666, experimental m/z = 179.10687.

4.2.1.7. Methyl 3-(4-nitrophenyl)propanoate (23). The carboxylic acid **15** (150 mg, 0.77 mmol) and MeOH (15 ml) were used, 142 mg (88%) of yellow crystalline solid were obtained. 1H NMR (500 MHz, acetone- d_6): 2.72 (t, J = 7.5, 2H), 3.07 (t, J = 8.2, 2H), 3.61 (s, 3H), 7.55–7.57 (m, 2H), 8.15–8.17 (m, 2H). ^{13}C NMR (125 MHz, acetone- d_6): 31.2, 35.2, 51.8, 124.3, 130.5, 147.6, 150.0, 173.0. MS (EI) m/z : $[M]^+$ = 208.9. Purity = >99%. Mp = 67–70 °C. HRMS: calculated m/z = 210.07608, experimental m/z = 210.07588.

4.2.1.8. Methyl 3-(4-aminophenyl)propanoate (24). The carboxylic acid **16** (150 mg, 0.91 mmol) and MeOH (15 ml) were used. The crude dried reaction mixture was dissolved in anhydrous THF (2 ml) and cooled with an ice-water bath. HCl 4N in dioxane (2 ml) was added dropwise to the solution until the formation of a precipitate isolated by filtration, 98 mg (74%) of a yellow crystalline solid were obtained. 1H NMR (500 MHz, acetone- d_6): 2.68 (t, J = 7.6, 2H), 2.99 (t, J = 8.0, 2H), 3.62 (s, 3H), 7.45 (s, 4H). ^{13}C NMR (125 MHz, acetone- d_6): 31.0, 35.6, 51.7, 125.4, 130.3, 135.0, 143.8, 173.2. MS (ESI) m/z : $[M+H]^+$ = 180.12. Purity = >99%. Mp = 178–180 °C. HRMS: calculated m/z = 180.10191, experimental m/z = 180.10197.

4.2.1.9. Methyl 3-(3,4-dihydroxyphenyl)propanoate (25). The carboxylic acid **17** (500 mg, 2.74 mmol) and MeOH (50 ml) were used, 433 mg (80%) of yellow crystalline solid were obtained. 1H NMR (500 MHz, acetone- d_6): 2.53 (t, J = 7.9, 2H), 2.76 (t, J = 8.0, 2H), 3.60 (s, 3H), 6.54 (dd, J = 8.0, J = 2.0, 1H), 6.70–6.73 (m, 2H), 7.60 (ws, 1H), 7.65 (ws, 1H). ^{13}C NMR (125 MHz, acetone- d_6): 31.0, 36.5, 51.5, 116.0, 116.2, 120.3, 133.4, 144.2, 145.8, 173.5. MS (ESI) m/z : $[M + H_2O]^+$ = 213.95. Purity = >99%. Mp = 77–79 °C. HRMS: calculated m/z = 197.08084, experimental m/z = 197.08106.

4.2.1.10. Ethyl 3-(3,4-dihydroxyphenyl)propanoate (26). The carboxylic acid **17** (150 mg, 0.82 mmol) and EtOH (15 ml) were used, 145 mg (84%) of yellow oil were obtained. 1H NMR (500 MHz, acetone- d_6): 1.18 (t, J = 6.9, 3H), 2.52 (t, J = 7.4, 2H), 2.75 (t, J = 7.9, 2H), 4.06 (qua, J = 7.3, 2H), 6.55 (dd, J = 7.9, J = 2.0, 1H), 6.71 (m, 2H), 7.63 (s, 1H), 7.68 (s, 1H). ^{13}C NMR (125 MHz, acetone- d_6): 14.5, 31.0, 36.8, 60.5, 116.0, 116.3, 120.4, 133.4, 144.2, 145.8, 173.0. MS (ESI) m/z : $[M+H]^+$ = 210.88. Purity = 95.11%. HRMS: calculated m/z = 211.09649, experimental m/z = 211.09626.

4.2.1.11. Isopropyl 3-(3,4-dihydroxyphenyl)propanoate (27). The carboxylic acid **17** (250 mg, 1.37 mmol) and *i*PrOH (25 ml) were used, 270 mg (88%) of yellow oil were obtained. 1H NMR (500 MHz, acetone- d_6): 1.17 (d, J = 6.2, 6H), 2.49 (t, J = 7.3, 2H), 2.75 (t, J = 7.9, 2H), 4.93 (hep, J = 6.3, 1H), 6.55 (dd, J = 7.9, J = 2.2, 1H), 6.71–6.73 (m, 2H), 7.64 (ws, 1H). ^{13}C NMR (125 MHz, acetone- d_6): 22.0, 31.1, 37.1, 67.8, 116.0, 116.3, 120.4, 133.4, 144.2, 145.7, 172.6. MS (ESI) m/z : $[M+H]^+$ = 225.10. Purity = >99%. HRMS: calculated m/z = 225.11214, experimental m/z = 225.11201.

4.2.1.12. Methyl 2-(3,4-dihydroxyphenyl)acetate (28). The carboxylic acid **18** (100 mg, 0.59 mmol) and MeOH (10 ml) were used, 60 mg (56%) of yellow crystalline solid were obtained. 1H NMR (500 MHz, acetone- d_6): 3.46 (s, 2H), 3.61 (s, 3H), 6.60 (dd, J = 8.0, J = 2.4, 1H), 6.75 (d, J = 8.2, 1H), 6.78 (d, J = 2.5, 1H), 7.78 (s, 2H). ^{13}C NMR (125 MHz, acetone- d_6): 40.7, 51.9, 116.0, 117.2, 121.5, 127.0, 144.9, 145.8, 172.6. MS (ESI) m/z : $[M + H_2O]^+$ = 199.88. Purity = >99%. Mp = 52–55 °C. HRMS: calculated m/z = 183.06519, experimental m/z = 183.06534.

4.2.1.13. Methyl 4-(3,4-dimethoxyphenyl)butanoate (29). The carboxylic acid **19** (1.00 g, 4.46 mmol) and MeOH (100 ml) were used, 900 mg (85%) of yellow crystalline solid were obtained. 1H NMR (500 MHz, acetone- d_6): 1.88 (qui, J = 7.2, 2H), 2.30 (t, J = 7.2, 2H), 2.57 (t, J = 7.6, 2H), 3.61 (s, 3H), 3.76 (s, 3H), 3.79 (s, 3H), 6.71 (dd, J = 8.3, J = 2.4, 1H), 6.82 (d, J = 2.1, 1H), 6.84 (d, J = 8.0, 1H). ^{13}C NMR (125 MHz, acetone- d_6): 27.6, 33.7, 35.3, 51.5, 56.1, 56.2, 113.0, 113.5, 121.2, 135.2, 148.8, 150.4, 174.0. MS (ESI) m/z : $[M+H]^+$ = 238.97. Purity = >99%. Mp = 32–34 °C. Intermediate **29** was used as is for the synthesis of **30**.

4.2.2. Synthesis of compound 30

4.2.2.1. Methyl 4-(3,4-dihydroxyphenyl)butanoate (30). After dissolving **29** (400 mg, 1.68 mmol) in CH_2Cl_2 (20 ml), the solution was cooled with an ice-water bath. BBr_3 1.0 N in CH_2Cl_2 (10 ml, 10 mmol) was added dropwise and the reaction mixture was stirred for 2 h at 0 °C under N_2 atmosphere. Ice was added to the mixture and the system was stirred overnight warming up to room temperature. Brine was added to the mixture and, then, it was extracted three times with CH_2Cl_2 ; the organic layers were collected, dried over Na_2SO_4 and the solvent was evaporated under reduced pressure. The crude extract was purified by column chromatography (hexane/ethyl acetate 8:2) yielding 258 mg (73%) of **30** as a yellow oil. 1H NMR (500 MHz, acetone- d_6): 1.83 (qui, J = 7.2, 2H), 2.28 (t, J = 7.5, 2H), 2.49 (t, J = 7.8, 2H), 3.61 (s, 3H), 6.52 (dd, J = 8.0, J = 2.3, 1H), 6.68 (d, J = 2.1, 1H), 6.72 (d, J = 8.0, 1H), 7.62 (ws, 2H). ^{13}C NMR (125 MHz, acetone- d_6): 27.7, 33.6, 35.0, 51.5, 116.0, 116.3, 120.5, 134.2, 144.0, 145.8, 174.0. MS (ESI) m/z : $[M-OMe]^+$ = 179.09. Purity = 98.10%. HRMS: calculated m/z = 211.09649, experimental m/z = 211.09649.

4.2.3. Synthesis of compound 32

4.2.3.1. 3-(3,4-Bis(tert-butyl dimethylsilyloxy)phenyl)propanoic acid (32). After dissolving **17** (1.00 g, 5.48 mmol) in DMF (11 ml), imidazole (3.73 g, 54.80 mmol) and TBDMSCl (3.72 g, 24.66 mmol) were added and the reaction mixture was stirred for 48 h at room temperature. Saturated solution of NH_4Cl (40 ml) was added to the reaction and the mixture was extracted three times with ethyl acetate. The organic layers were collected together, washed with brine, dried over Na_2SO_4 and the solvent was evaporated under reduced pressure. The crude extract was dissolved in a mixture of THF/MeOH/ H_2O 1:3:1 (25 ml), K_2CO_3 (757 mg, 5.48 mmol) was added in the solution and the system was stirred for 30 min at room temperature. The mixture was concentrated under vacuum at room temperature. Water was added to the crude mixture and drops of HCl 1 N were added until the pH = 7. The aqueous solution was diluted with brine and extracted three times with ethyl acetate. The organic layers were collected together, dried over Na_2SO_4 and the solvent was evaporated under reduced pressure. The crude extract was purified by column chromatography (hexane/ethyl acetate 9:1) yielding 2.14 g (95%) of **32** as a white crystalline solid. 1H NMR (500 MHz, acetone- d_6): 0.21 (s, 6H), 0.22 (s, 6H), 0.99–1.01 (m, 18H), 2.56 (t, J = 7.8, 2H), 2.80 (t, J = 7.7, 2H), 6.72 (dd, J = 8.1, J = 2.3, 1H), 6.79 (d, J = 8.1, 1H), 6.81 (d, J = 2.1, 1H), 10.53 (ws, 1H). ^{13}C NMR (125 MHz, acetone- d_6): -3.86, -3.81, 19.02, 19.04, 26.35, 26.37,

30.8, 36.1, 121.8, 122.1, 122.2, 135.5, 145.8, 147.3, 173.9. MS (ESI) m/z : $[M+H]^+$ = 410.84. Purity = >99%, Mp = 92–93 °C. Intermediate **32** was used as is for the synthesis of **33** and **35**.

4.2.4. General synthesis of compounds **31** and **35**

After dissolving the carboxylic acid in toluene (10 ml), SOCl₂ (1 ml) was added and the reaction mixture was refluxed. The toluene was removed under vacuum and the crude mixture was dissolved in CH₂Cl₂ under N₂ atmosphere. The alcohol and Et₃N were added together to the solution and the reaction mixture was stirred at room temperature for some hours. Brine was added to the mixture and, then, it was extracted three times with CH₂Cl₂; the organic layers were collected, dried over Na₂SO₄ and the solvent was evaporated under reduced pressure.

4.2.4.1. Methyl 3-(benzo[d][1,3]dioxol-5-yl)propanoate (**31**)

The carboxylic acid **20** (100 mg, 0.51 mmol) was used and the mixture was refluxed for 4 h; MeOH (1 ml) and Et₃N (1.5 ml) were added in the second step and the mixture was stirred overnight. The crude extract was purified by column chromatography (hexane/ethyl acetate 8:2) yielding 21 mg (20%) of **31** as a colorless oil. ¹H NMR (500 MHz, acetone-*d*₆): 2.57 (t, *J* = 7.4, 2H), 2.83 (t, *J* = 7.4, 2H), 3.61 (s, 3H), 5.94 (s, 2H), 6.69 (ddd, *J* = 7.9, *J* = 1.7, *J* = 1.0, 1H), 6.73 (d, *J* = 7.8, 1H), 6.77 (d, *J* = 1.7, 1H). ¹³C NMR (125 MHz, acetone-*d*₆): 31.3, 36.4, 51.6, 101.8, 108.9, 109.6, 122.0, 135.6, 146.9, 149.6, 173.4. MS (ESI) m/z : $[M + MeCN + H]^+$ = 249.86. Purity = 96.14%. HRMS: calculated m/z = 209.08084, experimental m/z = 209.08058.

4.2.4.2. Benzyl 3-(3,4-bis((tert-butyl)dimethylsilyloxy)phenyl)propanoate (**35**)

The carboxylic acid **32** (410 mg, 1.0 mmol) was used and the mixture was refluxed for 3 h; benzyl alcohol (104 μl, 1.0 mmol) and Et₃N (140 μl, 1.0 mmol) were added in the second step and the mixture was stirred for 2 h. The crude extract was purified by column chromatography (hexane/ethyl acetate 9:1) yielding 408 mg (81%) of **35** as an orange oil. ¹H NMR (500 MHz, acetone-*d*₆): 0.20–0.22 (m, 12H), 0.99–1.01 (m, 18H), 2.64 (t, *J* = 7.7, 2H), 2.84 (t, *J* = 7.5, 2H), 5.10 (s, 2H), 6.70 (dd, *J* = 8.2, *J* = 2.0, 1H), 6.78 (d, *J* = 8.2, 1H), 6.80 (d, *J* = 2.6, 1H), 7.33–7.36 (m, 5H). ¹³C NMR (125 MHz, acetone-*d*₆): -3.85, -3.80, 19.0, 26.35, 26.37, 30.8, 36.5, 66.4, 121.8, 122.1, 122.3, 128.78, 128.83, 129.3, 135.1, 137.5, 145.9, 147.4, 172.9. MS (ESI) m/z : $[M+H]^+$ = 501.07. Purity = >99%. Intermediate **35** was used as is for the synthesis of **36**.

4.2.5. Synthesis of compound **33**

4.2.5.1. 3-(3,4-Bis((tert-butyl)dimethylsilyloxy)phenyl)-*N*-methylpropanamide (**33**). After dissolving **32** (200 mg, 0.49 mmol) and Et₃N (165 μl, 1.18 mmol) in DMF (5 ml), the solution was cooled with an ice-water bath. NH₄Cl (40 mg, 0.59 mmol) was added to the mixture; BOP (217 mg, 0.49 mmol) was dissolved in CH₂Cl₂ (5 ml) and, then, added to the reaction mixture. The solution was stirred for 2 h at 0 °C under N₂ atmosphere. HCl 1 N (15 ml) was added to the reaction and the mixture was extracted three times with ethyl acetate. The organic layers were collected together, washed in sequence with a saturated solution of NaHCO₃ and brine, dried over Na₂SO₄ and the solvent was evaporated under reduced pressure. The crude extract was purified by column chromatography (hexane/ethyl acetate 1:1) yielding 121 mg (58%) of **33** as a white crystalline solid. ¹H NMR (500 MHz, acetone-*d*₆): 0.20 (s, 6H), 0.21 (s, 6H), 0.99–1.01 (m, 18H), 2.37 (t, *J* = 7.6, 2H), 2.66 (d, *J* = 4.7, 3H), 2.78 (t, *J* = 7.9, 2H), 6.67 (dd, *J* = 8.2, *J* = 2.1, 1H), 6.76–6.78 (m, 2H), 6.88 (ws, 1H). ¹³C NMR (125 MHz, acetone-*d*₆): -3.85, -3.80, 19.0, 26.0, 26.36, 26.38, 31.5, 38.6, 121.7, 122.1, 122.2, 136.1, 145.6, 147.3, 172.5. MS (ESI) m/z : $[M+H]^+$ = 423.85. Purity = 98.26%. Mp = 98–100 °C. Intermediate **33** was used as is for the synthesis of **34**.

4.2.6. Synthesis of compounds **34** and **36**

After dissolving the silyl ether compound in THF (4 ml), the solution was cooled with an ice-water bath. HCl 1 N (1 ml) and TFA (0.5 ml) were added to the solution and the mixture was stirred at room temperature for 24 h. Drops of saturated solution of NaHCO₃ were added to the mixture until the pH was adjusted to 7; brine was added to the mixture which was extracted three times with ethyl acetate. The organic layers were collected together, dried over Na₂SO₄ and the solvent was evaporated under reduced pressure.

4.2.6.1. 3-(3,4-Dihydroxyphenyl)-*N*-methylpropanamide (**34**)

The silyl ether **33** (100 mg, 0.24 mmol) was used. The crude extract was purified by column chromatography (pure ethyl acetate) yielding 36 mg (77%) of **34** as a colorless oil. ¹H NMR (500 MHz, acetone-*d*₆): 2.33–2.36 (m, 2H), 2.66 (d, *J* = 4.8, 3H), 2.72–2.75 (m, 2H), 6.52 (dd, *J* = 7.9, *J* = 2.2, 1H), 6.68–6.70 (m, 2H), 6.88 (ws, 1H), 7.65 (ws, 2H). ¹³C NMR (125 MHz, acetone-*d*₆): 26.0, 31.8, 38.9, 115.9, 116.2, 120.3, 134.2, 144.1, 145.7, 172.8. MS (ESI) m/z : $[M+H]^+$ = 196.05. Purity = 96.03%. HRMS: calculated m/z = 196.09682, experimental m/z = 196.09659.

4.2.6.2. Benzyl 3-(3,4-dihydroxyphenyl)propanoate (**36**)

The silyl ether **35** (200 mg, 0.40 mmol) was used. The crude extract was purified by semi-preparative HPLC (mobile phase: water, acetonitrile; flow rate: 5 ml/min; gradient: 0–35 min, linear gradient 30%–70% acetonitrile) yielding 24 mg (22%) of **36** as a yellow crystalline solid. ¹H NMR (500 MHz, acetone-*d*₆): 2.61 (t, *J* = 7.2, 2H), 2.79 (t, *J* = 7.9, 2H), 5.10 (s, 2H), 6.55 (dd, *J* = 8.2, *J* = 2.2, 1H), 6.70–6.72 (m, 2H), 7.29–7.37 (m, 5H), 7.64 (s, 1H), 7.68 (s, 1H). ¹³C NMR (125 MHz, acetone-*d*₆): 31.0, 36.7, 66.3, 116.1, 116.3, 120.4, 128.7, 128.8, 129.3, 133.3, 137.6, 144.3, 145.8, 173.0. MS (ESI) m/z : $[M+H]^+$ = 272.84. Purity = 95.34%. Mp = 50–53 °C. HRMS: calculated m/z = 273.11214, experimental m/z = 273.11207.

4.3. Biology

4.3.1. Expression and purification of recombinant PqsD

The procedure for expressing and purifying recombinant PqsD was conducted as recently described by us [15]. BL21 (λDE3) *E. coli* were transformed with the plasmid encoding PqsD (pT28b(+)/pqsD) and the expression of the protein was induced with IPTG overnight. After collecting the cells and lysis through sonication, the recombinant His₆-tag PqsD was separated from the lysate via immobilized metal ion affinity chromatography (IMAC) followed by gel filtration. In the SPR experiments, His₆-PqsD was used without cleaving the tag as previously reported [20]; in the enzyme inhibition assay, protein without the histidine-tag was employed. The His₆-tag was cleaved treating the His₆-tag PqsD with thrombin and a second IMAC was run obtaining the purified protein.

4.3.2. Enzyme inhibition assay using recombinant PqsD

The IC₅₀ values were determined checking the enzyme activity by measuring the HHQ concentration as described in our previous work [16]. PqsD was incubated with the compound for 10 min before the addition of the substrates ACoA and β-ketodecanoic acid. The in-house PqsD inhibitor 4-(3-(*N,N*-diethylsulfamoyl)benzamido)-[1,1'-biphenyl]-3,4'-dicarboxylic acid (IC₅₀ = 2.7 μM) published by Weidel et al. [20] was used as positive control. All compounds were tested in sextuplicates.

4.3.3. Surface plasmon resonance

SPR experiments were carried out using a Reichert SR7500DC instrument optical biosensor (Reichert Technologies, Buffalo, NY, USA) and CMD500 M sensor chips obtained by XanTec (XanTec Bioanalytics, Düsseldorf, Germany). Processing and analysis of the

data were performed using Scrubber software. Changes in refractive index due to DMSO-dependent solvent effects were corrected by use of a calibration curve (seven solutions, 4.25%–5.75% DMSO in buffer solutions).

The immobilization of His-tagged protein was performed following the procedure developed by Henn et al. [26] at 18 °C using standard amine coupling chemistry. His-PqsD (38.4 kDa, >90% pure based on SDS PAGE) was immobilized at densities of 5521 μ RIU for the binding affinity assay and 5959 μ RIU for the binding studies with ACoA.

The binding assays were carried out using the protocol set up by Weidel et al. [20] with some modifications. At a constant flow rate of 30 μ l/min using instrument running buffer (10 mM Hepes, pH 7.4, 150 mM NaCl, 5% DMSO (v/v), 0.05% P-20 (v/v)), **9**–**11**, **27**, **30** and **36** were tested at two concentrations, 500 μ M and 250 μ M. The compounds were injected consecutively employing 120 s of association and 300 s of dissociation. Experiments were performed twice. In the second experiment, ACoA (100 μ M) was injected for 40 min with a constant flow of 5 μ l/min to saturate the ACoA binding site. Afterwards, the flow rate was increased to 50 μ l/min and kept stable for 30 min in order to flush all unreacted reagents and residue CoA away until reaching the stability of the baseline signal. The flow was decreased to 30 μ l/min and additional ACoA (10 μ M) was injected for 120 s association and 300 s dissociation to investigate if the binding site is fully blocked (no signal was observed). Then, the compounds (tested at 500 μ M and 250 μ M) were injected again for 120 s of association and 300 s of dissociation. The obtained binding signals in the equilibrium were compared to those obtained without ACoA pretreatment. Experiments were performed twice.

4.3.4. Cultivation of *P. aeruginosa* PA14 pqsH⁻ mutant

The cultivation of bacterial cells for the measurement of extracellular HHQ levels was set up following the protocol developed by Lépine et al. [27]: cultures of *P. aeruginosa* PA14 pqsH⁻ transposon mutant (initial OD₆₀₀ = 0.02) were incubated with or without compound (final DMSO concentration 1%, v/v) at 37 °C, 200 rpm and a humidity of 75% for 16 h in 24-well Greiner Bio-One Cellstar plates (Frickenhausen, Germany) filled in 1.5 ml medium per well. Cultures were generally grown in PPGAS medium (20 mM NH₄Cl, 20 mM KCl, 120 mM Tris–HCl, 1.6 mM MgSO₄, 0.5% (w/v) glucose, 1% (w/v) Bacto™ Tryptone). For each sample, cultivation and sample work-up were performed in triplicates.

4.3.5. Determination of extracellular HHQ

Extracellular levels of HHQ were measured following the procedure of Lépine et al. with the modifications described subsequently [27]. 50 μ l of a 10 μ M methanolic solution of the internal standard (IS) 5,6,7,8-tetradeuterio-2-heptyl-4(1H)-quinolone (HHQ-d₄) were added in an aliquot of 500 μ l of bacterial culture and, then, extracted with ethyl acetate (1 ml) by vortexing. After centrifugation, 400 μ l of the organic layer were evaporated in LC glass vials. The crude extract was dissolved in methanol. UHPLC-MS/MS analysis was set up as described in our previous work [15]. The following ions were monitored (mother ion [m/z], product ion [m/z], scan time [s], scan width [m/z], collision energy [V], tube lens offset [V]): HHQ: 244, 159, 0.5, 0.01, 30, 106; HHQ-d₄ (IS): 248, 163, 0.1, 0.01, 32, 113. The data was acquired using Xcalibur software and quantified through a calibration curve relative to the area of the IS. The in-house PqsR antagonist 2-heptyl-6-nitro-4-oxo-1,4-dihydroquinoline-3-carboxamide published by Lu et al. [28] was used as positive control of the assay and it was tested at 15 μ M resulting in 54% of reduction.

Acknowledgment

The authors are grateful to Christine Maurer, Benjamin Kirsch, Carina Scheid and Simone Amann for performing PqsD and *in celulo* assays, to Michael Hoffmann for recording the HR mass spectra and Prof. Dr. Susanne Häußler for kindly supplying the PA14 pqsH⁻ mutant strain. This project was funded by BMBF through grant 1616038B.

Appendix A. Supplementary data

Supplementary data related to this article can be found at <http://dx.doi.org/10.1016/j.ejmech.2014.11.055>.

References

- [1] D.S. Blanc, C. Petignat, B. Janin, J. Bille, P. Francioli, Frequency and molecular diversity of *Pseudomonas aeruginosa* upon admission and during hospitalization: a prospective epidemiologic study, *Clin. Microbiol. Infect.* 4 (1998) 242–247.
- [2] M. Gomez, A. Prince, Opportunistic infections in lung disease: *Pseudomonas* infections in cystic fibrosis, *Curr. Opin. Pharmacol.* 7 (2007) 244–251.
- [3] R.E.W. Hancock, D.P. Speert, Antibiotic resistance in *Pseudomonas aeruginosa*: mechanisms and impact on treatment, *Drug Resist. Updat.* 3 (2000) 247–255.
- [4] S. Swift, J.A. Downie, N.A. Whitehead, A.M. Barnard, G.P. Salmond, P. Williams, Quorum sensing as a population-density-dependent determinant of bacterial physiology, *Adv. Microb. Physiol.* 45 (2001) 199–270.
- [5] R.S. Smith, B.H. Iglewski, *P. aeruginosa* quorum-sensing systems and virulence, *Curr. Opin. Pharmacol.* 6 (2003) 56–60.
- [6] J.F. Dubert, S.P. Diggle, Quorum sensing by 2-alkyl-4quinolones in *Pseudomonas aeruginosa* and other bacterial species, *Mol. Biophys.* 4 (2008) 882–888.
- [7] E. Déziel, S. Gopalani, A.P. Tampakaki, F. Lépine, K.E. Padfield, M. Saucier, G. Xiao, L.C. Rahme, The contribution of MvR to *Pseudomonas aeruginosa* pathogenesis and quorum sensing circuitry regulation: multiple quorum sensing-regulated genes are modulated without affecting *lasR*, *rhlR* or the production of N-acyl-L-homoserine lactones, *Mol. Microbiol.* 55 (2005) 998–1014.
- [8] S.P. Diggle, K. Winzer, S.R. Chhabra, K.E. Worrall, M. Cámara, P. Williams, The *Pseudomonas aeruginosa* quinolone signal molecule overcomes the cell density-dependency of the quorum sensing hierarchy, regulates *rhl*-dependent genes at the onset of stationary phase and can be produced in the absence of *LasR*, *Mol. Microbiol.* 50 (2003) 29–43.
- [9] L.A. Gallagher, S.L. McKnight, M.S. Kuznetsova, E.C. Pesci, C. Manoil, Function required for extracellular quinolone signaling by *Pseudomonas aeruginosa*, *J. Bacteriol.* 184 (2002) 6472–6480.
- [10] C.L. Duley, V. Dekimpe, D.-A. Favuelle, S. Milot, M.-C. Groleau, N. Doucet, L.G. Rahme, F. Lépine, E. Déziel, The end of an old hypothesis: the *Pseudomonas* signaling molecules 4-hydroxy-2-alkylquinolones derive from fatty acids, not 3-keno fatty acids, *Chem. Biol.* 20 (2013) 1481–1491.
- [11] A.K. Bera, V. Aranasova, H. Robinson, E. Eisenstein, J.P. Coleman, E.C. Pesci, J.F. Parson, Structure of PqsD, a *Pseudomonas* quinolone signal biosynthetic enzyme, in complex with anthranilate, *Biochem.* 48 (2009) 8644–8655.
- [12] J.-L. Ferrer, J.M. Jex, M.E. Bowman, R.A. Dixon, J.P. Noel, Structure of chalcone synthase and the molecular basis of plant polyketide biosynthesis, *Nat. Struct. Biol.* 6 (1999) 755–783.
- [13] T.T.H. Dao, H.J.M. Linthorst, R. Verpoorte, Chalcone synthase and its functions in plant resistance, *Phytochem. Rev.* 10 (2011) 397–412.
- [14] J. Schröder, The family of chalcone synthase-related proteins: functional diversity and evolution, in: R. Ibrahim, L. Varin, V. De Luca, J. Romeo (Eds.), *Evolution of Metabolic Pathways*, Elsevier Science Ltd, Oxford, 2000, pp. 55–90.
- [15] M.P. Storz, C.K. Maurer, C. Zimmer, N. Wagner, C. Brengel, J.C. de Jong, S. Lucas, M. Miesken, S. Häussler, A. Steinbach, R.W. Hartmann, Validation of PqsD as an anti-biofilm target in *Pseudomonas aeruginosa* by development of small-molecule inhibitors, *J. Am. Chem. Soc.* 134 (2012) 16143–16146.
- [16] D. Pistocci, A. Ullrich, S. Lucas, R.W. Hartmann, U. Kazmaier, R. Müller, Biosynthesis of 2-alkyl-4-(1H)-quinolones in *Pseudomonas aeruginosa*: potential for therapeutic interference with pathogenicity, *ChemBioChem* 12 (2011) 850–853.
- [17] I. Abe, H. Murita, A. Numura, H. Naguchi, Substrate specificity of chalcone synthase: enzymatic formation of unnatural polyketides from synthetic cinnamoyl-CoA analogues, *J. Am. Chem. Soc.* 122 (2000) 11242–11243.
- [18] D. Mulliner, D. Wondrusch, G. Schürmann, Predicting Michael-acceptor reactivity and toxicity and through quantum chemical transition-state calculations, *Org. Biomol. Chem.* 9 (2011) 8400–8412.
- [19] M.P. Storz, C. Brengel, E. Weidel, M. Hoffmann, K. Hollemeyer, A. Steinbach, R. Müller, M. Empting, R.W. Hartmann, Biochemical and biophysical analysis of a chiral PqsD inhibitor revealing tight-binding behavior and enantiomers with contrary thermodynamic signatures, *ACS Chem. Biol.* 8 (2013) 2794–2801.

- [20] E. Weidel, J.C. de Jong, C. Brengel, M.P. Storz, A. Braunschauen, M. Negri, A. Plaza, A. Steinbach, R. Müller, R.W. Hartmann, Structure optimization of 2-benzamidobenzoic acids as PqsD inhibitors for *Pseudomonas aeruginosa* infections and elucidation of binding mode by SPR, STD NMR, and molecular docking, *J. Med. Chem.* 56 (2013) 6146–6155.
- [21] J.H. Sahner, C. Brengel, M.P. Storz, M. Groh, A. Plaza, R. Müller, R.W. Hartmann, Combining in silico and biophysical methods for the development of *Pseudomonas aeruginosa* quorum sensing inhibitors: an alternative approach for structure-based drug design, *J. Med. Chem.* 56 (2013) 8656–8664.
- [22] D.J. O'Shannessy, M. Brigham-Burke, K.K. Sooson, P. Hensley, I. Brooks, Determination of rate and equilibrium binding constants for macromolecular interactions using surface plasmon resonance: use of nonlinear least squares analysis methods, *Anal. Biochem.* 212 (1993) 457–468.
- [23] M.P. Storz, G. Allegrè, B. Kirsch, M. Ergöveg, R.W. Hartmann, From in vitro to in cellulo: structure-activity relationship of (2-nitrophenyl)methanol derivatives as inhibitors of PqsD in *Pseudomonas aeruginosa*, *Org. Biomol. Chem.* 12 (2014) 6094–6104.
- [24] H. Nikaido, Molecular basis of bacterial outer membrane permeability revisited, *Microbiol. Mol. Biol. Rev.* 67 (2003) 593–656.
- [25] H. Nikaido, J.-M. Pages, Broad-specificity efflux pumps and their role in multidrug resistance of Gram-negative bacteria, *Microbiol. Rev.* 36 (2012) 340–363.
- [26] C. Henn, S. Boettcher, A. Steinbach, R.W. Hartmann, Catalytic enzyme activity on a biosensor chip: combination of surface plasmon resonance and mass spectroscopy, *Anal. Biochem.* 428 (2012) 28–30.
- [27] F. Lépine, E. Dziel, S. Milot, L.G. Rahme, A stable isotope dilution assay for the quantification of the *Pseudomonas* quinolone signal in *Pseudomonas aeruginosa* cultures, *Biochim. Biophys. Acta* 1622 (2003) 36–41.
- [28] C. Lu, C.K. Maurer, B. Kirsch, A. Steinbach, R.W. Hartmann, Overcoming the unexpected functional inversion of a PqsR antagonist in *Pseudomonas aeruginosa*: an in vivo potent antivirulence agent targeting pqs quorum sensing, *Angew. Chem. Int. Ed. Engl.* 53 (2014) 1109–1112.

9.3 Elucidation of the profile of MvfR-regulated small molecules in *Pseudomonas aeruginosa* after Quorum Sensing Inhibitors treatment

Introduction

Pseudomonas aeruginosa is a ubiquitous Gram-negative bacterium able to cause severe chronic infections in immuno-compromised patients, for example in people affected by cystic fibrosis (Gómez, Prince, 2007) or thermally injured individuals (Tredget *et al.*, 2004). The eradication of this pathogen with antibiotic treatments is becoming more and more difficult because of its intrinsic and acquired resistance (Hancock, Speert, 2000; Aloush *et al.*, 2006) and tolerance (Mulcahy *et al.*, 2010) toward these drugs. A new promising strategy for treating *Pseudomonas aeruginosa* infections is blocking its pathogenicity without killing the bacteria targeting a cell-to-cell communication system called Quorum Sensing (QS) (Hurley *et al.*, 2012).

This bacterium employs four interconnected QS systems, namely *las*, *iqs*, *pqs*, and *rhl* that regulate the expression of several toxins needed for adjusting its metabolism and virulence during the course of infection (Lee, Zhang, 2015). The *pqs* QS system is selectively expressed by *P. aeruginosa* and utilizes the signal molecule *Pseudomonas* Quinolone Signal (PQS) and its precursor 4-hydroxy-2-heptylquinoline (HHQ) for activating the transcriptional regulator MvfR (Multiple Virulence Factor Regulator), also called PqsR. This protein induces the production of different toxins, such as lectins, pyocyanin, and hydrogen cyanide. It also regulates the expression of enzymes needed for the biosynthesis of its natural ligands encoded by the *pqsABCDE* operon (Xiao *et al.*, 2006) and has been shown to be essential for persister cells development (Que *et al.*, 2013).

Briefly, the synthesis of HHQ and PQS starts with the conversion of anthranilic acid (AA) into its Coenzyme A (CoA) thioester derivative by the action of CoA-ligase PqsA. The activated molecule is then condensed with malonyl-CoA by PqsD leading to the formation of 2'-aminobenzoylacetyl-CoA (2-ABA-CoA), which is subsequently hydrolyzed by the thioesterase PqsE into 2'-aminobenzoylacetate (2-ABA) (Dulcey *et al.*, 2013; Drees, Fetzner, 2015). This reactive intermediate is transformed into HHQ by the heterodimer PqsBC bearing an octanoyl chain (Dulcey *et al.*, 2013). Finally, PqsH oxidizes HHQ into PQS (Schertzer, *et al.*, 2010) (Fig. 1).

Furthermore, 2-ABA-CoA and 2-ABA are intermediates for the biosynthesis of other important metabolites. Actually, both compounds can cyclize leading to the formation of dihydroxyquinoline (DHQ), which has been shown to be fundamental in *P. aeruginosa* pathogenicity (Gruber *et al.*, 2016), and in reducing the growth of epithelial cells (Zhang *et al.*, 2008). Moreover, after decarboxylation, 2-ABA is converted into 2'-aminoacetophenone (2-AA), an important signal molecule that coordinates the transition from acute to chronic infection and the development of persister cells (Kesarwani *et al.*, 2011; Que *et al.*, 2013). In addition, 2-ABA could be converted into its hydroxylamine form by the oxidase PqsL and, then, transformed into 4-hydroxy-2-heptylquinoline-N-oxide (HQNO) by the complex octanoyl-PqsBC (Dulcey *et al.*, 2013). HQNO is

essential for biofilm formation because it favors extracellular DNA release by programmed cell lyses of the bacteria (Hazan *et al.*, 2016).

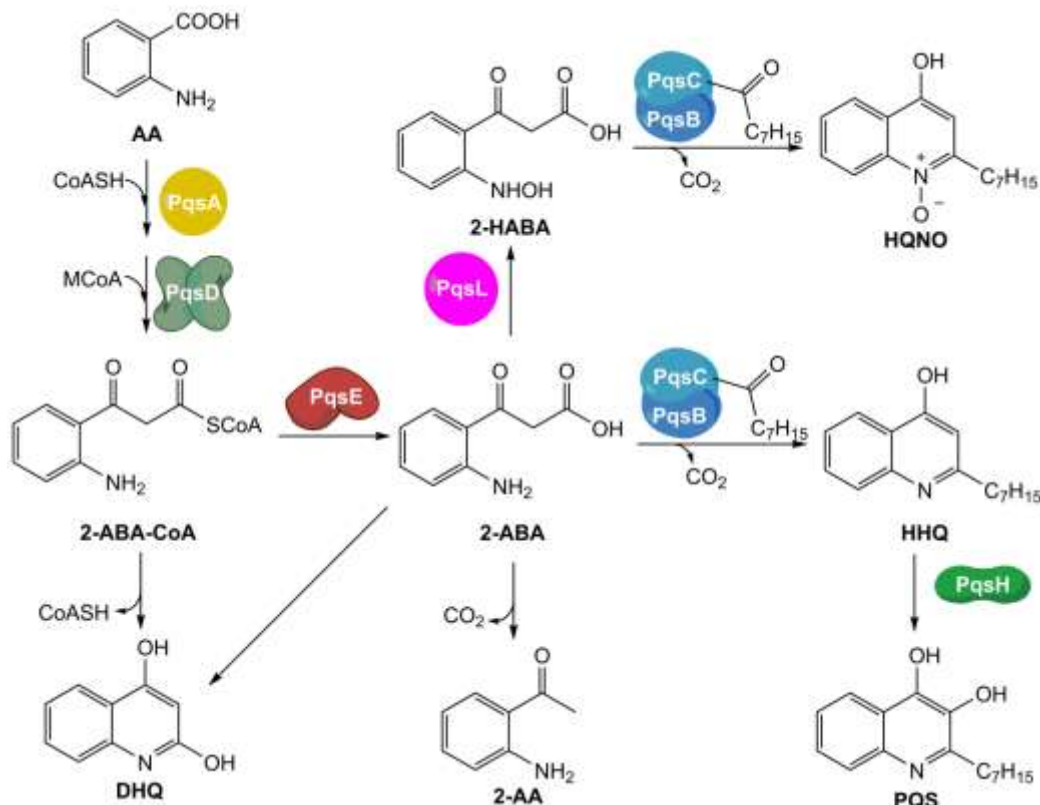


Figure 1 Current model of the biosynthetic pathway of MvfR-related small molecules. AA: anthranilic acid. CoASH: Coenzyme A. MCoA: malonyl-CoA. 2-ABA-CoA: 2'-aminobenzoyl-CoA. 2-ABA: 2'-aminobenzoylacetate. DHQ: dihydroxyquinoline. 2-AA: 2'-aminoacetophenone. 2-HABA: 2'-hydroxylaminobenzoylacetate. HHQ: 4-hydroxy-2-heptylquinoline. HQNO: 4-hydroxy-2-heptylquinoline-N-oxide. PQS: Pseudomonas Quinolone Signal.

Among the potential targets for blocking the *pqs* system, we herein discuss the transcriptional regulator MvfR and the biosynthetic enzyme PqsBC. So far, a number of MvfR antagonists and PqsBC inhibitors has been developed that efficiently reduced HHQ and PQS production in *P. aeruginosa* (Zender *et al.*, 2013; Lu *et al.*, 2014a; Starkey *et al.*, 2014). The aim of this work was to gather detailed information about the effects of these QS Inhibitors (QSIs) on the production of MvfR-related small molecules including 2-AA, DHQ, HQNO, HHQ, and PQS. Furthermore, we monitored the expression of the *pqs* operon in a time-dependent manner upon treatment with the aforementioned QSIs.

Among the QS molecules, 2-AA was proven to be important in the development of *P. aeruginosa* persister cells (Kesarwani *et al.*, 2011; Que *et al.*, 2013), which are metabolically inactive individuals within the bacterial population (Lewis, 2010). Due to their dormant state, antibiotic efficacy is severely impaired in this bacterial sub-group. Targeting persistence by blocking 2-AA production through QS inhibition was shown to be a promising strategy (Starkey *et al.*, 2014). Consequently, an additional goal of the work was to quantify persister phenotype of *P. aeruginosa* after treatment with QSIs.

Material and Methods:

Chemicals and growth media

1, **2** and **3** were synthesized as described in literature (Rahme *et al.*, 2012; Zender *et al.*, in press; Storz *et al.*, 2014). *d*₄-HHQ was synthesized following the procedure of HHQ using *d*₅-aniline (Lu *et al.*, 2012). **4** and amitriptyline were purchased from ChemDiv (USA) and Alfa Aesar (Germany), respectively.

Water (Th. Geyer, Germany), acetonitrile (VWR, Germany) methanol (Sigma-Aldrich, USA) and formic acid (Fluka, USA) were LC–MS grade and used for HPLC–MS/MS experiments.

Yeast extract (Fluka, Germany), sodium chloride (VWR, Germany) and peptone from casein (Merck, Germany) were used for the preparation of Luria Bertani (LB) broth needed for performing the quantification experiments of *pqs*-related signal molecules. Ready-made mixture of LB broth (Fisher, USA) and Tryptic Soy Broth (TSB) 1% [w/v] (BD, USA) were used for *pqsA*-GFP_{ASV} and persister cells experiments.

Bacterial strains

P. aeruginosa PA14 and its isogenic transposon mutants *pqsA*, *pqsC*, *pqsH* and *pqsE* kindly provided by Susanne Häussler (Twincore, Hannover, Germany) were used in the experiments for the quantification of MvfR-related small molecules with and without QSIs. *P. aeruginosa* PA14, its isogenic *pqsBC* transposon mutant, and its *myfR* single mutant were employed for performing persister cells assays. *P. aeruginosa* PA14 transformed with pAC37 carrying *pqsA*-GFP_{ASV} and gentamicin resistance cassette was used in *pqsA* expression experiments. The bacterial strains were maintained at –80°C in 25 % [v/v] glycerol stocks.

MvfR-related small molecule quantification

P. aeruginosa strains were cultivated as previously described (Maurer *et al.*, 2013). After letting PA14 strains grow for 6 h in LB, an aliquot of bacterial culture was centrifuged for 10 min at 4835 x *g* and 25 °C using a Rotina 380R Centrifuge (Hettich, Germany). The supernatant was discarded, the pellet was resuspended in fresh LB, and the bacterial cells were spun down using the previous centrifugation settings. After repeating the wash step a second time, the OD₆₀₀ of the washed cells was measured using a BioPhotometer plus Spectrophotometer (Eppendorf, Germany) in order to prepare a final bacterial suspension with OD₆₀₀ = 0.02 in LB. Aliquots of 1.5 mL were added in each well of a 24-well Cellstar plate (Greiner Bio-One, Frickenhausen, Germany). 15 µL of dimethylsulfoxide (DMSO) or DMSO stock solutions of the target compound were added in each well. Triplicates of each condition were evaluated in every assay. The plates were incubated for 17 h at 37 °C with 75 % humidity and shaken at 200 rpm. The quantification of anthranilic acid derivatives was performed following a previously described protocol (Lépine *et al.*, 2003) with slight modifications. 750 µL of culture from each well were diluted with 750 µL of Internal Standard (IS) stock solution in acetonitrile. The IS employed in experiments with PA14 *wt* and *pqsC*

mutant was *d₄*-HHQ at a final concentration of 500 nM, while the experiments in PA14 *pqsH* mutant required amitriptyline as IS at a final concentration of 1 μ M. After mixing the diluted cell culture for 5 min, the mixture was spun down for 15 min at 18,620 $\times g$ and 15 $^{\circ}$ C using a Mikro 220R Centrifuge (Hettich, Germany). 1 mL of supernatant was transferred in glass vial and analyzed with the Accela HPLC system (Thermo Fisher Scientific, Germany) coupled to a triple quadrupole mass spectrometer TSQ Quantum Access Max (Thermo Fisher Scientific Germany) equipped with an HESI-II source. Separation was achieved by a Macherey-Nagel Nucleodur C₁₈ Pyramid column (150 \times 2 mm, 3 μ m) heated at 40 $^{\circ}$ C. The mobile phase consisted of 10:90 MeOH:H₂O for 0.5 min, followed by a linear gradient of 1.5 min for reaching 100 % MeOH, which was kept constant for 1 min. Then, the initial eluents composition was pumped for 2 min. The flow rate employed was 600 μ L \cdot min⁻¹. A final concentration of 0.1 % formic acid was present in the eluents. Compounds were ionized using heated electrospray ionization (hESI) in positive ion mode with the following parameters: spray voltage: 3500 V; vaporizer temperature: 370 $^{\circ}$ C; sheath gas pressure (nitrogen): 35 units; auxiliary gas pressure (nitrogen): 30 units; skimmer offset voltage: 0 V; capillary temperature: 270 $^{\circ}$ C. Selected reaction monitoring was used for detecting DHQ (161.971 \rightarrow 115.979, collision energy: 28 V, tube lens: 95 V), 2-AA (136.016 \rightarrow 91.048, collision energy: 24 V, tube lens: 68 V), HHQ (244.050 \rightarrow 158.944; collision energy: 31 V; tube lens: 100 V), HQNO (260.036 \rightarrow 158.908; collision energy: 28 V; tube lens: 110 V), PQS (260.048 \rightarrow 174.927; collision energy: 30 V; tube lens: 110 V), *d₄*-HHQ (248.081 \rightarrow 162.965; collision energy: 32 V; tube lens: 100 V) and amitriptyline (278.061 \rightarrow 232.932; collision energy: 16 V; tube lens: 90 V) employing a scan width of 0.010 *m/z*, a scan time of 0.100 s, and a peak width of 0.70. Calibration curves were prepared following the same protocol and using PA14 *pqsA* mutant as matrix without compounds and spiked with known concentrations of analytes and IS after the overnight growth. The assays were repeated at least three times.

***pqsA* expression assay**

The assays were performed following the protocol previously published (Kesarwani *et al.*, 2011) with few modifications. After let PA14 *wt* transformed with pAC37 grow overnight in LB with 60 μ g/mL of gentamicin, an aliquot of bacterial culture was centrifuged for 5 min at 8000*g* at 25 $^{\circ}$ C using a 5810R Centrifuge (Eppendorf, USA). The supernatant was discarded, the pellet was resuspended in fresh LB with the same antibiotic and the bacterial cells were spun down using the previous centrifugation settings. After repeating the wash step a second time, the OD₆₀₀ of the washed cells was measured using a Spectronic Unicam Genesys 10 UV spectrophotometer (Thermo Fisher, USA) in order to prepare a final bacterial suspension with OD₆₀₀ = 0.02 in LB with 60 μ g/mL of gentamicin. 100 μ L of the prepared culture was poured in each well of a 96-well plate (Corning Inc. Corning, USA) and the compounds were added in triplicates. The final concentration of DMSO was 1% v/v. The plates were incubated at 37 $^{\circ}$ C under static condition in Infinite F200

plate reader (Tecan Group Ltd, Männedorf, Switzerland) monitoring GFP fluorescence ($\lambda_{\text{ex}} = 485$ nm; $\lambda_{\text{em}} = 535$ nm) and OD₆₀₀ every 15 min. The assays were repeated at least three times.

Persister cells assay

The effects of QSIs on persistence were evaluated following the published protocol (Starkey *et al.*, 2014) with some modifications. After streaking the bacteria on LB agar and overnight incubation at 37 °C, one colony was dispersed in 5 mL of LB and the bacteria were grown at 37 °C up to OD₆₀₀ = 0.5. 30 μ L of the culture were transferred into glass tubes with 5 mL of TSB 1 % [w/v] and incubated overnight at 37°C under shaking condition. Then, an aliquot of *P. aeruginosa* culture was centrifuged for 5 min at 8,000 x *g* and 25 °C using a 5810R Centrifuge (Eppendorf, USA). The supernatant was discarded, the pellet was resuspended in fresh LB, and the bacterial cells were spun down using the previous centrifugation settings. After repeating the wash step a second time, the OD₆₀₀ of the washed cells was measured using a Spectronic Unicam Genesys 10 UV spectrophotometer (Thermo Fisher, USA) in order to prepare a final bacterial suspension with OD₆₀₀ = 0.02 in 5 mL of TSB 1% [w/v] in each glass tube. The target compounds were added in the tubes and the final concentration of DMSO was 0.5 % [v/v]. The bacterial suspension was incubated at 37 °C under shaking condition for 4 h. An aliquot of 100 μ L of culture from each tube was used for dilution plating on LB agar plates and colony forming units (CFU) quantification (normalizers). 50 μ L of meropenem 1 mg/mL were added in each tube and the cultures were incubated at 37 °C for 24 h under shaking condition. Aliquots of 600 μ L of bacterial suspension were utilized for dilution plating on LB agar plates and CFU quantification (persisters). The survival fractions were calculated as the ratio of normalizers over persisters. Triplicates per each condition were employed in each assay and the experiments were repeated at least three times.

Results and Discussion

The QSIs evaluated in this study were the two MvfR antagonists **1** (Starkey *et al.*, 2014) and **2** (Zender *et al.*, unpublished results), and the two PqsBC inhibitors **4** (Starkey *et al.*, 2014) and **3** (unpublished results) shown in Figure 2. As previously published, these compounds were able to inhibit the production of the signal molecules HHQ and PQS in PA14 *pqsH* mutant and *wt*, respectively. However, the effects of these QSIs on the other MvfR-related small molecules were not studied. Considering that 2-AA, HQNO, and DHQ are pathogenicity-promoting molecules in *P. aeruginosa* infections, it was important to analyze the behavior of the inhibitors on the production of all these anthranilic acid derivatives. To ensure a convenient analytic procedure, we developed an “all-in-one” method for the simultaneous evaluation of these bacterial metabolites. Following the protocol by Lépine and coworkers (Lépine *et al.*, 2003) with some optimizations, a single assay for quantification of the relevant *pqs*-related small molecules was established allowing medium

throughput, easy sample processing, low material consumption, without relevant interference between analytes.

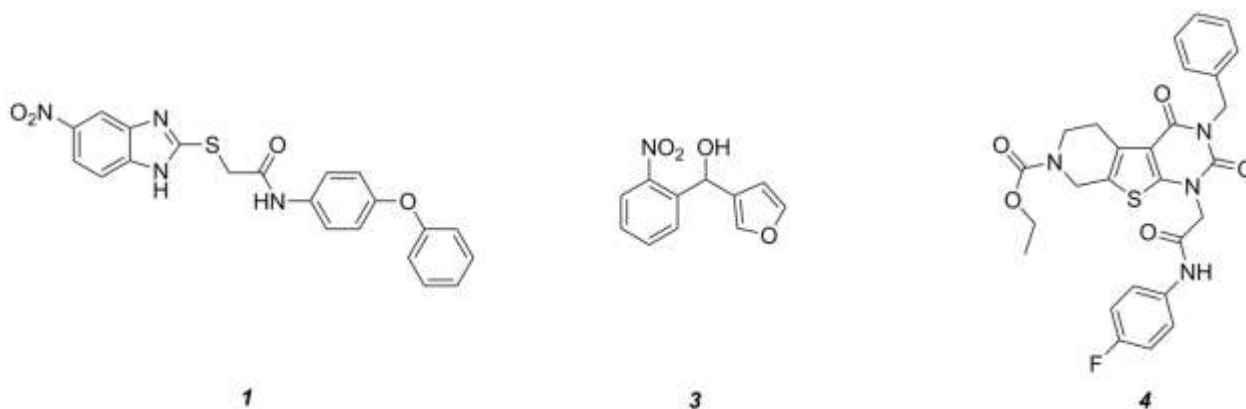


Figure 2 Structures of the compounds evaluated in this work. MvfR antagonist **1**, PqsBC inhibitors **3** and **4**.

Effects of MvfR antagonists on pqs-related small molecules

The MvfR antagonists **1** and **2** were able to reduce dose-dependently the production of the alkyl-quinolones (AQs) and 2-AA in PA14 *wt* with an IC₅₀ of 1.1 μM and 3.1 μM, respectively (Table 1, Figure 3AB). Interestingly, the sigmoidal curves of each of these metabolites were very steep with a Hill coefficient over 1 giving the idea of a possible exponential effect of the MvfR natural ligands on the *pqs* regulon expression. Moreover, while DHQ production was inhibited at high concentrations, its biosynthesis was enhanced up to 330 % and 396 % after the respective incubation of *P. aeruginosa* with **1** and **2** at a concentration close to the compounds' IC₅₀s (inhibitor concentration causing half maximum inhibition). The basal levels of DHQ were reached at lower doses of the two QSIs. Nevertheless, **1** and **2** were able to reduce dose-dependently the overall biosynthesis of these metabolites with an IC₅₀ of 1.2 μM and 3.8 μM, respectively.

Table 1 Effects of MvfR antagonists on production of MvfR-related small molecules in PA14 *wt*.

Compounds	2-AA IC ₅₀ [μM]	Maximal DHQ production [%]	HQNO IC ₅₀ [μM]	HHQ + PQS IC ₅₀ [μM]	Overall IC ₅₀ [μM]
1	1.3 (1.1–1.2) ^a	330 ± 12 ^b @ 1 μM	1.2 (1.1–1.3) ^a	1.1 (1.0–1.2) ^a	1.2 (1.1–1.3) ^a
2	3.6 (3.3–3.9) ^a	396 ± 25 ^b @ 3 μM	3.8 (3.5–4.0) ^a	3.1 (2.9–3.3) ^a	3.8 (3.6–4.1) ^a

^a 95 % Confidence Intervals. ^b Standard Error of the Mean intervals.

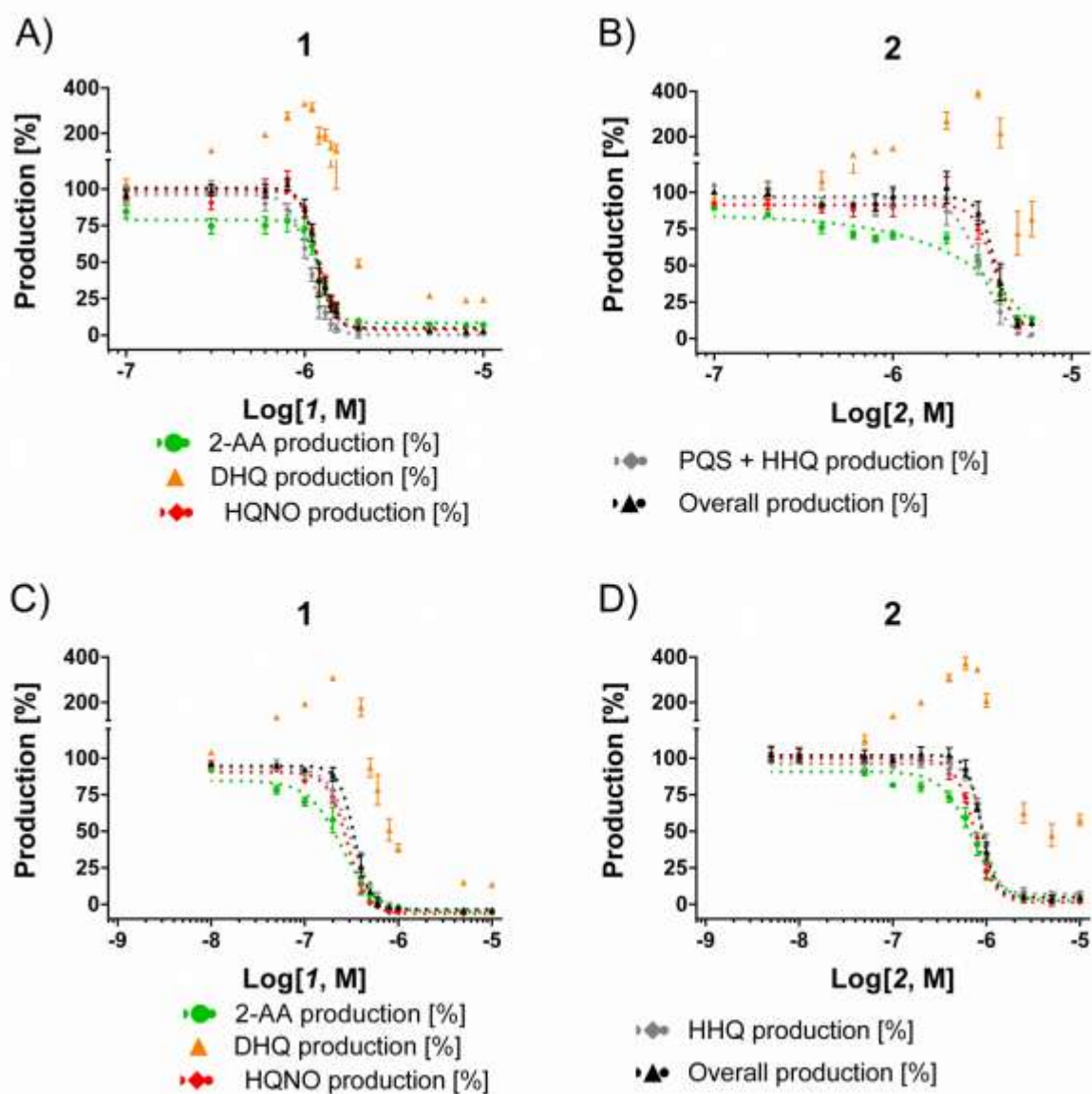


Figure 3 Dose-response curves of MvfR antagonists acting on MvfR-related small molecules production in PA14 strains. *1* (A) and *2* (B) in PA14 *wt*. 2-AA: green. DHQ: orange. PQS + HHQ: grey. HQNO: red. Sum of all anthranilic acid derivatives: black. *1* (C) and *2* (D) in PA14 *pqsH* mutant. 2-AA: green. DHQ: orange. HHQ: grey. HQNO: red. Sum of all anthranilic acid derivatives: black. The “x” axes indicate the logarithm of the concentration of the antagonists in molar units (M). The error bars indicate Standard Error of the Mean.

These compounds were also evaluated in PA14 *pqsH* mutant strain, which does not convert HHQ into PQS. Notably, in a clinical setting, it has been observed that *P. aeruginosa* tends to produce much more HHQ than the hydroxylated analog (Que *et al.*, 2011) and used as potential biomarker of early stage infections (Barr *et al.*, 2016). Our experiments with the PQS-deficient *pqsH* mutant revealed that the QSIs showed similar profiles on the other *pqs*-related molecules production compared to PA14 *wt*. Indeed, *1* and *2* efficiently inhibited AQS and 2-AA production displaying an IC_{50} of circa 0.30 μ M and 0.85 μ M, respectively, and very steep inhibitory curves as in PA14 *wt* (Table 2, Figure 3CD). Likewise, they enhanced DHQ formation up to 300 % and 373 % at their

respective IC₅₀ concentration. Considering that PQS is more active than HHQ in inducing *pqs* expression (Xiao *et al.*, 2006), it is not surprising that the MvfR antagonists were more potent in repressing the biosynthesis of *pqs*-related signal molecules in PA14 *pqsH* mutant than in *wt*.

Table 2 Effects of MvfR antagonists on production of anthranilic acid derivatives in PA14 *pqsH* mutant.

Compounds	2-AA IC ₅₀ [μM]	Maximal DHQ production [%]	HQNO IC ₅₀ [μM]	HHQ IC ₅₀ [μM]	Overall IC ₅₀ [μM]
<i>1</i>	0.19 (0.16–0.22) ^a	304 ± 2 ^b @ 0.2 μM	0.27 (0.25–0.30) ^a	0.27 (0.25–0.30) ^a	0.32 (0.30–0.34) ^a
<i>2</i>	0.69 (0.59–0.81) ^a	373 ± 18 ^b @ 0.6 μM	0.73 (0.67–0.80) ^a	0.91 (0.85–0.96) ^a	0.86 (0.81–0.91) ^a

^a 95 % Confidence Intervals. ^b Standard Error of the Mean intervals.

The characteristic profiles in *wt* and *pqsH* mutant of this class of QSIs, such as the steep inhibitory dose-dependent curves and the overproduction of DHQ close to the IC₅₀ for AQ inhibition, suggest the *pqs* autoloop as a reason. Actually, PQS and HHQ have high activity toward MvfR in the nanomolar range (Lu *et al.*, 2014b; Xiao *et al.*, 2006) and the actual QS signal is amplified through expression of enzymes, which produce again a multitude of additional MvfR natural ligands. Antagonizing the transcriptional regulator would thus have a higher-order effect on the downstream products resulting from pseudo-cooperative effects. Each decrease in signal molecule synthesis achieved by MvfR antagonism would have an additional impact on MvfR deactivation due to less competing autoinducers. In the concentration range close to the antagonist IC₅₀, it would be plausible that the biosynthetic pathway cannot convert the major amount of anthranilic acid into HHQ and PQS maybe because of a slow kinetic step in the biosynthesis. Considering the low affinity of 2-ABA toward PqsBC (Drees *et al.*, 2016), it is feasible to claim that the slow step is the condensation and cyclization reaction performed by PqsBC. This would lead to an accumulation of the reactive intermediate 2-ABA that quickly cyclizes into DHQ.

For confirming these hypotheses, the compounds were evaluated in PA14 *pqsC* mutant, which synthesizes only 2-AA and DHQ, in an experimental setup with and without exogenous addition of the signal molecule PQS. Since these bacteria do not produce any MvfR natural ligands, the *pqs* autoloop is consequently absent and it was possible to control its expression with external administration of PQS. Exogenous addition of the quinolone of 1 μM and 10 μM reduced the potency of the QSIs on MvfR-related small molecules synthesis of circa one and two orders of magnitude, respectively, and increased the steepness of the inhibitory curves (Table 3, Figure 4).

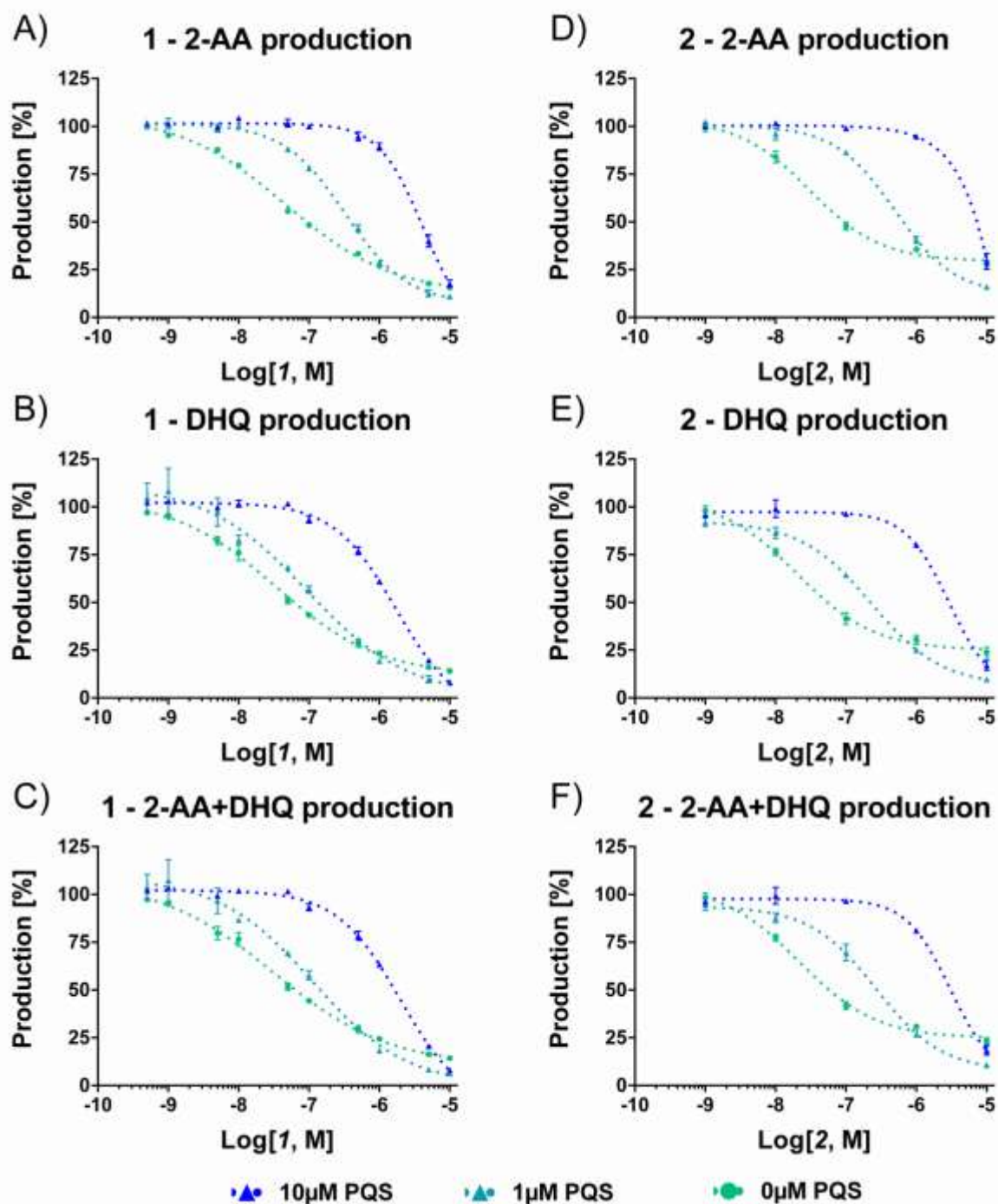


Figure 4 Dose-response curves of MvfR antagonists acting on 2-AA and DHQ production in PA14 *pqsC* mutant with and without external addition of PQS. Effect of **1** on 2-AA (A), DHQ (B) and 2-AA + DHQ (C) synthesis. Effect of **2** on 2-AA (D), DHQ (E) and 2-AA + DHQ (F) synthesis. Concentration of PQS: 0 μM (green curves), 1 μM (light blue curves), 10 μM (dark blue curves). The “x” axes indicate the logarithm of the concentration of the antagonists in molar units (M). The error bars indicate Standard Error of the Mean.

Actually, the IC_{50} of **1** on 2-AA production worsened from 50 nM (without PQS) over 0.3 μM (with 1 μM PQS) to 4.2 μM (with 10 μM PQS). In addition, the concentration of compound needed to reduce DHQ production to 50 % shifted from 30 nM (without PQS) over 90 nM (1 μM PQS) to 1.7

μM (10 μM PQS). Consequently, the overall effect of the QSI on the production of *pqs*-related molecules within the PqsADE biosynthetic pipeline present in the *pqsC* mutant was also affected by PQS administration. Hence, an increase of $\text{IC}_{50\text{s}}$ from 30 nM (no PQS) over 0.11 μM (1 μM PQS) to 2.0 μM (10 μM PQS) was observed. In a similar manner, compound **2** showed higher $\text{IC}_{50\text{s}}$ on 2-AA formation revealing an enhancement from 30 nM (without PQS) to 0.49 μM (1 μM PQS) and 4.8 μM (10 μM PQS). Similarly, the DHQ IC_{50} increased from 20 nM (without PQS) to 0.23 μM (1 μM PQS) and 2.9 μM (10 μM PQS). The IC_{50} on the total biosynthesis of the MvfR-related molecules shifted from 20 nM (without PQS) to 0.27 μM (1 μM PQS) and 3.0 μM (10 μM PQS).

Table 3 Effects of MvfR antagonists on 2-AA and DHQ production in PA14 *pqsC* mutant with and without external addition of PQS.

Compounds	Exogenous PQS [μM]	2-AA IC_{50} [μM]	DHQ IC_{50} [μM]	2-AA + DHQ IC_{50} [μM]
1	0	0.05 (0.04–0.06)	0.03 (0.03–0.04)	0.03 (0.02–0.04)
	1	0.33 (0.28–0.38)	0.09 (0.05–0.18)	0.11 (0.07–0.19)
	10	4.2 (3.0–5.8)	1.7 (1.3–2.3)	2.0 (1.4–2.8)
2	0	0.03 (0.02–0.05)	0.02 (0.01–0.04)	0.02 (0.01–0.03)
	1	0.49 (0.37–0.65)	0.23 (0.17–0.31)	0.27 (0.17–0.41)
	10	4.8 (4.0–2.9)	2.9 (2.4–3.6)	3.0 (2.5–3.8)

The data are reported with 95 % Confidence Interval.

These findings confirmed that the presence of PQS in the bacterial culture plays an important role in controlling the biosynthesis of *pqs*-related molecules. Indeed, when the natural ligand is present, the efficiency of the compounds was strongly reduced as the shifts in IC_{50} confirmed. In addition, the increased steepness of the inhibitory curves after addition of PQS to the PA14 *pqsC* mutant culture displayed that, in case of a small reduction in concentration of QSIs, the MvfR-related compounds were quickly restored to the basal production level.

Furthermore, the expression levels of *pqsA* were monitored under MvfR antagonist treatment using the PA14 *wt* transformed with the plasmid carrying the construct *pqsA*-GFP_{ASV} (Yang *et al.*, 2007). The kinetic studies showed that the expression of the plasmidic *pqsA* promoter occurred in the

exponential phase of bacterial growth as for the genomic *pqs* operon (Déziel *et al.*, 2004) and the tested QSIs were highly efficient in reducing it. In detail, *1* and *2* inhibited the expression displaying IC_{50} s of 16 nM and 1.5 μ M, respectively (Figure 5).

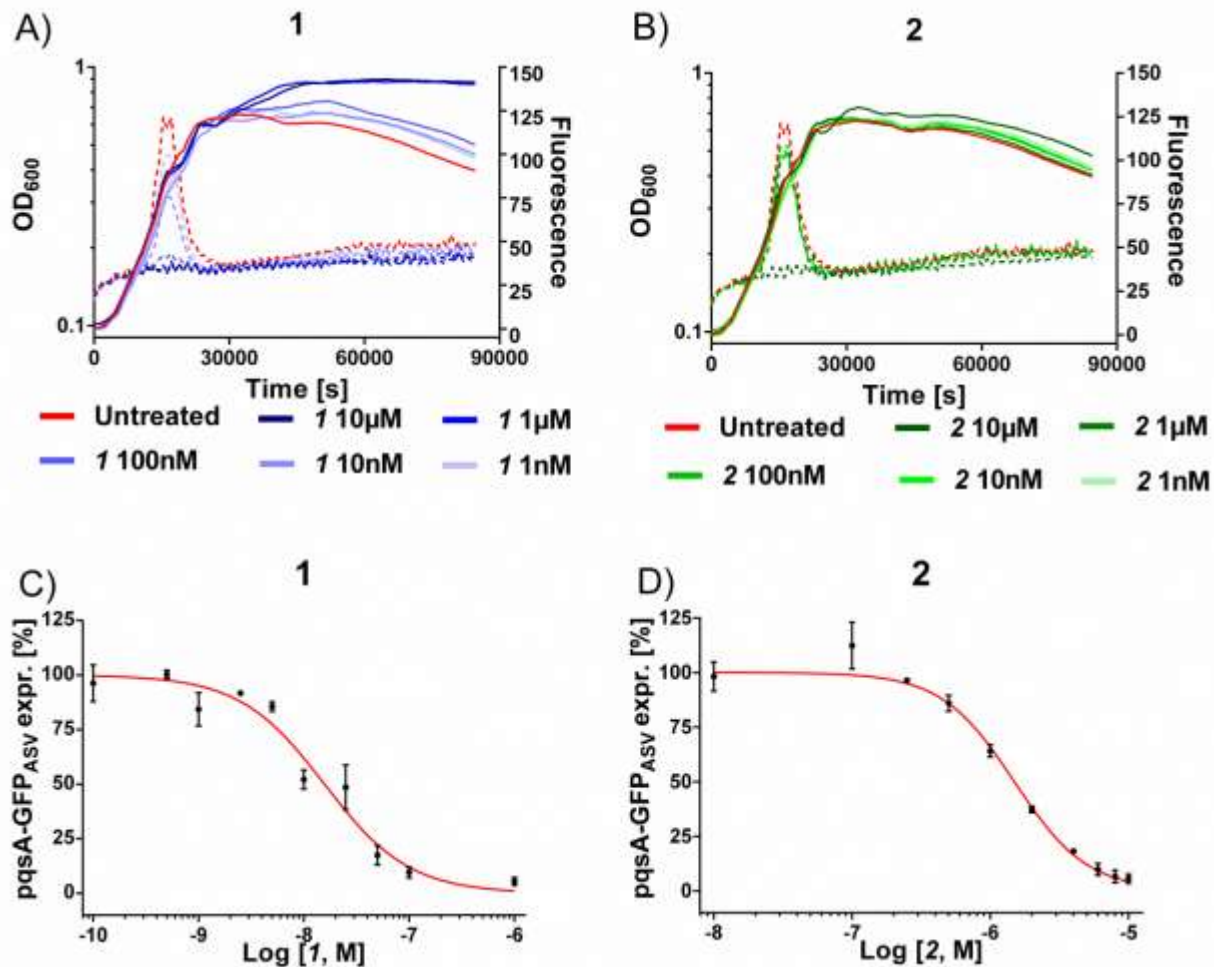


Figure 5 Expression of *pqsA*-GFP_{ASV} (dotted lines) and growth curves (solid lines) of *Pseudomonas aeruginosa* treated with *1* (A) and *2* (B). IC_{50} curves of *1* (C) and *2* (D). The “x” axes indicate the logarithm of the concentration of the antagonists in molar units (M). The error bars indicate Standard Error of the Mean.

Combining these findings with the results in PA14 *wt* and *pqsH* mutant indirectly confirmed that the action of autoinducers HHQ and PQS within this positive feedback loop is the explanation for the pronounced steepness of the sigmoidal dose-response curves for 2-AA, HHQ, PQS, and HQNO levels. The fact that down-regulation of the *pqsA* operon results in an initial increase in DHQ, while the other investigated components show the expected sigmoidal dose-response curves, suggests that either 2-ABA-CoA or 2-ABA accumulate in this scenario, which can be spontaneously degraded to the shunt product. From published studies on the whole PQS biosynthesis cassette, it can be assumed that the reactions mediated by the PqsAD-cascade proceed quickly enough also at lowered enzyme concentrations to enable sufficient 2-ABA-CoA production. These initial steps should be more dependent on the cellular availability of the substrates anthranilic acid and malonyl-CoA. The hydrolysis catalyzed by PqsE can also be performed by housekeeping thioesterases like TesB. But,

an analysis of a *pqsE* transposon mutant by Drees *et al.* regarding the profile of PQS-related molecules showed increased DHQ levels (Drees, Fetzner, 2015). We corroborated and extended the data on this strain with the established *pqs*-related small molecule quantification method (Figure 6). As expected for this strain, 2-AA levels are reduced while DHQ concentration is dramatically increased hinting at accumulation of the reactive intermediate 2-ABA-CoA. Finally, insufficient action of PqsBC and, thus, accumulation of 2-ABA should lead to both increased DHQ and 2-AA levels.

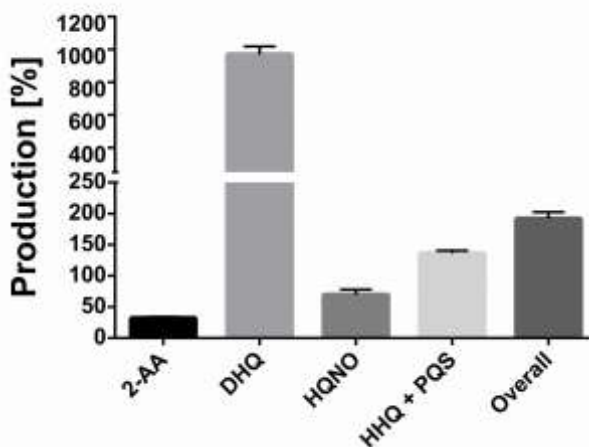


Figure 6 Relative production of 2-AA, DHQ, HQNO, HHQ + PQS and overall amount of AQs in PA14 *pqsE* mutant compared to PA14 *wt*. The error bars indicate Standard Error of the Mean.

Hence, the gathered information suggests that through the MvfR-antagonist-induced down-regulation of the *pqsA* operon an initial accumulation of 2-ABA-CoA rather than 2-ABA takes place (as in the *pqsE* mutant). Interestingly, it has been shown that the condensation reaction mediated by PqsBC should be the rate-limiting step in this biosynthetic cascade (Drees, Fetzner, 2015). Thus, we consider it rather surprising that we observe a metabolite profile that hints more towards the role of 2-ABA-CoA upon partial inactivation of the *pqsA* operon.

Nevertheless, at very low levels of MvfR activity, DHQ is finally reduced as the diminished PqsAD cascade ceases to operate efficiently resulting in the observed metabolite profiles.

Among the *pqs*-related molecules produced by this pathogen, 2-AA was shown to be a key factor for switching the infection from acute to chronic state favoring the formation of persister cells (Kesarwani *et al.*, 2011; Que *et al.*, 2013). Actually, high levels of this QS compound enhanced the genesis of these metabolically inactive bacteria within the population reducing the killing activity of antibiotics. Considering the high efficiency of the MvfR antagonists in reducing 2-AA (Starkey *et al.*, 2014), these QSIs were evaluated in their capability to modify the survival fraction of the pathogen after treatment with meropenem. A dose of 10 μ M of **1** and **2** reduced significantly persisters development in PA14 *wt* from 1.2×10^{-6} of the untreated control to 2.3×10^{-7} and 3.7×10^{-7} , respectively, reaching the same levels of the 2-AA non-producing strain PA14 *mvfR* mutant, that is 2.7×10^{-7} (Figure 7). These findings corroborated the importance of suppressing the

biosynthesis of this carbonyl compound via blockage of the transcriptional regulator for achieving a more efficient antibiotic therapy against *P. aeruginosa* infections.

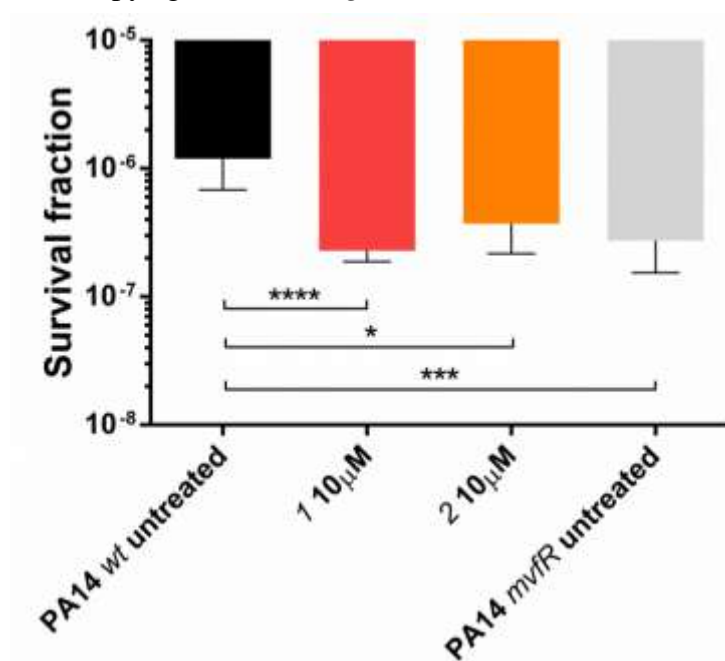


Figure 7 Persister cells survival of PA14 *wt* with and without MvfR antagonists and PA14 *mvfR* mutant after the treatment with 10 μ g/mL of meropenem for 24 h. The error bars indicate 95% Confidence Interval of the geometric mean. Statistical analysis performed with non-parametric one-way ANOVA ($\alpha = 0.05$; **** = $p < 0.0001$; *** = $p < 0.003$; * = $p < 0.05$).

Effects of PqsBC inhibitors on mvfR-related small molecules

The PqsBC inhibitors **3** and **4** reduced the production of the MvfR natural ligands in PA14 *wt* down to 34 % and 35 %, respectively, at their highest concentration (Table 4, Figure 8A). As expected (*vide supra*), the levels of 2-AA and DHQ strongly increased after the treatment with such inhibitors up to 188 % and 389 % after incubation with 250 μ M of **3** and 415 % and 654 % with 10 μ M of **4**. Surprisingly, the synthesis of HQNO was also enhanced up to two times compared to the untreated bacteria. Interestingly, the overall production of the *pqs* signal molecules was not significantly affected. Reducing the concentration of these QSIs led to a reduced inhibitory activity on HHQ and PQS production and a relapse of 2-AA, DHQ and HQNO to the respective basal levels.

The compounds were also evaluated in PA14 *pqsH* mutant giving similar results obtained with the isogenic *wt* (Table 5, Figure 8B). Here, **3** and **4** reduced at their highest dosage the formation of HHQ down to 62% and 73%, respectively. Moreover, the production of 2-AA, DHQ, and HQNO was increased by 157 %, 581 %, and 265 % after treatment with 250 μ M of **3** and 150 %, 264 %, and 141 % after incubation with 10 μ M of **4** compared to the untreated control. In addition, as in PA14 *wt*, the overall amount of the MvfR-related compounds was not affected by the addition of these QSIs.

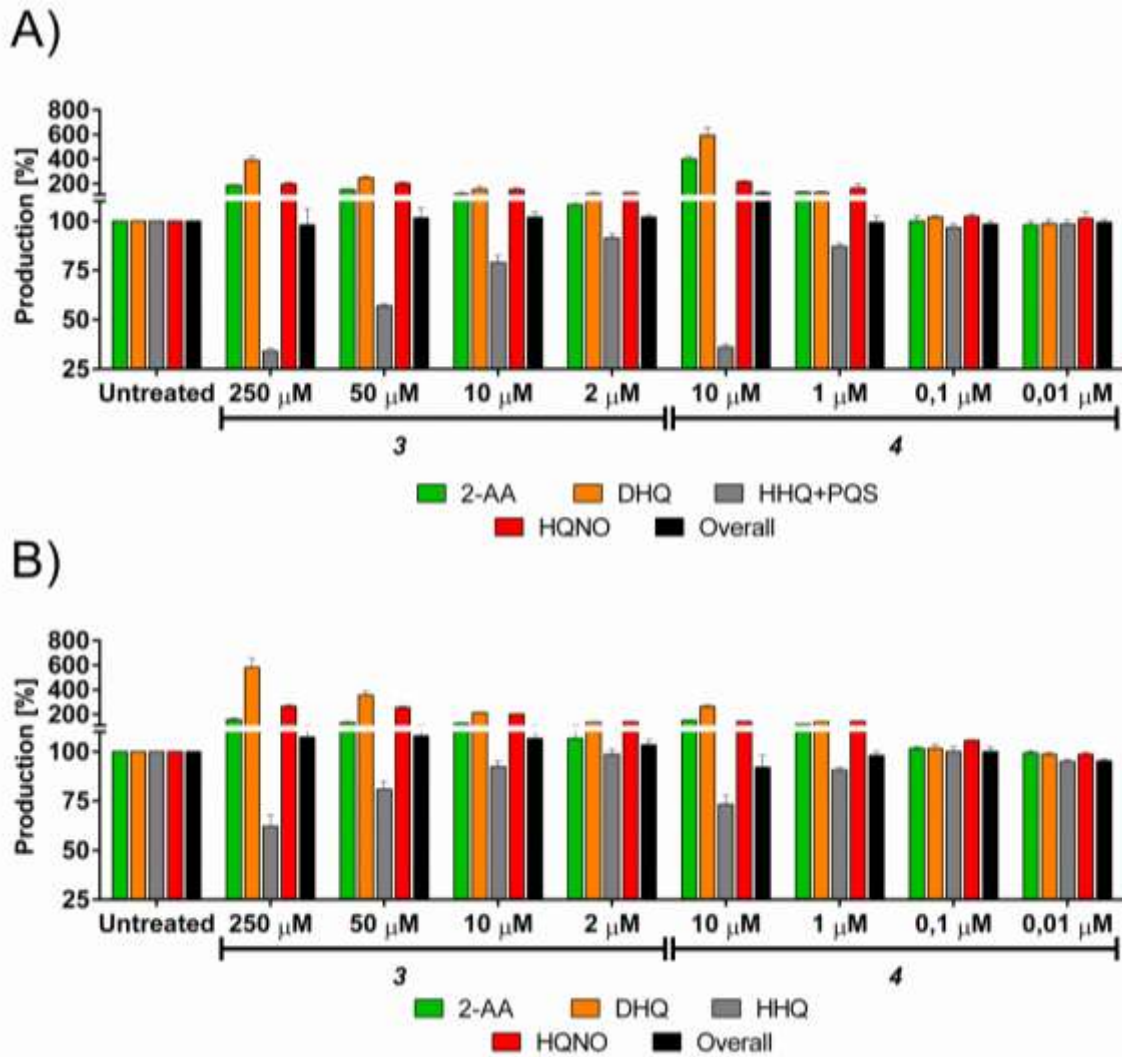


Figure 8 Effects of PqsBC inhibitors on *pqs* related signal molecules production in PA14 strains. (A) **3** and **4** in PA14 *wt*. 2-AA: green. DHQ: orange. PQS + HHQ: grey. HQNO: red. Sum of all anthranilic acid derivatives: black. (B) **3** and **4** in PA14 *pqsH* mutant. 2-AA: green. DHQ: orange. HHQ: grey. HQNO: red. Sum of all anthranilic acid derivatives: black. The error bars indicate Standard Error of the Mean. Statistical analysis performed with one-way ANOVA ($\alpha = 0.05$).

Table 4 Production of *pqs* signal molecules in PA14 *wt* after the treatment with PqsBC inhibitors.

Compounds	Concentration [μ M]	2-AA [%]	DHQ [%]	HQNO [%]	HHQ + PQS [%]	Overall [%]
3	250	188 \pm 4	389 \pm 33	198 \pm 12	34 \pm 1	98 \pm 8
	50	152 \pm 4	249 \pm 15	201 \pm 10	57 \pm 1	101 \pm 5
	10	111 \pm 8	141 \pm 31	148 \pm 19	81 \pm 6	100 \pm 3
	2	107 \pm 2	115 \pm 7	128 \pm 1	93 \pm 4	102 \pm 2
4	10	415 \pm 39	654 \pm 49	218 \pm 16	35 \pm 3	136 \pm 5
	1	134 \pm 7	131 \pm 12	181 \pm 39	86 \pm 2	100 \pm 5
	0.1	99 \pm 4	102 \pm 1	103 \pm 2	96 \pm 3	98 \pm 3
	0.01	99 \pm 4	100 \pm 4	97 \pm 2	103 \pm 5	99 \pm 3

100% is the level of metabolite produced in the untreated PA14 *wt*. The data are reported with Standard Error of the Mean intervals.

Table 5 Production of *pqs* signal molecules in PA14 *pqsH* mutant after the treatment with PqsBC inhibitors.

Compounds	Concentration [μ M]	2-AA [%]	DHQ [%]	HQNO [%]	HHQ [%]	Overall [%]
3	250	157 \pm 8	581 \pm 76	265 \pm 8	62 \pm 6	107 \pm 4
	50	134 \pm 5	355 \pm 31	255 \pm 10	81 \pm 4	108 \pm 3
	10	126 \pm 6	215 \pm 3	199 \pm 2	91 \pm 4	104 \pm 4
	2	102 \pm 2	133 \pm 2	138 \pm 1	97 \pm 2	101 \pm 2
4	10	150 \pm 3	264 \pm 11	141 \pm 1	73 \pm 4	92 \pm 6
	1	121 \pm 2	139 \pm 3	143 \pm 2	91 \pm 1	98 \pm 2
	0.1	102 \pm 1	102 \pm 2	106 \pm 1	100 \pm 3	100 \pm 2
	0.01	99 \pm 1	99 \pm 1	99 \pm 1	95 \pm 1	95 \pm 1

100% is the level of metabolite produced in the untreated PA14 *pqsH* mutant. The data are reported with Standard Error of the Mean intervals.

Additionally, **3** and **4** were examined in PA14 *pqsC* mutant for confirming their target selectivity. Both compounds turned out to be inactive in reducing 2-AA and DHQ production independently from the concentration of PQS added into the culture (Figure 9) supporting the *in vitro* characterization of the two inhibitors (unpublished results; Starkey *et al.*, 2014).

Considering their efficiency in reducing the production of the MvfR natural ligands in PA14 *wt* and *pqsH* mutant, these inhibitors were analyzed in the *pqsA*-GFP_{ASV} construct for monitoring their potential ability for reducing the expression of the *pqs* operon. Actually, **3** and **4** reduced the operon transcription down to 36 % and 15 %, respectively, at their highest dosage (Figure 10).

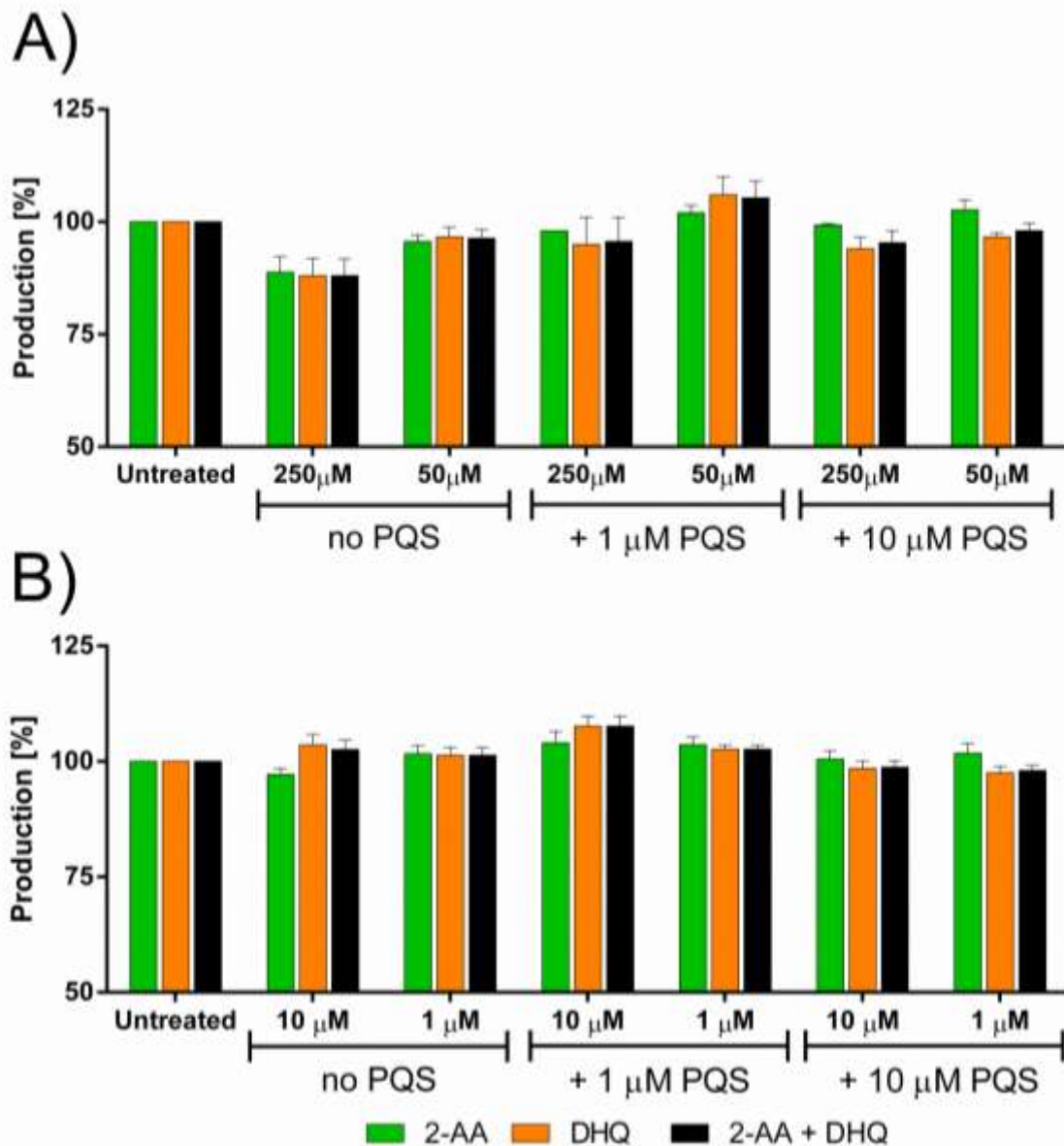


Figure 9 Effects of PqsBC inhibitors on 2-AA and DHQ production in PA14 *pqsC* mutant. (A) **3** and (B) **4**. 2-AA: green. DHQ: orange. Sum of all anthranilic acid derivatives: black. The error bars indicate Standard Error of the Mean. Statistical analysis performed with one-way ANOVA ($\alpha = 0.05$).

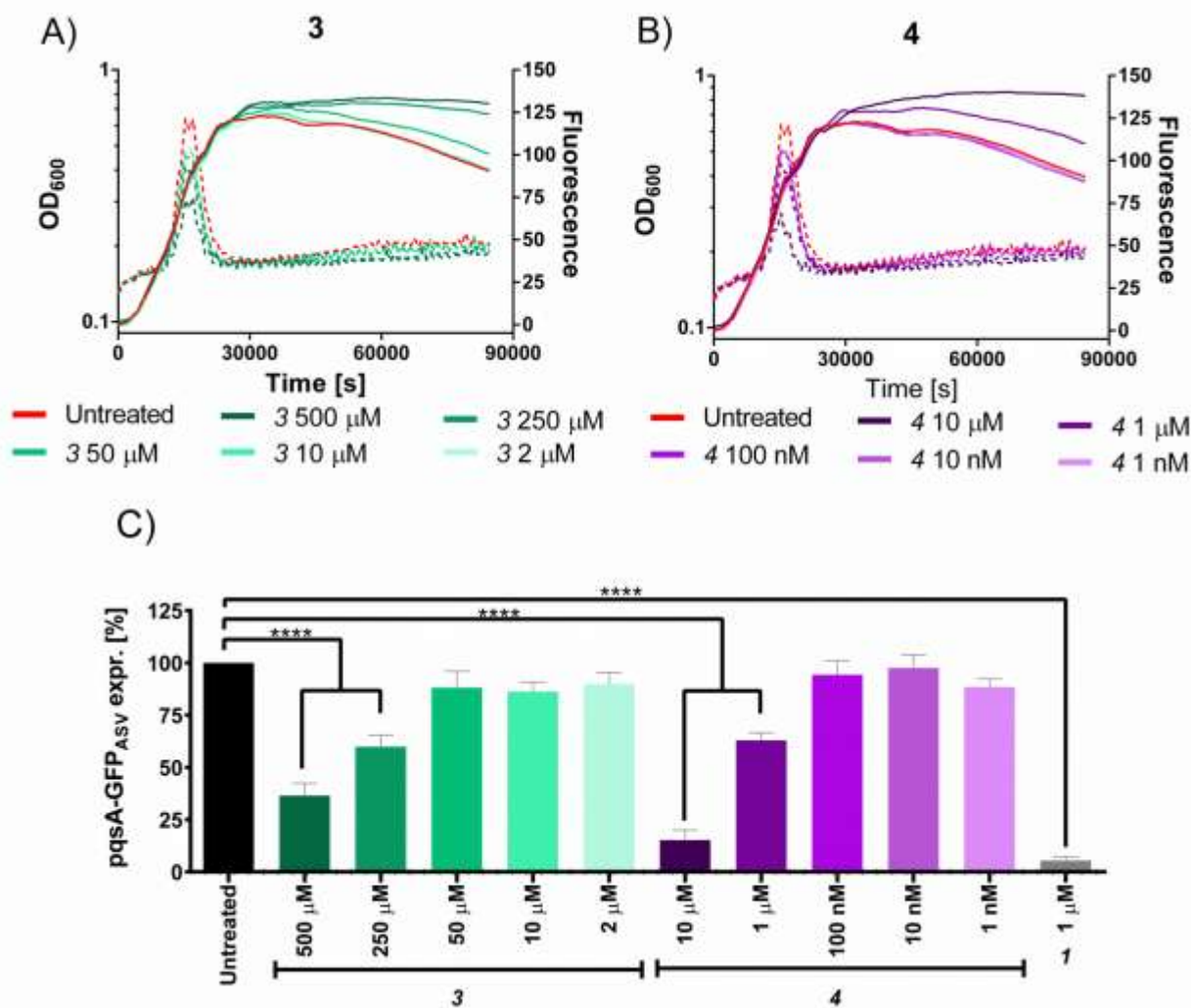


Figure 10 Expression of pqsA-GFP_{ASV} (dotted lines) and growth curves (solid lines) of *Pseudomonas aeruginosa* treated with 3 (A) and 4 (B). (C) Percentage of pqsA-GFP_{ASV} expression after PqsBC inhibitors addition. The error bars indicate Standard Error of the Mean. Statistical analysis performed with one-way ANOVA ($\alpha = 0.05$; **** = $p < 0.0001$).

Taking into consideration the obtained results, the effects of the PqsBC inhibitors on the MvfR natural ligands, 2-AA, and DHQ production fitted to the expected behavior of blocking the hetero-dimer PqsBC. Actually, its inhibition would lead to a reduced conversion of the reactive 2-ABA into HHQ with consequently reduced expression of the *pqs* operon. The excess of this intermediate would be consequently transformed more into the stable molecules 2-AA and DHQ, conversions that do not require PqsBC. According to the current model of HQNO synthesis, 2-ABA is *N*-oxidized by the oxidase PqsL into its hydroxylamine form, 2-HABA. We assume that this moiety of the intermediate should be a more reactive nucleophile (Ningst *et al.*, 2012) than the amine of 2-ABA or a better substrate and that, consequently, the reaction of condensation and cyclization performed by the hetero-dimer proceeds faster. Moreover, it is plausible to expect that the enzyme complex has a different affinity towards the amine and the hydroxylamine intermediates and, due to this fact, the inhibitors would have also different activities in blocking both reactions. Based on the

obtained results, this hypothesis would reasonably explain the overproduction of HQNO after incubation of PA14 with PqsBC inhibitors. But, we do not exclude that an additional, yet unknown bypass reaction towards HQNO might cause this unexpected observation. In addition, the analysis of the overall amount of the *pqs*-related small molecules revealed that these QSIs modify only the ratio of the QS compounds without affecting the total content.

Because of the different QS profiles of PqsBC inhibitors compared to MvfR antagonists and, in particular, the inductive effects on 2-AA production, **3** and **4** were examined regarding their capability to affect persister cells development. We found that only **3** significantly enhanced the persistence phenotype of PA14 *wt* increasing the survival fraction from 1.2×10^{-6} (untreated) up to 4.6×10^{-6} cells. This corresponds to the levels of PA14 *wt* treated with 2-AA as well as the untreated PA14 *pqsBC* mutant showing persister rates of 7.2×10^{-6} and 4.1×10^{-6} , respectively (Figure 11). These findings confirmed that targeting PqsBC led to an enhanced survival of the bacteria. This might ultimately result in a reduced efficiency of antibiotic therapy.

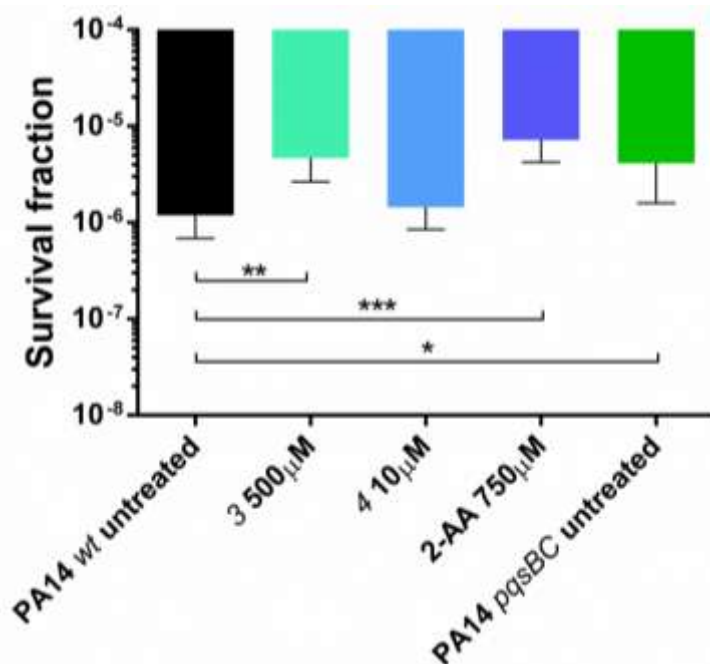


Figure 11 Persister cells survival of PA14 *wt* with and without PqsBC inhibitors or 2-AA and PA14 *pqsBC* mutant after the treatment with $10 \mu\text{g}/\text{mL}$ of meropenem for 24 h. The error bars indicate 95% Confidence Interval of the geometric mean. Statistical analysis performed with non-parametric one-way ANOVA ($\alpha = 0.05$; *** = $p < 0.003$; ** = $p < 0.01$; * = $p < 0.05$).

Conclusions

The profiling of *Pseudomonas aeruginosa* MvfR antagonists and PqsBC inhibitors emphasized the importance in selecting the target for the development of new anti-infectives. The analysis of the *pqs*-related small molecules after the incubation of PA14 strains with MvfR antagonists showed the high efficiency of these QSIs at the highest concentration to strongly reduce the formation of the bacterial metabolites. However, the treatment of the bacteria at lower concentration of MvfR

antagonists revealed a characteristic profile featuring an overproduction of DHQ at concentrations close to the compounds' IC₅₀. The PqsBC inhibitors showed to be less efficient in reducing the MvfR natural ligands synthesis at the highest dosages and, moreover, lead to an increased production of 2-AA, DHQ, and HQNO. Actually, they mainly affected the ratio of QS molecules generated within a bacterial population without modifying the overall production. Finally, we could corroborate the importance of reducing 2-AA production through MvfR antagonism for achieving lower persistence and, consequently, more efficient antibiotic therapy. In the end, we recommend that the preferable target for blocking the *pqs* system is the transcriptional regulator MvfR. In case of PqsBC inhibitors, a combination with other QSIs (e.g., MvfR antagonists) might still be a valid route towards novel anti-infectives.

Funding

The research was supported by the Helmholtz Centrum for Infection Research, Massachusetts General Hospital and by “GradUS global” – promoted by the German Academic Exchange Service (DAAD) and funded by the Federal Ministry of Education and Research (BMBF).

Acknowledgement

I would like to thank Prof. Dr. Susanne Häussler for kindly supplying *Pseudomonas aeruginosa* PA14 *wt* and its isogenic *pqsA*, *pqsC*, *pqsE* and *pqsH* mutants. Furthermore, I would like to thank Simone Amann for having helped me in performing some *pqs*-small molecules quantification experiments. Finally, I would like to thank Dr. Jens Eberhard, Dr. Martin Empting, Dr. Christine K. Maurer and Prof. Dr. Rolf W. Hartmann for supervising the project.

References

- Aloush, V., Navon-Venezia, S., Seigman-Igra, Y., Cabili, S., Carmeli, Y. (2006). Multidrug-resistant *Pseudomonas aeruginosa*: risk factors and clinical impact. *Antimicrob. Agents Chemother.* 50 (1), 43–48.
- Barr, H., L., Halliday, N., Barrett, D., A., Williams, P., Forrester, D., L., Peckham, D., Williams, K., Smyth, A., R., Honeybourne, D., Whitehouse, J., L., Nash, E., F., Dewar, J., Clayton, A., Knox, A., J., Cámara, M., Fogarty, A., W. (2016). Diagnostic and prognostic significance and systemic alkyl quinolones for *P. aeruginosa* in cystic fibrosis: a longitudinal study. *J. Cyst. Fibros.* doi: 10.1016/j.jcf.2016.10.005.
- Déziel, E., Lépine, F., Milot, S., He, J., Mindrinos, M. N., Tompkins, R. G., Rahme, L. G. (2004) Analysis of *Pseudomonas aeruginosa* 4-hydroxy-2-alkylquinolines (HAQs) reveals a role for 4-hydroxy-2-heptylquinoline in cell-to-cell communication. *PNAS.* 101 (5), 1339–1344.
- Drees, S. L., Fetzner, S. (2015). PqsE of *Pseudomonas aeruginosa* acts as pathway-specific thioesterase in the biosynthesis of alkylquinolone signaling molecules. *Chem. Biol.* 22 (5), 611–618.
- Drees, S. L., Li, C., Prasetya, F., Saleem, M., Dreveny, I., Williams, P., Hennecke, U., Emsley, J., Fetzner, S. (2016). PqsBC, a condensing enzyme in the biosynthesis of the *Pseudomonas aeruginosa* quinolone signal: crystal structure, inhibition, and reaction mechanism. *J. Biol. Chem.* 291 (13), 6610–6624.

- Dulcey, C. E., Dekimpe, V., Fauvelle, D.-A., Milot, S., Groleau, M.-C., Doucet, N., Rahme, L. G., Lépine, F., Déziel, E. (2013). The end of an old hypothesis: the *Pseudomonas* signaling molecules 4-hydroxy-2-alkylquinolines derive from fatty acids, not 3-ketofatty acids. *Chem. Biol.* 20, 1481–1491.
- Gómez, I. M., Prince, A. (2007). Opportunistic infections in lung disease: *Pseudomonas* infections in cystic fibrosis. *Curr. Opin. Pharmacology.* 7, 244–251.
- Gruber, J., D., Chen, W., Parnham, S., Beauchesne, K., Moeller, P., Flume, P., A., Zhang, Y., M. (2016). The role of 2,4-dihydroxyquinoline (DHQ) in *Pseudomonas aeruginosa* pathogenicity. *PeerJ.* 4:e1495. doi: 10.7717/peerj.1495.
- Hancock, R. E. W., Speert, D. P. (2000). Antibiotic resistance in *Pseudomonas aeruginosa*: mechanisms and impact on treatment. *Drug Resist. Updat.* 3, 247–255.
- Hazan, R., Que, Y.-A., Maura, D., Strobel, B., Majcherczyk, P. A., Hopper, L. R., Wilbur, D. J., Hreha, T. N., Barquera B., Rahme, L. G. (2016). Auto poisoning of the respiratory chain by a quorum-sensing-regulated molecule favors biofilm formation and antibiotic tolerance. *Curr. Biol.* 26 (2), 195–206.
- Hurley, M. N., Cámara, M., Smyth, A. R. (2012). Novel approaches to the treatment of *Pseudomonas aeruginosa* infections in cystic fibrosis. *Eur. Respir. J.* 40, 1014–1023.
- Lee, J., Zhang, L. (2015). The hierarchy quorum sensing network in *Pseudomonas aeruginosa*. *Protein Cell.* 6 (1), 26–41.
- Lépine, F., Deziel, E., Milot, S., Rahme, L. G. (2003). A stable isotope dilution assay for the quantification of the *Pseudomonas* quinolone signal in *Pseudomonas aeruginosa* cultures. *Biochim. Biophys. Acta.* 1622 (1), 36–41.
- Lewis, K. (2010). Persister cells. *Annu. Rev. Microbiol.* 64, 357–372.
- Lu, C., Kirsch, B., Zimmer, C., de Jong, J. C., Henn, C., Maurer, C. K., Müsken, M., Häussler, S., Steinbach, A., Hartmann, R. W. (2012). Discovery of antagonists of PqsR, a key player in 2-alkyl-4-quinolone-dependent quorum sensing in *Pseudomonas aeruginosa*. *Chem. Biol.* 19, 381–390.
- Lu, C., Kirsch, B., Maurer, C. K., de Jong, J. C., Braunshausen, A., Steinbach, A., Hartmann, R. W. (2014a). Optimization of anti-virulence PqsR antagonists regarding aqueous solubility and biological properties resulting in new insights in structure-activity relationship. *Eur. J. Med. Chem.* 79, 173–183.
- Lu, C., Maurer, C. K., Kirsch, B., Steinbach, A., Hartmann, R. W. (2014b). Overcoming the unexpected functional inversion of a PqsR antagonist in *Pseudomonas aeruginosa*: an in vivo potent antivirulence agent targeting pqs Quorum Sensing. *Angew. Chem. Int. Ed.* 53, 1109–1112.
- Kesarwani, M., Hazan, R., He, J., Que, Y.-A., Apidianakis, Y., Lesic, B., Xiao, G., Dekimpe, V., Milot S., Deziel, E., Lépine, F., Rahme, L. G. (2011). A quorum sensing regulated small volatile molecule reduces acute virulence and promotes chronic infection phenotypes. *PLoS Pathog.* 7:8. doi: 10.1371/journal.ppat.1002192.
- Maurer, C. K., Steinbach, A., Hartmann, R. W. (2013). Development and validation of a UHPLC–MS/MS procedure for quantification of the *Pseudomonas* Quinolone Signal in bacterial culture after acetylation for characterization of new quorum sensing inhibitors. *J. Pharm. Biomed. Anal.* 86, 127–134.
- Mulcahy, L. R., Burns, J. L., Lory, S., Lewis, K. (2010). Emergence of *Pseudomonas aeruginosa* strains producing high levels of persister cells in patients with cystic fibrosis. *J. Bacteriol.* 192 (23), 6191–6199.
- Ningst, T. A., Antipova, A., Mayr, H. (2012). Nucleophilic reactivities of hydrazines and amines: the futile search for the α -effect in hydrazine reactivities. *J. Org. Chem.* 77 (18), 8142–8155.
- Pistorius, D., Ullrich, A., Lucas, C., Hartmann, R. W., Kazmaier, U., Müller, R. (2011). Biosynthesis of 2-alkyl-4(1H)-quinolones in *Pseudomonas aeruginosa*: potential for therapeutic interference with pathogenicity. *Chembiochem.* 12 (6), 850–853.
- Que, Y.-A., Hazan, R., Ryan, C. M., Milot, S., Lépine, F., Lydon, M., Rahme, L. G. (2011). Production of *Pseudomonas aeruginosa* intercellular small signal molecules in human burn wounds. *J. Pathog.* 2011:549302. doi: 10.4061/2011/549302.

- Que, Y.-A., Hazan, R., Strobel, B., Maura, D., He, J., Kesarwani, M., Panopoulos, P., Tsurumi, A., Giddey, M., Wilhelmy, J., Mindrinos, M. N., Rahme, L. G. (2013). A quorum sensing small volatile molecule promotes antibiotic tolerance in bacteria. *PLoS One*. **8**:12. doi: 10.1371/journal.pone.0080140.
- Rahme, L. G., Lépine, F., Starkey, M., Lesic-Arsic, B. (2012). *Antibiotic Tolerance Inhibitor*. US Patent No 61/445,448. Washington, DC: U. S. Patent and Trademark Office.
- Schertzer, J. W., Brown, S. A., Whiteley, M. (2010). Oxygen levels rapidly modulate *Pseudomonas aeruginosa* social behaviours via substrate limitation of PqsH. *Mol. Microbiol.* **77** (6), 1527–1538.
- Starkey, M., Lépine, F., Maura, D., Bandyopadhyaya, A., Lesic, B., He, J., Kitao, T., Righi, V., Milot, S., Tzika, A., Rahme, L. (2014) Identification of anti-virulence compounds that disrupt Quorum-Sensing regulated acute and persistent pathogenicity. *PLoS Pathog.* **10**:8. doi:10.1371/journal.ppat.1004321.
- Storz, M. P., Allegretta, G., Kirsch, B., Empting, M., Hartmann, R. W. (2014). From in vitro to in cellulose: structure–activity relationship of (2-nitrophenyl)methanol derivatives as inhibitor of PqsD in *Pseudomonas aeruginosa*. *Org. Biomol. Chem.* **12**, 6094–6104.
- Tredget, E. E., Shankowsky, H. A., Rennie, R., Burrell, R. E., Logsetty, S.. (2004). *Pseudomonas* infections in the thermally injured patient. *Burns*. **30**, 3–26.
- Xiao G., Déziel, E., He, J., Lépine, F., Lesic, B., Castonguay, M.-H., Milot, S., Tampakaki, A. P., Stachel, S. E., Rahme, L. G. (2006). MvfR, a key *Pseudomonas aeruginosa* pathogenicity LTTR-class regulatory protein, has dual ligands. *Mol. Microbiol.* **62** (6), 1689–1699.
- Yang, L., Barken, K. B., Skindersoe, M., Christensen, A. B., Givskov, M., Toler-Nielsen, T. (2007) Effects of iron on DNA release and biofilm development in *Pseudomonas aeruginosa*. *Microbiol.* **153**, 1318–1328.
- Zender, M., Klein, T., Henn, C., Kirsch, B., Maurer, C. K., Kail, D., Ritter, C., Dolezal, O., Steinbach, A., Hartmann, R. W. (2013). Discovery and biophysical characterization of 2-amino-oxadiazoles as novel antagonists of PqsR, an important regulator of *Pseudomonas aeruginosa* virulence. *J. Med. Chem.* **56**, 6761–6774.
- Zhang, Y. M., Frank, M. W., Zhu, K., Mayasundari, A., Rock, C. O. (2008). PqsD is responsible for the synthesis of 2,4-dihydroxyquinoline, an extracellular metabolite produced by *Pseudomonas aeruginosa*. *J. Biol. Chem.* **283** (43), 28788–28794.

10 DISCUSSION

10.1 Development of PqsD inhibitors

One of the main goals of the thesis was to develop and optimize inhibitors against the enzyme PqsD because of its key role in the *pqs*-related signal molecules biosynthesis. Two strategies were applied: a ligand-based and a similarity-guided approach.

10.1.1 Ligand-based approach

Based on the results of Storz and coworkers (Storz *et al.*, 2012), the PqsD inhibitor **I** was identified simplifying and rigidifying the scaffold of the tetrahedral intermediate of A-CoA in the catalytic pocket of the enzyme. Considering the potential noxious effects of the nitro group (Kovacic, Somanathan, 2014), it was attempted to exchange it with other electron withdrawing groups (EWGs) as trifluoromethyl, nitril and halogens. However, all these derivatives revealed to be completely inactive in the PqsD cell-free assay highlighting the importance of the nitro group in the enzyme inhibition. Consequently, compound **I** was evaluated in toxicity and mutagenesis assays using respectively human THP-1 macrophages and *Salmonella typhimurium* (Ames test). These tests revealed that this QSI did not show neither toxic nor mutagenic effects. Consequently, the optimization of the scaffold was attempted for improving the activity of the compound class both *in vitro* and *in cellulo* assays. Around 50 compounds were designed and synthesized as fully described in the publication **A** changing the substitution pattern on the nitrophenyl and the *R* substituents (Fig. 5).

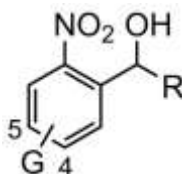


Fig. 5 Molecular scaffold of the (2-nitrophenyl)methanol compounds. *G* could be EWG, or EDG, or H. *R* could be alkyl chains, or (hetero)aromatic rings, or alkyl chain with terminal amine or phthalimide moiety, or H.

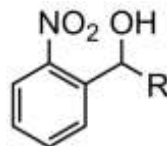
Compound **I** was shown to bind tightly the bacterial enzyme in its active site with a slow onset kinetic and displaying, as a consequence, a higher potency in case of longer pre-incubation time with PqsD (Storz *et al.*, 2013). Consequently, the potency of the compounds was evaluated quantifying the concentration of inhibitor necessary for blocking the 50% of conversion (IC_{50}) of A-CoA into HHQ using different pre-incubation times (10 and 30 minutes) of the enzyme with the QSIs (Storz *et al.*, 2012; Storz *et al.*, 2013). Actually, compound **I** showed an IC_{50} of $3.2 \pm 0.1 \mu\text{M}$ using 10 min pre-incubation protocol and an IC_{50} of $0.5 \pm 0.1 \mu\text{M}$ after 30 min incubation with PqsD. So, **I** was taken as reference compound for studying the SAR of this QSI class. The different properties of the substituents added in position 4 and 5 on the nitrophenyl ring affected interestingly the compound behavior. The analysis of the inhibitors with the short pre-incubation protocol revealed that while the addition of EWGs, as chlorine or nitro, diminished activity compared to **I**,

the analogues having electron donating groups (EDGs), as methyl or methoxy groups, resulted to be as potent as **I**. Furthermore, the comparison of the results between short and long pre-incubation time assay revealed that substituents in position 4 can modulate the binding kinetics. Actually, while EWGs slowed down the onset of the compound, the EDGs accelerated it. On the contrary, substituents in 5 did not modify the kinetic onset. Dealing with a slow tight binder would be beneficial, as it would imply a longer residency of the inhibitor in the enzyme and, consequently, a more efficient blockage of the protein functionality. So, the nitrophenyl ring was not additionally substituted and the scaffold optimization was continued on the *R* side. The phenyl in *R* of **I** was replaced with alkyl chains and saturated rings of different size and molecular volume. PqsD inhibition analysis revealed that compounds with bulky and/or long aliphatic moieties showed lower potency than the QSIs with smaller linear chains. It is plausible that big substituents have steric clashes and need high entropic penalties for binding PqsD. Considering the positive effect of short alkyl chains in inhibiting PqsD, *R* was replaced with short saturate linkers bearing at the end functional groups, as phenyl ring, amine, phthalimide and fluorophores. Only the phthalimide derivatives resulted to be as potent as **I** showing IC_{50} s in the high nanomolar range with the longer pre-incubation time as compound **II** which displayed an IC_{50} of $0.3 \pm 0.1 \mu\text{M}$. The compounds with an amino moiety at the end of an alkenyl chain were inactive or weakly active as expected. Actually, it is plausible that at physiological pH the amino group is protonated and, consequently, an electrostatic repulsion occurs between the compound and the positively charged entrance channel. The derivatives carrying phenyl rings and fluorophores showed to have acceptable IC_{50} s in the single digit micromolar range, but still less potent than **I** maybe due to steric clashes and/or entropic penalties. Furthermore, the phenyl group present in **I** at *R* was exchanged with several heteroaromatic rings. While compounds with thiophene and pyridine did not show a better inhibitory activity on PqsD compared to **I**, the derivatives with furan displayed a particular behavior. Actually, the 2-furyl **VI** derivative showed to be as potent as **I**; on the contrary, the 3-furyl analogue **VII** was almost inactive. A deep analysis of this specific compound revealed that it is a selective PqsBC inhibitor (unpublished data) (Table1).

The most *in vitro* active QSIs were, then, tested in bacterial cultures of *P. a. pqsH* mutant capable to produce all the biosynthetic products of the *pqs* system down to HHQ with the exception of PQS. Consequently, it was monitored the reduction of HHQ after overnight incubation of PqsD inhibitors with the bacteria. The compounds were evaluated at a final concentration of 250 μM , if soluble. Considering that **I** inhibited HHQ production of $43 \pm 4\%$, the compounds having additional substituents on the nitrophenyl ring resulted to be less active or completely inactive. On the other side, modification of *R* moiety affected the activity of the compounds in the cell based assay depending on its chemical properties. The QSIs having alkyl chains showed a particular profile. Starting from the hydrogen derivative, the compounds displayed increasing activity up to the ethyl analogue **III** capable to reduce HHQ of $61 \pm 2\%$. Then, the enlargement of *R* reduced the cellular potency of the analogues. Furthermore, all the PqsD inhibitors characterized by having a saturated

linker bearing specific functional groups were completely inactive. The introduction of heteroaromatic rings on *R*, on the contrary, led to the identification of the most potent QSIs of the class in the cellular settings capable (Table 1).

Table 1 Most potent compounds of the class in cell-free and/or whole-cell assays using PA14 *pqsH* mutant.



I - VII

Compound	<i>R</i>	IC ₅₀ [μM] (10 min preinc.) ^a	IC ₅₀ [μM] (30 min preinc.) ^b	% HHQ inhibition in PA14 <i>pqsH</i> mutant
I	Ph	3.2 ± 0.1	0.5 ± 0.1	43 ± 6 ^c
II	(CH ₂) ₂ Phth	1.2 ± 0.1	0.3 ± 0.1	Inactive ^d
III	Et	1.1 ± 0.2	0.8 ± 0.1	61 ± 2 ^c
IV	2-Thienyl	14.3 ± 1.9	1.5 ± 0.2	64 ± 6 ^c
V	3-Thienyl	5.9 ± 0.9	6.4 ± 1.9	74 ± 6 ^c
VI	2-Furyl	1.8 ± 0.4	0.9 ± 0.1	51 ± 15 ^c
VII	3-Furyl	28 % @ 50 μM	13.1 ± 2.8	73 ± 2 ^c

Errors indicate Standard Deviation. ^a Cell-free PqsD assay with 10 minutes pre-incubation protocol of enzyme with compound. ^b Cell-free PqsD assay with 30 minutes pre-incubation protocol of enzyme with compound. ^c Compounds tested at 250 μM. ^d Compounds tested at 125 μM.

A comparison of the results between *in vitro* and *in cellulo* assays revealed that there was not a clear correlation of the activities between the two protocols. Actually, only few compounds that were highly active in the PqsD assay efficiently reduced also HHQ production in *P. a.* cultures as **I**, **III** and **VI**. A deeper analysis of the compounds properties disclosed that most of the inhibitors active in the cellular setting have a molecular weight below 250 Da, a cut off value much smaller compared to the one reported for Gram-negative active drugs of 600 Da (O'Shea, Moser, 2008). This finding highlighted the characteristic low permeability of the membranes of this class of bacteria, especially of the outer layer which is rich in proteins involved in transporting compounds inside and outside the cell (Nikaido, 2003). So, it should not be excluded that these QSIs require transporters or porins for entering into the cells, or are expelled by the bacterium through the usage efflux pumps. In addition, *P. a.* expresses also some enzymes for xenobiotic metabolism as nitroreductases, needed for the reduction of the nitro to an amino group, and acetylases, necessary for the conjugation of acetyl moieties (Noguera, Freedman, 1996; Schackmann, Müller, 1991). Consequently, the requirement of high concentrations of compounds could be also due to their possible inactivation by proteins involved in xenobiotic metabolism.

10.1.2 Similarity-guided approach

Taking into consideration functional and mechanistic properties, PqsD has some common features with the Polyketide Synthase (PKS) family and, in particular, with the Chalcone Synthase (CHS2), a vegetable protein expressed by *Medicago sativa* (known also as *alfalfa*) (Bera *et al.*, 2009; Ferrer *et al.*, 1999). CHS2, as PqsD, is a condensing enzyme and it favors the conversion of *p*-coumaric acid into the flavone naringenin employing three molecules of M-CoA (Ferrer *et al.*, 1999) (Fig. 6). In addition, the vegetable protein can catalyze in unnatural condition the conversion of other compounds belonging to cinnamic acid family, as caffeic acid, cinnamic acid and ferulic acid, into the respective flavones (Dao *et al.*, 2011; Schröder, 2000).

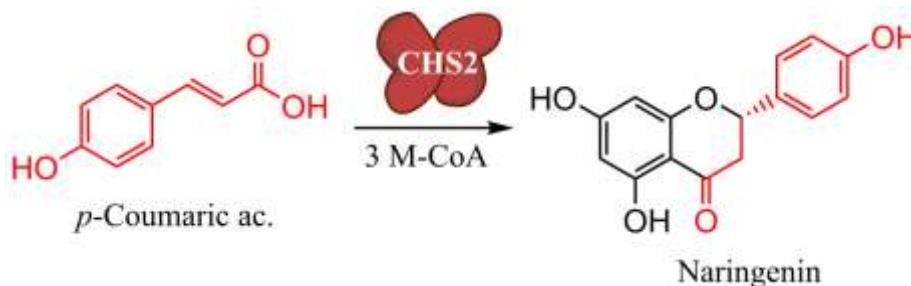


Fig. 6 Conversion of *p*-coumaric acid into naringenin by CHS2

Even if CHS2 and PqsD are not homologues, the enzymes share several characteristics. Firstly, both proteins employ the triad cysteine-histidine-asparagine for their condensation reactions. Moreover, maybe due to the use of the same secondary substrate M-CoA, CHS2 and PqsD have similar active site volume, comparable deepness of the CoA binding pocket and the entrance of the catalytic site is surrounded by basic aminoacids (Bera *et al.*, 2009; Ferrer *et al.*, 1999; Dao *et al.*, 2011). Encouraged by the positive results obtained in the application of a similarity-guided approach between the bacterial enzymes PqsD and FabH for the development of new QSIs (Weidel *et al.*, 2013), a similar strategy was employed with CHS2 and the *P. a.* protein. Starting from the scaffold of the CHS2 substrates, more than 30 compounds were designed and synthesized as fully described in the publication **B**.

The evaluation of the cinnamic acids analogues and their respective methyl esters in the PqsD cell-free assay revealed that only the methyl caffeate (**VIII**) showed a significant inhibition of the enzymatic conversion with an $IC_{50} = 51 \pm 4 \mu\text{M}$. However, this compound contains an α,β -unsaturated system that could act as Michael-acceptor. Consequently, it might react with nucleophiles in the cell and display toxic effects (Mulliner *et al.*, 2011). So, the olefinic linker was exchanged with a saturated congener as in compound **IX** which resulted to be much more potent exhibiting an $IC_{50} = 23 \pm 1 \mu\text{M}$. The next step of scaffold optimization involved the modification of different moieties of the molecule, as the substitution pattern on the phenyl ring, the carboxylic part and the linker (Fig. 7).

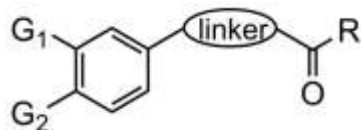


Fig. 7 Molecular scaffold of the CHS2 substrate-like compounds. G_1 and G_2 could be substituents with different chemical properties, or H. R could be esters or amide bearing hydrocarbon moieties of different size.

Actually, the replacement of the catechol with any other substituents, as nitro, acetal and the isosters amino, fluorine and methyl, provoked a completely loss in activity highlighting the fundamental requirement of the 3,4-dihydroxy group for having PqsD inhibition. Consequently, this feature was kept and modification on the carboxylic moiety were attempted for improving activity. The introduction of bigger ester substituents from methyl to benzyl (**IX–XII**) enhanced compound potency in relation to the size of the group down to single digit micromolar IC_{50} s as for **XI** and **XII** (Table 2) suggesting that a favorable hydrophobic interaction could take place between the inhibitor and the enzyme. In addition, replacement of the ester with the isoster amide in **XIII** did not improve compound potency. The next step of scaffold optimization involved the linker length. The analysis of analogues having different bridge size revealed that longer alkenyl chain improved compound activity as the propylene congener **XIV** showing an $IC_{50} = 7.9 \pm 0.2 \mu\text{M}$ (Table 2). Actually, it is plausible that, as for the ester substituents, a favorable hydrophobic interaction is established between the QSI and the protein that would counter balance the higher entropic penalty due to the longer alkenyl chain.

Furthermore, the binding mode of this PqsD inhibitor class was analyzed by SPR monitoring the association and dissociation sensograms of the compounds on the enzyme (Weidel *et al.*, 2013). Actually, the experiment was constituted by two phases. In the first step it was measured the binding of compounds on free protein. Then, after washing PqsD with running buffer for removing the ligands, the second step consisted in pre-incubating the enzyme with A-CoA followed by addition of the inhibitor. Taking into consideration that the pre-treatment with A-CoA blocks the active site, the binders can interact with PqsD only in the entrance channel (Fig. 8).

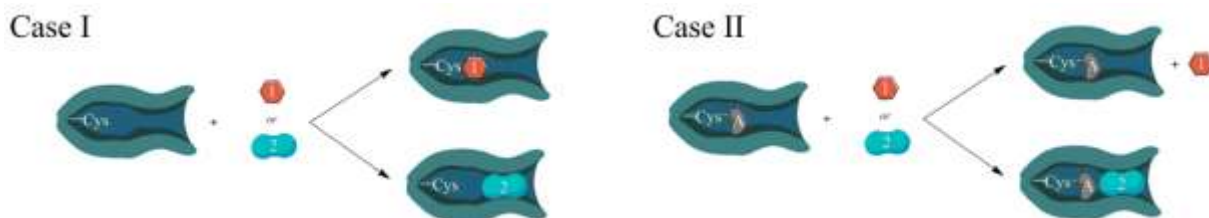


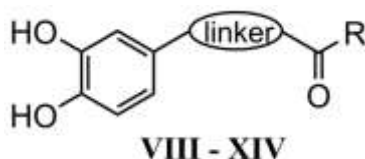
Fig. 8 Representative schemes of the two possible binding mode of inhibitors on PqsD. 1 is a competitor of A-CoA in the active site, 2 is an inhibitor that bind the channel before the active site. Case I: PqsD with the compounds. Case II: PqsD, preincubated with A-CoA (“A”), with the inhibitors.

Among the several analogues, six compounds were selected for binding mode evaluation, three having the unsaturated linker as **VIII** and three with the saturated chain as **XII**. Actually, the analysis revealed that these inhibitors are capable to interact with PqsD also after A-CoA treatment

and, consequently, they do not bind the enzyme in the catalytic pocket, but likely in the entrance channel.

Furthermore, it was investigated the capability of these pathoblockers to reduce HHQ production in PA14 *pqsH* mutant. As for the (2-nitrophenyl)methanol derivatives, the inhibitors were tested at 250 μ M. Interestingly, the most potent compounds in the cell-free assay **XI**, **XII**, **XIV** revealed to be weakly active or completely inactive in the cell-based test, while the unsaturated derivative **VIII** showed to be the most active inhibitor of the class capable to reduce HHQ production of $31 \pm 2\%$ at 250 μ M (Table 2). In addition, while the amide **XIII** was as potent as the analogue ester in the PqsD cell-free assay, in the cell-based is showed no effect on HHQ reduction.

Table 2 Most potent compounds of the class in cell-free and/or whole-cell assays using PA14 *pqsH* mutant.



Compound	Linker	R	IC ₅₀ [μ M] (10 min preinc.) ^a	% HHQ inhibition in PA14 <i>pqsH</i> mutant ^b
VIII	CH=CH (E)	OMe	51 ± 4	31 ± 2
IX	CH ₂ CH ₂	OMe	23 ± 1	17 ± 1
X	CH ₂ CH ₂	OEt	14 ± 1	17 ± 1
XI	CH ₂ CH ₂	OiPr	8.6 ± 0.6	16 ± 1
XII	CH ₂ CH ₂	OCH ₂ Ph	5.9 ± 1.2	Inactive
XIII	CH ₂ CH ₂	NHMe	20 ± 4	Inactive
XIV	CH ₂ CH ₂ CH ₂	OMe	7.9 ± 0.2	18 ± 2

Errors indicate Standard Deviation. ^a Cell-free PqsD assay with 10 minutes pre-incubation protocol of enzyme with compound. ^b Compounds tested at 250 μ M.

As for the (2-nitrophenyl)methanol QSIs, also these PqsD inhibitors showed to be efficient in reducing the enzymatic catalysis in *in vitro* settings and active *in cellulo* only at high concentrations without finding a clear correlation between the two assay conditions. Actually, the accessibility of the compounds to reach the bacterial target could be challenging due to the low permeability of the bacterial membranes as previously mentioned (Nikaido, 2003) and/or due to possible metabolization of the QSIs by bacterial esterases (Pesaresi *et al.*, 2005).

10.1.3 Common characteristics of the two classes

Even if the two approaches applied for the development of PqsD inhibitors were different and ended with the discovery of two completely diverse scaffolds, the two compound classes shares two main characteristics. Firstly, no correlation was found between high potency in cell-free and in

whole-cell assays in both classes. Secondly, high concentration of PqsD inhibitor, such as 250 μ M, was required for displaying a significant inhibition of the signal molecule. As previously mentioned, *P. a.* is known to have very selective low permeable cellular membranes, thanks also to high expression of efflux pumps, and a set of enzymes that can metabolize xenobiotics. However, it should not be excluded that targeting PqsD could not completely suppress the *pqs* system as, for example, the partial reduction of HHQ did not affect the production of the redox toxin pyocyanin (unpublished data). Consequently, it might be possible that other strategies for blocking this QS system should be taken into consideration.

10.2 Evaluation of PqsBC inhibitors and MvfR antagonists

Considering the high doses necessary for reducing HHQ production in *P. a.* cultures and the possibility that PqsD would not be the best target for blocking the *pqs* system, no further optimizations were made on the developed inhibitors. Consequently, a deeper study in the scientific literature highlighted the importance of PqsBC and MvfR in coordinating the functionality of this QS system, as Aqs biosynthesis and *P. a.* virulence. So, four tool compounds, such as the two PqsBC inhibitors **VII** (unpublished data) and **XV** (Starkey *et al.*, 2014), and the two most potent MvfR antagonists **XVI** (Starkey *et al.*, 2014) and **XVII** (Zender *et al.*, unpublished data) (Fig. 9) were used for investigating the *pqs* biosynthetic machinery in different *P. a.* strains as fully described in the manuscript C.

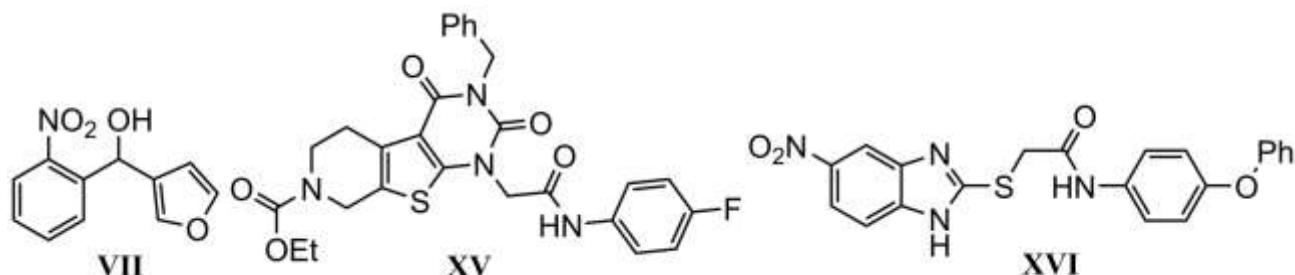


Fig. 9 Structures of the PqsBC inhibitors **VII** and **XV** and of the MvfR antagonist **XVI**. The chemical formula of **XVII** cannot be disclosed because of patent submission on going.

While it was previously described the activity of these compounds in reducing PQS and HHQ production in PA14 *wt* and its isogenic *pqsH* mutant, respectively, the effects of these QSIs on 2-AA, DHQ and HQNO were not elucidated. Consequently, an "all-in-one" assay using the HPLC-MS/MS was established for detecting the five major *pqs*-related small molecules in multiple *P. a.* strains modifying the published protocol of Lépine and coworkers (Lépine *et al.*, 2003). The two classes of inhibitors showed a characteristic profile regarding *mvfr*-related small molecule formation in PA14 *wt* and its isogenic *pqsH* mutant.

10.2.1 Effects of MvfR antagonists on pqs-small molecules

The MvfR antagonists **XVI** and **XVII** were capable to completely suppress the overall biosynthesis at the highest concentration in both strains. Reduction of the QSI dose provoked a quick restoration of the synthesis of AQs and 2-AA as highlighted by the observed very steep curves. Furthermore, while **XVI** and **XVII** showed respective AQs IC₅₀ of 1.2 μM and 3.8 μM in PA14 *wt*, the compounds were around one order of magnitude more potent in PA14 *pqsH* mutant displaying AQs IC₅₀ of 0.30 μM and 0.85 μM. Actually, this difference in activities between the two strains was expected as PQS is much more potent than HHQ in activating the transcriptional regulator (Xiao *et al.*, 2006a). Interestingly, the DHQ level tremendously increased at dosages of antagonist close to the 2-AA and AQs IC₅₀s for returning to basal levels at lower amounts of compound. These overall specific profiles suggested that the *pqs* autoloop could be one of the causing factors. Actually, MvfR antagonization would result in reduced *pqs* expression with subsequent lower amount of signal molecules capable to compete with the QSIs on the transcriptional regulator. This would have, in the end, a pseudo-positive cooperative effect on the MvfR antagonist efficacy. Furthermore, at concentrations of pathoblocker close to AQs IC₅₀s, the biosynthetic machinery would not be capable to convert the major amount of anthranilic acid into HHQ/PQS maybe because of slow kinetic step in it. Considering the low affinity of 2-ABA toward PqsBC (Drees *et al.*, 2016), it was assumed that the conversion of 2-ABA into HHQ was the slow step. Consequently, this would lead accumulation of the reactive intermediate which spontaneously cyclize in the stable molecule DHQ.

So, the compounds were evaluated in PA14 *pqsC* mutant with and without exogenous addition of PQS for modulating operon expression. Actually, **XVI** and **XVII** showed smooth inhibitory curves of 2-AA and DHQ in absence of signal molecule and IC₅₀s values in the two digits nanomolar range. The addition of quinolone increased both the steepness of the curves, and their respective IC₅₀s values up to the single digit micromolar range, similar to their inhibitory activity in *wt* strain. These results, consequently, confirmed that PQS and its autoloop would be two factors of the steepness of the inhibitory curves. Furthermore, analysis of *pqsA* expression after addition of MvfR antagonist revealed that these QSIs efficiently suppressed the transcription of the operon.

In addition, the profiling of the *pqs*-small molecules in PA14 *pqsE* mutant uncovered a profile characterized by a much higher levels of DHQ and lower production of 2-AA and HQNO compared to the isogenic *wt*. This specific distribution of *mvfR*-related compounds in *pqsE* mutant occurred because the thioester cleavage of 2-ABA-CoA into 2-ABA would be carried out by the slow unspecific thioesterase TesB (Drees, Fetzner, 2015). Considering the similar distribution of 2-AA, DHQ and HQNO between PA14 *pqsE* mutant and PA14 *wt* with AQs IC₅₀ doses of antagonist, it is plausible that an accumulation of the intermediate 2-ABA-CoA took place in PA14 *wt* instead of the hypothesized 2-ABA.

10.2.2 Effects of PqsBC inhibitors on pqs-small molecules

The analysis of the PqsBC inhibitors **VII** and **XV** on *pqs*-small molecule production in PA14 *wt* and *pqsH* mutant showed that these QSIs were not able to affect the overall formation of QS molecules. Actually, these QSIs mainly influenced the distribution of the *pqs* biosynthetic products favoring the increase of 2-AA, DHQ and HQNO amounts and the decrease of signal molecules levels. While the increase in 2-AA and DHQ was expected, the higher production of HQNO was surprising as the biosynthesis of this specific AQ requires the hetero-dimeric protein.

Consequently, it was preferable to confirm their target selectivity. So, these QSIs were evaluated in PA14 *pqsC* mutant in which they resulted to be completely inactive. Furthermore, analysis of the *pqsA* expression showed that 500 μ M of **VII** and 10 μ M of **XV** strongly suppressed the transcription of the operon in accordance with the efficient reduction of signal molecules at similar concentrations.

Taking into consideration the obtained results and the biosynthetic pathway, it is plausible to assume that PqsBC might have different kinetic parameters and affinities depending on the substrate to be used, 2-HABA for HQNO and 2-ABA for HHQ. Consequently, the designed PqsBC inhibitors would have different inhibitory activity depending on the reaction to be blocked. So, while the formation of the signal molecule is inhibited, the reactive intermediate 2-ABA is transformed into DHQ, 2-AA and 2-HABA which is, finally, converted into HQNO.

10.2.3 Effects of MvfR antagonists and PqsBC inhibitors on antibiotic tolerance

Considering the important role of 2-AA in antibiotic tolerance development, the four compounds were analyzed to assess their capability to influence the rate of persister cells and, consequently, modulate the killing rate of the employed antibiotic meropenem. Actually, the efficiency of the MvfR antagonists in reducing the 2-AA formation translated into their capability to reduced PA14 *wt* tolerance to the isogenic *mvfR* mutant levels with the consequent improvement of antibiotic efficacy. On the contrary, while both PqsBC inhibitors enhanced 2-AA production, only **VII** increased persistence to similar levels of PA14 *wt* incubated with 2-AA. A comparable result was obtained for the isogenic *pqsBC* mutant which led to a reduced antibacterial potency of meropenem.

10.2.4 Comparison between PqsBC inhibitors and MvfR antagonists

The combination of the findings from the *pqs*-small molecules profiling and persistence assessment revealed that targeting PqsBC would not be beneficial for blocking *P. a.* infections. Actually, higher production of 2-AA and HQNO in the infection site would be translated into higher chances to develop chronic infections characterized by biofilms richer in persistent cells. In addition, the overproduction of DHQ would lead to intoxication of the host cells. Consequently, the

eukaryotic cell growth would be inhibited and the mechanism of tissue repair would be strongly delayed.

On the contrary, targeting MvfR would efficiently inhibit the whole *pqs* system and, consequently, reduce *P. a.* pathogenicity and development of long-term infections. So, the employment of the transcriptional regulator antagonists would, firstly, help the host immune system in blocking the colonization and invasion of the pathogen in the tissues and, secondly, improve the efficacy of antibacterial drugs.

11 CONCLUSIONS AND OUTLOOKS

The evaluation of three different QSI groups, such as PqsD and PqsBC inhibitors and MvfR antagonists, helped in understanding more in depth the *pqs* system and the therapeutic efficiency in blocking singularly the proteins.

The application of two different strategies used in drug discovery, as the ligand-based and similarity-guided, helped in the development of PqsD inhibitors based on two diverse scaffolds. Deep SAR studies were conducted on both classes which resulted in the identification of potent compounds in cell-free settings with IC_{50} s values between single digit micromolar - high nanomolar range. In addition, while the (2-nitrophenyl)methanols were shown to bind the enzyme in its catalytic site, the catechols revealed to likely interact in the entrance channel of the protein. The *in cellulo* evaluation of the QSIs showed that some compounds potent in the PqsD assay were capable to efficiently reduce signal molecule production at 250 μ M. However, the usage of such high doses in the whole-cell assays suggested three possible explanations. Firstly, it could not be excluded that both compound classes were not be able to permeate easily through the bacterial membranes due to low import in the cell or high expulsion carried out by efflux pumps. Consequently, in a next step, the permeability of the QSIs could be analyzed as employing *in vitro* models mimicking the physicochemical properties of the bacterial membrane (Graef *et al.*, 2016). In case the compounds diffuse easily through the bacterial membrane, the PqsD inhibitors could be evaluated in strains lacking in the expulsion systems (El'Garch *et al.*, 2007) or tested in combination with efflux pumps inhibitors (Lomovskaya *et al.*, 2001). Secondly, based on the arsenal of metabolizing enzymes expressed, *P. a.* may transform the QSIs into inactive forms. So, their possible metabolic inactivation could be analyzed through quantification of the inhibitor during cellular incubation by HPLC-MS/MS (Said *et al.*, 2016; Bhat *et al.*, 2013). Thirdly, considering the high activity of the signal molecules in activating the *pqs* operon, it might be that PqsD inhibition does not fully suppress the expression of the gene cluster. Consequently, analysis of *pqs* operon expression could help such elucidation.

So, the evaluation of other targets was accomplished, such as the biosynthetic enzyme PqsBC and the transcriptional regulator MvfR. After the development of an "all-in-one" HPLC-MS/MS assays, an extended analysis of all the *pqs* biosynthetic products was performed using two tool compounds for each target protein. PqsBC inhibitors revealed that they mainly affected the distribution of the *mvfR*-related small molecules, but not the overall production. Actually, these compounds induced higher 2-AA, DHQ and HQNO biosynthesis, key molecules in persistence, host toxicity and biofilm formation, while reduced signal molecules levels. Consequently, the developed inhibitors of this heterodimeric protein would not block all its reactions, but only conversion of 2-ABA into HHQ. On the contrary, the designed MvfR antagonists showed to reduce 2-AA, Aqs and the overall production dose-dependently with very steep inhibitory curves. In addition, they induced

a boost of DHQ formation at Aqs IC₅₀ values. Comparing the activities of the compounds in the *pqsC* mutant with and without exogenous PQS, used for modulating operon expression, highlighted that the signal molecule and its autoloop are factors which influence the steepness of the curves. Furthermore, the similar distribution of the *pqs*-small molecules between the *pqsE* mutant and the *wt* with Aqs IC₅₀ concentration of antagonist highlighted that the overproduction of DHQ could be due to the accumulation of the reactive intermediate 2-ABA-CoA. In addition, considering the different effects of the two QSI groups on 2-AA production, their activities in modulating persistence was evaluated. While PqsBC inhibitors enhanced bacterial tolerance, MvfR antagonists efficiently reduced it displaying, in the end, the preferable profile.

In the end, this study highlighted that, among the three targets evaluated, blocking MvfR was identified as the optimal strategy to be applied for reducing *P. a.* pathogenicity. Consequently, further efforts should be put in the optimization of the known class of compounds designed to antagonize the transcriptional regulator and in the discovery of novel scaffolds. In addition, while a monotherapy with the studied PqsD or PqsBC inhibitors would not be ideal for treating *P. a.* infections, these compounds could be employed in combination therapies with MvfR antagonists for improving the anti-virulence effects of the transcriptional regulator blockers (Thomann *et al.*, 2016). Consequently, analysis of *pqs*-small molecules production and persistence assessments would be recommended to be performed after the incubation of *P. a.* with the combination therapy. Actually, these studies will give further information about the efficiency of this therapeutic approach in reducing bacterial virulence, and guide the scientific community in how to improve it.

12 REFERENCES

- Allen, R., C., Popat, R., Diggle, S., P., Brown, S., P. (2014). Targeting virulence: can we make evolution-proof drugs? *Nat. Rev. Microbiol.* *12*, 300 – 308.
- Bera, A., K., Atanasova, V., Robinson, H., Eisenstein, E., Coleman, J., P., Pesci, E., C., Parson, J., F. (2009). Structure of PqsD, a *Pseudomonas* Quinolone Signal biosynthetic enzyme, in complex with anthranilate. *Biochem.* *48*, 8644 – 8655.
- Bhat, J., Narayan, A., Venkatraman, J., Chatterji, M. (2013). LC-MS based assay to measure intracellular compound levels in *Mycobacterium smegmatis*: linking compound levels to cellular potency. *J. Microbiol. Meth.* *94*, 152 – 158.
- Brown., E., D., Wright, G., D. (2016). Antibacterial drug discovery in the resistance era. *Nature.* *529*, 336 – 343.
- Busi Rizzi, E., Schininá, V., Bordi, E., Buontempo, G., Narciso, P., Bibbolino, C. (2006). HIV-related bronchopulmonary infection by *Pseudomonas aeruginosa* in the HAART era: radiological findings. *Acta Radiol.* *47*, 793 – 797.
- Christensen, L., D., Moser, C., Jensen, P., Ø., Rasmussen, T., B., Christophersen, L., Kjelleberg, S., Kumar, N., Høiby, N., Givskov, M., Bjarnsholt, T. (2007). Impact of *Pseudomonas aeruginosa* quorum sensing on biofilm persistence in an *in vivo* intraperitoneal foreign-body infection model. *Microbiol.* *153*, 2312 – 2320.
- Cao, H., Krishnan, G., Goumnerov, B., Tsongalis, J., Tompkins, R., Rahme, L., G. (2001). A quorum sensing-associated virulence gene of *Pseudomonas aeruginosa* encodes a LysR-like transcriptional regulator with a unique self-regulatory mechanism. *Proc. Natl. Acad. Sci. U S A.* *98*, 14613 – 14618.
- Clatworthy, A., E., Pierson, E., Hung, D., T. (2007). Targeting virulence: a new paradigm for antimicrobial therapy. *Nature.* *3*, 541 – 548.
- Coleman, J., P., Hudson, L., L., McKight, S., L., Farrow III, J., M., Calfee, M., W., Lindsey, C., A., Pesci, E., C. (2008). *Pseudomonas aeruginosa* PqsA is an anthranilate-coenzyme A ligase. *J. Bacteriol.* *190*, 1247 – 1255.
- Dao, T., T., H., Linthorst, H., J., M., Verpoorte, R. (2011). Chalcone synthase and its functions in plant resistance. *Phytochem. Rev.* *10*, 397 – 412.
- Déziel, E., Lépine, F., Milot, S., He, J., Mindrinos, M., N., Tompkins, R., G., Rahme, L., G. (2004). Analysis of *Pseudomonas aeruginosa* 4-hydroxy-2-alkylquinolines (HAQs) reveals a role for 4-hydroxy-2-heptylquinoline in cell-to-cell communication. *Proc. Natl. Acad. Sci. U S A.* *101*, 1339 – 1344.
- Diggle, S., P., Lumjiaktase, P., Dipilato, F., Winzer, K., Kunakorn, M., Barrett, D., A., Chhabra, S., R., Cámara, M., Williams, P. (2006). Functional genetic analysis reveals a 2-alkyl-4-quinolone signaling sensing in the human pathogen *Burkholderia pseudomallei* and related bacteria. *Chem. Biol.* *13*, 701 – 710.
- Diggle, S., P., Matthijs, S., Wright, V., J., Fletcher, M., P., Chhabra, S., R., Lamont, I., L., Kong, X., Hider, R., C., Cornelis, P., Cámara, M., Williams, P. (2007). The *Pseudomonas aeruginosa* 4-quinolone signal molecules HHQ and PQS play multifunctional roles in Quorum Sensing and iron entrapment. *Chem. Biol.* *14*, 87 – 96.
- Drees, S., L., Fetzner, S. (2015). PqsE of *Pseudomonas aeruginosa* acts as pathway-specific thioesterase in the biosynthesis of alkylquinolone signaling molecules. *Chem. Biol.* *22*, 611 – 618.
- Drees, S., L., Li, C., Prasetya, F., Saleem, M., Dreveny, I., Williams, P., Hennecke, U., Emsley, J., Fetzner, S. (2016). PqsBC, a condensing enzyme in the biosynthesis of the *Pseudomonas aeruginosa* quinolone signal: crystal structure, inhibition, and reaction mechanism. *J. Biol. Chem.* *291*, 6610–6624.
- Dulcey, C., E., Dekimpe, V., Fauvelle, D., A., Milot, S., Groleau, M., C., Doucet, N., Rahme, L., G., Lépine, F., Déziel, E. (2013). The end of an old hypothesis: the *Pseudomonas* signaling molecules 4-hydroxy-2-alkylquinolines derive from fatty acids, not 3-ketofatty acids. *Chem. Biol.* *20*, 1481 – 1491.

- El'Garch, F., Jeannot, K., Hocquet, D., Llanes-Barakat, C., Plésiat, P. (2007). Cumulative effects of several nonenzymatic mechanisms on the resistance of *Pseudomonas aeruginosa* to aminoglycosides. *Antimicrob. Agents Chemother.* 51, 1016 – 1021.
- European Centre for Disease Prevention and Control/European Medicines Agency Joint Working Group (ECDC/EMA). (2009). The bacterial challenge: time to react. Available at www.ecdc.europa.eu/en/publications/Publications/0909_TER_The_Bacterial_Challenge_Time_to_React.pdf.
- Feldman, M., Bryan, R., Rajan, S., Scheffler, L., Brunnert, S., Tang, H., Prince, A. (1998). Role of flagella in pathogenesis of *Pseudomonas aeruginosa* pulmonary infection. *Infect. Immun.* 66, 43 – 51.
- Ferrer, J., L., Jez, J., M., Bowman, M., E., Dixon, R., A., Noel, J., P. (1999). Structure of chalcone synthase and the molecular basis of plant polyketide biosynthesis. *Nat. Struct. Biol.* 6, 755 – 783.
- Fleming, A. (1929). On the antibacterial action of cultures of a penicillium, with special reference to their use in the isolation of *B. influenzae*. *Br. J. Exp. Pathol.* 10, 226 – 236.
- Flemming, H., C., Wingender, J. (2010). The biofilm matrix. *Nat. Rev. Microbiol.* 8, 623 – 633.
- Fugua, C., Parsek, M., R., Greenberg, E., P. (2001). Regulation of gene expression by cell-to-cell communication: acyl-homoserine lactone quorum sensing. *Annu. Rev. Genet.* 35, 439 – 468.
- Gallagher, L., A., McKnight, S., L., Kuznetsova, M., S., Pesci, E., C., Manoil, C. (2002). Functions required for extracellular quinolone signaling by *Pseudomonas aeruginosa*. *J. Bacteriol.* 184, 6472 – 6480.
- Galoway, D., R. (1991). *Pseudomonas aeruginosa* elastase and elasolysis revisited: recent developments. *Mol. Microbiol.* 5, 2315 – 2321.
- Gómez, I., M., Prince, A. (2007). Opportunistic infections in lung disease: *Pseudomonas* infections in cystic fibrosis. *Curr. Opin. Pharmacology.* 7, 244 – 251.
- Graef, F., Vukosavljevic, B., Michel, J., P., Wirth, M., Ries, O., De Rossi, C., Windbergs, M., Rosilio V., Ducho, C., Gordon, S., Lehr, C., M. (2016). The bacterial cell envelope as delimiter of anti-infective bioavailability - An *in vitro* permeation model of the Gram-negative bacterial inner membrane. *J. Control Release.* 243, 214 – 224.
- Gruber, J., D., Chen, W., Parnham, S., Beauchesne, K., Moeller, P., Flume, P., A., Zhang, Y., M. (2016). The role of 2,4-dihydroxyquinoline (DHQ) in *Pseudomonas aeruginosa* pathogenicity. *PeerJ.* 4:e1495. doi: 10.7717/peerj.1495.
- Hall-Stoodley, L., Costerton, J., W., Stoodley, P. (2004). Bacterial biofilms: from the natural environment to infectious diseases. *Nat. Rev. Microbiol.* 2, 95 – 108.
- Hancock, R., E. (1998). Resistance mechanisms in *Pseudomonas aeruginosa* and other nonfermentative gram-negative bacteria. *Clin. Infect. Dis. Suppl.* 1, S93 – S99.
- Hazan, R., Que, Y., A., Maura, D., Strobel, B., Majcherczyk, P., A., Hopper, L., R., Wilbur, D., J., Hreha, T., N., Barquera B., Rahme, L., G. (2016). Auto poisoning of the respiratory chain by a quorum-sensing-regulated molecule favors biofilm formation and antibiotic tolerance. *Curr. Biol.* 26, 195 – 206
- Hill, D., Rose, B., Pajkos, A., Robinson, M., Bye, P., Bell, S., Elkins, M., Thompson, B., Macleod, C., Aaron, S., D., Harbour, C. (2005). Antibiotic susceptibilities of *Pseudomonas aeruginosa* isolates derived from patients with cystic fibrosis under aerobic, anaerobic, and biofilm conditions. *J. Clin. Microbiol.* 43, 5085 – 5090.
- Hinsberger, S., de Jong, J., C., Groh, M., Haupenthal, J., Hartmann, R., W. (2014). Benzamidobenzoic acids as potent PqsD inhibitors for the treatment of *Pseudomonas aeruginosa* infections. *Eur. J. Med. Chem.* 76, 343 – 351.
- Hoergy, F., Mislin, G., L., Schalk, I., J. (2014). Pyoverdine and pyochelin measurements. *Methods Mol. Biol.* 1149, 293 – 301.
- Hurley, M., N., Cámara, M., Smyth, A., R. (2012). Novel approaches to the treatment of *Pseudomonas aeruginosa* infections in cystic fibrosis. *Eur. Respir. J.* 40, 1014 – 1023.

- Ilangonav, A., Fletcher, M., Rampioni, G., Pustelny, C., Rumbaugh, K., Heeb, S., Cámara, M., Truman, A., Chhabra, S., R., Emsley, J., Williams, P. (2013). Structural basis for native agonist and synthetic inhibitor recognition by the *Pseudomonas aeruginosa* Quorum Sensing regulator PqsR (MvfR). *PLoS Pathog.* 9(7):e1003508. doi: 10.1371/journal.ppat.1003508.
- Kang, C., I., Kim, S., H., Kim, H., B., Park, S., W., Choe, Y., J., Oh, M., D., Kim, E., C., Choe, K., W. (2003). *Pseudomonas aeruginosa* bacteremia: risk factors for mortality and influence of delayed receipt of effective antimicrobial therapy on clinical outcome. *Clin. Infect. Dis.* 37, 745 – 751.
- Kesarwani, M., Hazan, R., He, J., Que, Y., A., Apidianakis, Y., Lesic, B., Xiao, G., Dekimpe, V., Milot S., Deziel, E., Lépine, F., Rahme, L., G. (2011). A quorum sensing regulated small volatile molecule reduces acute virulence and promotes chronic infection phenotypes. *PLoS Pathog.* 7:8. doi: 10.1371/journal.ppat.1002192.
- Klein, T., Henn, C., de Jong, J., C., Zimmer, C., Kirsch, B., Maurer, C., K., Pistorius, D., Müller, R., Steinbach, A., Hartmann, R., W. (2012). Identification of small-molecule antagonists of the *Pseudomonas aeruginosa* transcriptional regulator PqsR: biophysically guided hit discovery and optimization. *ACS Chem. Biol.* 7, 1496 – 1501.
- Kovacic, P., Somanathan, R. (2014). Nitroaromatic compounds: environmental toxicity, carcinogenicity, mutagenicity, therapy and mechanism. *J. Appl. Toxicol.* 34, 810 – 824.
- Laarman, A., J., Bardoel, B., W., Ruyken, M., Fernie, J., Milder, F., J., van Strijp, J., A., G., Rooijackers, S., H., M. (2012). *Pseudomonas aeruginosa* alkaline protease blocks complement activation via the classical and lectin pathways. *J. Immunol.* 188, 386 – 393.
- Lamarche, M., G., Déziel, E. (2011). MexEF-OprN efflux pump exports the *Pseudomonas* Quinolone Signal (PQS) precursor HHQ (4-hydroxy-2-heptylquinoline). *PLoS ONE.* 6(9):e24310. doi:10.1371/journal.pone.0024310.
- Lee, J., Wu, J., Deng, Y., Wang, J., Wang, C., Wang, J., Chang, C., Dong, Y., Williams, P., Zhang, L., H. (2013). A cell-cell communication signal integrates quorum sensing and stress response. *Nat. Chem. Biol.* 9, 339 – 343.
- Lee, J., Zhang, L. (2014). The hierarchy quorum sensing network in *Pseudomonas aeruginosa*. *Protein Cell.* 6, 26 – 41.
- Lépine, F., Deziel, E., Milot, S., Rahme, L., G. (2003). A stable isotope dilution assay for the quantification of the *Pseudomonas* Quinolone Signal in *Pseudomonas aeruginosa* cultures. *Biochim. Biophys. Acta.* 1622, 36 – 41.
- Lépine, F., Milot, S., Déziel, E., He, J., Rahme, L., G. (2004). Electrospray/mass spectrometric identification and analysis of 4-hydroxy-2-alkylquinolines (HAQs) produced by *Pseudomonas aeruginosa*. *J. Am. Soc. Mass. Spectrom.* 15, 862 – 869.
- Lewis, K. (2010). Persister cells. *Annu. Rev. Microbiol.* 64, 357 – 372.
- Lister, P., D., Wolter, D., J., Hanson, N., D. (2009). Antibacterial-resistant *Pseudomonas aeruginosa*: clinical impact and complex regulation of chromosomally encoded resistance mechanisms. *Clin. Microbiol. Rev.* 22, 582 – 610.
- Livermore, D., M., Woodford, N. (2006). The beta-lactamase threat in *Enterobacteriaceae*, *Pseudomonas* and *Acinetobacter*. *Trends Microbiol.* 14, 413 – 420.
- Lomovskaya, O., Warren, M., S., Lee, A., Galazzo, J., Fronko, R., Lee, M., Blais, J., Cho, D., Chamberland, S., Renau, T., Leger, R., Hecker, S., Watkins, W., Hoshino, K., Ishida, H., Lee, V., J. (2001). Identification and characterization of inhibitors of multidrug resistance efflux pumps in *Pseudomonas aeruginosa*: novel agents for combination therapy. *Antimicrob. Agents Chemother.* 45, 105 – 116.
- Lu, C., Kirsch, B., Maurer, C., K., de Jong, J., C., Braunshausen, A., Steinbach, A., Hartmann, R., W. (2014). Optimization of anti-virulence PqsR antagonists regarding aqueous solubility and biological properties resulting in new insights in structure-activity relationships. *Eur. J. Med. Chem.* 79, 173 – 183.
- Machan, Z., A., Taylor, G., W., Pitt, T., L., Cole, P., J., Wilson, R. (1992). 2-heptyl-4-hydroxyquinoline *N*-oxide, an antistaphylococcal agent produced by *Pseudomonas aeruginosa*. *J. Antimicrob. Chemother.* 30, 615 – 623.

- Mariencheck, W., I., Alcorn, F., F., Palmer, S., M., Wright, J., R. (2003). *Pseudomonas aeruginosa* elastase degrades surfactant proteins A and D. *Am. J. Respir. Cell. Mol. Biol.* 28, 528 – 537.
- Mashburn, L., M., Whiteley, M. (2005). Membrane vesicles traffic signals and facilitate group activities in a prokaryote. *Nature.* 437, 422 – 425.
- Maura, D., Ballock, A., E., Rahme, L., G. (2016). Considerations and caveats in anti-virulence drug development. *Curr. Opin. Microbiol.* 33, 41 – 46.
- Maura, D., Hazan, R., Kitao, T., Ballock, A., E., Rahme, L., G. (2016). Evidence for direct control of virulence and defense gene circuits by the *Pseudomonas aeruginosa* Quorum Sensing regulator, MvfR. *Sci. Rep.* 6:34083. doi:10.1038/srep34083.
- McGrawth, S., Wade, D., S., Pesci, E., C. (2004). Dueling quorum sensing systems in *Pseudomonas aeruginosa* control the production of the *Pseudomonas* quinolone signal (PQS). *FEMS Microbiol. Lett.* 230, 27 – 34.
- Miller, M., B., Bassler, B., L. (2001). Quorum sensing in bacteria. *Annu. Rev. Microbiol.* 55, 165 – 199.
- Mulliner, D., Woundrousch, D., Schüürmann, G. (2011). Predicting Michael-acceptor reactivity and toxicity through quantum chemical transition-state calculations. *Org. Biomol. Chem.* 9, 8400 – 8412.
- Nikaido, H. (2003). Molecular basis of bacterial outer membrane permeability revised. *Microbiol. Mol. Biol. Rev.* 67, 593 – 656.
- Noguera, D., R., Freedman, D., L. Reduction and acetylation of 2,4-dinitrotoluene by a *Pseudomonas aeruginosa* strain. *Appl. Environ. Microbiol.* 62, 2257 – 2263.
- Obritsch, M., D., Douglas, N., F., MacLaren, R., Jung, R. (2004). National surveillance of antimicrobial resistance in *Pseudomonas aeruginosa* isolates obtained from intensive care unit patients from 1993 to 2002. *Antimicrob. Agents Chemother.* 48, 4606 – 4610.
- O'Shea, R., Moser, H., E. (2008). Physicochemical properties of antibacterial compounds: implications for drug discovery. *J. Med. Chem.* 51, 2871 – 2878.
- Pendleton, J., N., Gorman, S., P., Gilmore, B., F. (2013) Clinical relevance of the ESKAPE pathogens. *Expert Rev. Anti Infect. Ther.* 11, 297 – 308.
- Persat, A., Inclan, Y., F., Engel, J., N., Stone, H., A., Gitai, Z. (2015). Type IV pili mechanochemically regulate virulence factors in *Pseudomonas aeruginosa*. *Proc. Natl. Acad. Sci. U S A.* 112, 7563 – 7568.
- Pesaresi, A., Devescovi, G., Lamba, D., Venturi, V., Degrassi, G. (2005). Isolation, characterization, and heterologous expression of a carboxylesterase of *Pseudomonas aeruginosa* PAO1. *Curr. Microbiol.* 50, 102 – 109.
- Pesci, E., C., Milbank, J., B., J., Pearson, J., P., McNight, S., Kende, A., S., Greenberg, E., P., Iglewski, B., H. (1999). Quinolone signaling in the cell-to-cell communication system of *Pseudomonas aeruginosa*. *Proc. Natl. Acad. Sci. USA.* 96, 11229 – 11234.
- Pistorius, D., Ullrich, A., Lucas, S., Hartmann, R., W., Kazmaier, U., Müller, R. (2011). Biosynthesis of 2-alkyl-4(1H)-quinolones in *Pseudomonas aeruginosa*: potential for therapeutic interference with pathogenicity. *Chembiochem.* 12, 850 – 853.
- Que, Y., A., Hazan, R., Ryan, C., M., Milot, S., Lépine, F., Lydon, M., Rahme, L., G. (2011). Production of *Pseudomonas aeruginosa* intercellular small signal molecules in human burn wounds. *J. Pathog.* 2011:549302. doi: 10.4061/2011/549302.
- Que, Y., A., Hazan, R., Strobel, B., Maura, D., He, J., Kesarwani, M., Panopoulos, P., Tsurumi, A., Giddey, M., Wilhelmy, J., Mindrinos, M., N., Rahme, L., G. (2013). A quorum sensing small volatile molecule promotes antibiotic tolerance in bacteria. *PLoS One.* 8:12. doi: 10.1371/journal.pone.0080140.
- Rasko, D., A., Sperandio, V. (2010). Anti-virulence strategies to combat bacteria-mediated disease. *Nat. Rev. Drug Discov.* 9, 117 – 128.

- Rumbaugh, K., P., Griswold, J., A., Iglewski, B., H., Hamood, A., N. (1999). Contribution of Quorum Sensing to the virulence of *Pseudomonas aeruginosa* in burn wound infections. *Infect. Immun.* 67, 5854 – 5862.
- Said, I., H., Shah, R., L., Ullrich, M., S., Kuhnert, N. (2016). Quantification of microbial uptake of quercetin and its derivatives using an UHPLC-ESI-QTOF mass spectrometry assay. *Food Funct.* 7, 4082 – 4091.
- Schäberle, T., F., Hack, I., M. (2014). Overcoming the current deadlock in antibiotic research. *Trends Microbiol.* 22, 165 – 167.
- Schackmann, A., Müller, R. (1991). Reduction of nitroaromatic compounds by different *Pseudomonas* species under aerobic conditions. *Appl. Microbiol. Biotechnol.* 34, 809 – 813.
- Schell, M., A. (1993). Molecular biology of the LysR family of transcriptional regulators. *Annu. Rev. Microbiol.* 47, 597 – 626.
- Schertzer, J., W., Brown, S., A., Whiteley, M. (2010). Oxygen levels rapidly modulate *Pseudomonas aeruginosa* social behaviors via substrate limitation of PqsH. *Mol. Microbiol.* 77, 1527 – 1538.
- Schröder, J. The family of chalcone synthase-related proteins: functional diversity and evolution. In: Ibrahim, R., Varin, L., De Luca, V., Romeo, J. *Evolution of metabolic pathways.* Elsevier Science Ltd. Oxford 2000. 55 – 90.
- Smith, R., S., Iglewski, B., H. (2003). *P. aeruginosa* quorum-sensing systems and virulence. *Curr. Opin. Microbiol.* 6, 56 – 60.
- Starkey, M., Lépine, F., Maura, D., Bandyopadhyaya, A., Lesic, B., He, J., Kitao, T., Righi, V., Milot, S., Tzika, A., Rahme, L., G. (2014). Identification of anti-virulence compounds that disrupt quorum-sensing regulated acute and persistent pathogenicity. *PLoS Pathog.* 10(8):e1004321. doi: 10.1371/journal.ppat.1004321.
- Storz, M., P., Brengel, C., Weidel, E., Hoffmann, M., Hollemeyer, K., Steinbach, A., Müller, R., Empting, M., Hartmann, R., W. (2013). Biochemical and biophysical analysis of a chiral PqsD inhibitor revealing tight-binding behaviour and enantiomers with contrary thermodynamic signatures. *ACS Chem. Biol.* 8, 2794 – 2801.
- Storz, M., P., Maurer, C., K., Zimmer, C., Wagner, N., Brengel, C., de Jong, J., C., Lucas, S., Müsken, M., Häussler, S., Steinbach, A., Hartmann, R., W. (2012). Validation of PqsD as an anti-biofilm target in *Pseudomonas aeruginosa* by development of small-molecule inhibitors. *J. Am. Chem. Soc.* 134, 16143 – 16146.
- Strateva, T., Mitov, I. (2011). Contribution of an arsenal of virulence factors to pathogenesis of *Pseudomonas aeruginosa* infections. *Ann. Microbiol.* 61, 717 – 732.
- Thomann, A., de Mello Martins, A., G., G., Brengel, C., Empting, M., Hartmann, R., W. (2016). Application of dual inhibition concept within looped autoregulatory systems toward antivirulence agents against *Pseudomonas aeruginosa*. *ACS Chem. Biol.* 11, 1279 – 1286.
- Todar, K. (2009). Opportunistic infections caused by *Pseudomonas aeruginosa*. In: Kenneth Todar's Online Textbook of Bacteriology. University of Wisconsin-Madison, Department of Bacteriology, <http://www.textbookofbacteriology.net/>.
- Tredget, E., E., Shankowsky, H., A., Rennie, R., Burrell, R., E., Logsetty, S. (2004). *Pseudomonas* infections in the thermally injured patient. *Burns.* 30, 3 – 26.
- Vial, L., Lépine, F., Milot, S., Groleau, M., C., Dekimpe, V., Woods, D., E., Déziel, E. (2008). *Burkholderia pseudomallei*, *B. thailandensis*, and *B. ambifaria* produce 4-hydroxy-2-alkylquinoline analogues with a methyl group at the 3 position that is required for Quorum-Sensing regulation. *J. Bacteriol.* 190, 5339 – 5352.
- Wagner, S., Sommer, R., Hinsberger, S., Lu, C., Hartmann, R., W., Empting, M., Titz, A. (2016). Novel strategies for the treatment of *Pseudomonas aeruginosa* infections. *J. Med. Chem.* 59, 5929 – 5969.
- Walter III, M., C., Roe, F., Bugnicourt, A., Franklin, M., J., Stewart, P., S. (2003). Contributions of antibiotic penetration, oxygen limitation, and low metabolic activity to tolerance of *Pseudomonas aeruginosa* biofilms to ciprofloxacin and tobramycin. *Antimicrob. Agents. Chemother.* 47, 317 – 323.

- Weidel, E., de Jong, J., C., Brengel, C., Storz, M., P., Braunshausen, A., Negri, M., Plaza, A., Steinbach, A., Müller, R., Hartmann, R., W. (2013). Structure optimization of 2-benzamidobenzoic acids as PqsD inhibitors for *Pseudomonas aeruginosa* infections and elucidation of binding mode by SPR, STD NMR, and molecular docking. *J. Med. Chem.* *56*, 6146 – 6155.
- Xiao, G., Déziel, E., He, J., Lépine, F., Lesic, B., Castonguay, M., H., Milot, S., Tampakaki, A., P., Stachel, S., E., Rahme, L., G. (2006a). MvfR, a key *Pseudomonas aeruginosa* pathogenicity LTTR-class regulatory protein, has dual ligands. *Mol. Microbiol.* *62*, 1689 – 1699.
- Xiao, G., He, J., Rahme, L., G. (2006b). Mutation analysis of the *Pseudomonas aeruginosa* *mvfR* and *pqsABCDE* gene promoters demonstrates complex quorum-sensing circuitry. *Microbiol.* *152*, 1679 – 1686.
- Zhang, Y., J., Li, S., Gan, R., Y., Zhou, T., Xu, D., P., Li, H., B. (2015). Impacts of gut bacteria on human health and diseases. *Int. J. Mol. Sci.* *16*, 7493 – 7519.
- Zhang, Y. M., Frank, M. W., Zhu, K., Mayasundari, A., Rock, C., O. (2008). PqsD is responsible for the synthesis of 2,4-dihydroxyquinoline, an extracellular metabolite produced by *Pseudomonas aeruginosa*. *J. Biol. Chem.* *283*, 28788 – 28794.

13 ANKNOWLEDGEMENTS

I would like to thank my supervisor Prof. Dr. Rolf W. Hartmann for having supported me during these years at the Helmholtz and transmitted me his passion on Science. Especially I am grateful of his precious guide in let me find solutions to problems connected to my PhD project.

Moreover, I am thankful to Prof. Dr. Rolf Müller and Dr. Alexander Titz for their assistance as being co-supervisors of my PhD work.

An important and big "Dankeschön" to all the colleagues I met at Saarland University and at the Helmholtz, in particular to Dr. Martin Empting for his precious advices, Dr. Christine Maurer for her patience in guiding me in the field of biology, Dr. Jens Eberhard for being my HPLC-MS/MS mentor, Simone Amann and Jeannine Jung for their sympathy and passion in working.

Furthermore, a huge "Thanks a lot" to Prof. Dr. Laurence G. Rahme and her team for having given to me the honor and the opportunity to work with them in the place I have always dreamed about (n.d.r., Harvard Medical School), showing me other approaches to Science and opening my mind to new horizons

A special "Grazie mille", "Merci beaucoup", "Muito obrigado", "جزيد لا شكرا" to all the friendly expatriates I had the pleasure to meet in Saarbrücken, mostly Marco Gargano, Antonio Martins and Ahmed Ashraf which were with me when I was facing both good and bad moments and helping me in finding always the light at the end of the tunnel.

Moreover, I really appreciated the support of my parents, my parents-in-law, the whole family and friends during these years in which, even if I was far away from them, they always let me feel close to their homes and hearts.

Last but not least, I thank my wife, Annachiara, for having supported me every day in facing difficulties, problems, for let me relax during stressing periods, in saying always "Try!" and "Never give up!", for being, in the end, the best wife a man looks for. "Grazie Amore!".